Becker, K., Foss, G., et al., 1992
Proceedings of the Ocean Drilling Program, Initial Reports, Vol. 137

2. SITE 504[1]

Shipboard Scientific Party[2]

HOLE 504B

Date occupied: 7 April 1991

Date departed: 29 April 1991

Time on hole: 21 days, 12.25 hr

Position: 1°13.61′N, 83°43.818′W

Seafloor (rig floor, m): 3475

Total depth (mbsf): 1621.5

Penetration (m): 59.2 (during Leg 137)

Number of cores: 8

Total length of cored section (m): 48.6

Total core recovered (m): 8.77

Core recovery (%): 18.0%

Basement rocks:
Depth sub-bottom (mbsf): 1621.5
Nature: basalt, massive units and sheeted dikes
Measured velocity (km/s): 6.1

Principal results: *JOIDES Resolution* arrived at Hole 504B for Leg 137 on 7 April 1991 with 3 weeks allocated to reconditioning the deepest hole ever drilled into oceanic crust in preparation for future deepening.

Temperature Data and Water Samples from the Undisturbed Borehole. Before engineering operations were begun, temperatures in the undisturbed hole were logged, and 36 hr was devoted to sampling borehole fluids. Temperatures in the deeper kilometer of the hole were consistent with values logged during Leg 111, with a linear gradient of 61°C/km. This gradient extrapolates to a temperature of 165°C at the bottom of the hole at 1562 mbsf. In the upper 350 m of the hole, temperatures were considerably depressed, suggesting an unexpected renewal of the downhole flow of ocean bottom water into the upper levels of basement. Such downhole flow was fairly vigorous when the hole was first drilled during Legs 69 and 70 in 1979, but had decayed to less than 1% of the original rate when Leg 111 revisited the hole in 1986. The Leg 137 temperatures are similar to those measured during Leg 83 in 1981, suggesting that the rate of downhole flow has increased since 1986. This is a surprising result that raises many intriguing questions about the hydrogeology at the site.

Using tools provided by Los Alamos and Lawrence Berkeley National Laboratories, eight fluid samples were obtained from the hole, at depths ranging from 350 to 1540 mbsf. Initial chemical analyses indicate that seven of these samples contain borehole fluid with characteristics in agreement with past sampling studies of the hole. Some contamination of the samples appears to have occurred, either by entrainment of fluids during the trip down prior to sampling or as a result of leakage during the ascent as the hot sampled fluids cooled and contracted. The fluid chemistry indicates bottom water present down to at least 350 mbsf, corroborating the inference of downhole flow from the temperature log. An interesting note: during subsequent engineering operations at the bottom of the hole, many small pieces of platy anhydrite were recovered, consistent with predictions that anhydrite should reach saturation in the borehole fluids near 150°C and 1500 mbsf.

Primary Objective: Clean-out Operations. The primary purpose of Leg 137 was to salvage Hole 504B, perhaps the most important reference hole for the structure of the oceanic crust. In 1986, a diamond coring assembly broke off near the end of Leg 111, which was left with insufficient time to recover all the lost hardware. Leg 111 had to abandon the large diamond bit and assorted hardware at the bottom of the hole. There were also suggestions of possible problems with the casing, but these did not materialize during Leg 137. A further worry was the possibility that wall rocks might have caved in on top of the junk since Leg 111, but we were able to run straight to the junk from virtually the beginning of engineering operations. Starting on 11 April, we ran one fishing attempt with a junk basket and five mills with boot baskets to capture pieces of broken-up metal. These returned with parts or whole pieces of all the lost hardware, including recognizable pieces of the diamond bit. Thus, during only 6 days of remedial operations, the application of straightforward fishing and milling techniques succeeded in breaking up the diamond bit and in cleaning out the hole.

Coring Tests. After successfully achieving its most important priority, cleaning the lost diamond bit from the bottom of Hole 504B, Leg 137 proceeded with another important priority: to test coring systems and assess the feasibility of coring ahead during a full scientific leg to the hole. Once the hole was verified to be clean of all remnants of junk, two coring systems were tested: the standard ODP RCB wireline coring system and a conventional oilfield diamond core barrel. These tests yielded mixed results, and unfortunately ended with a frustrating loss of very fishable coring equipment in the hole.

Two runs with the RCB system in a clean hole yielded penetration rates of 1–2 m/hr and average recovery of 14%. This is comparable to results with the same system during Legs 83 and 111. The cutting inserts of the bits failed quickly in a manner that suggested that the formation is extremely hard and abrasive and that a more appropriate grade of bit could make more hole. But, while rotary core and drill bits could be used to advance the hole at a reasonable rate, it is clear that the RCB system cannot be expected to yield core recovery any better than 20% in this lithology and environment.

The diamond core barrel also yielded mixed results, with extremely slow penetration but very good recovery. Two runs resulted in a recorded advance of only 3.1 m (which could be in error because of the effects of tides) and a calculated recovery of 79%. The first diamond bit was extremely worn after less than 2 m of penetration, indicating that the bit matrix material was too soft for the hard, abrasive formation. The second diamond bit behaved in a similar manner downhole, but was not recovered, because all 18 m of outer core barrel broke off in the hole, with the bit at the bottom.

Such a long, narrow piece is normally the easiest kind of junk to fish from a hole with the appropriate tools, and in fact the first fishing overshot apparently did engage and lift it some distance up the hole. However, the fishing overshot itself broke off, leaving a compound fish that remains eminently fishable with the appropriate fishing tools. Unfortunately, the proper tools were not on board, although a second fishing attempt was made with a modified taper tap. When this failed, the decision was made not to risk damage to the fish by attempting to retrieve it with a "rig-engineered" solution, but instead to leave the fish in its easily

[1] Becker, K., Foss, G., et al., 1992. *Proc. ODP, Init. Repts.,* 137: College Station, TX (Ocean Drilling Program).

[2] Shipboard Scientific Party is as given in the list of participants preceding the contents.

retrievable condition, in a position to be removed with proper equipment during a future leg.

Coring Results. Drilling on Leg 137 deepened Hole 504B by 59.2 m, to a total depth of 1621.5 mbsf or 1347 m into basement. Of this interval, 48.6 m was cored, with a recovery of 8.77 m. The recovered rocks are all interpreted as a continuation of the sheeted dike complex, although no intrusive dike margins were actually recovered. The physical properties of recovered core support the inference that the formation is very hard and dense massive basalt, and therefore difficult to core. Chlorite and actinolite veins and actinolite-bearing alteration halos are common in the diamond cores with good recovery. It would therefore appear that the trend of increasing proportion of actinolite in the secondary mineral assemblage recognized on Leg 111 continues with depth.

Final Logging. Attempts to fish the lost outer core barrel left time for only an abbreviated program of downhole measurements at the end of the leg. The planned open-hole packer inflation was cancelled because it posed the greatest risk of somehow disturbing or compounding the presentation of the fish. A digital BHTV log of the casing was successfully conducted, but the tool failed shortly after logging only 85–90 m of the open-hole section. The complicated flowmeter/injection experiment was an operational success during two packer inflations in casing, but each time was cut short by premature packer deflations. The packer was recovered in good condition (with outer rubber fully intact), so the most plausible explanation for the packer deflations is that the inflation pressure was insufficient to maintain a grip against the smooth casing.

The casing inspection by borehole televiewer disclosed that the casing flaw suspected after Leg 111 is simply a casing expansion joint, but that some casing damage, apparently due to wear, does exist. The most severe degradation is in the lowermost 30–40 m, where the casing appears to have several small holes connected by some sort of vertical split or separation. To date this has not affected operations at the hole, and it does not appear to require casing repair for the single science leg approved for the 1991–1992 schedule.

Conclusions and Recommendations for Future Operations at Hole 504B. Leg 137 achieved its primary objective, cleaning Hole 504B of the serious junk lost at the end of Leg 111. Operations throughout the leg showed no indication of the supposed problems with the casing, although a borehole televiewer inspection during the last day on site showed flaws with the lower 30–40 m of casing. Leg 137 clearly succeeded in demonstrating that Hole 504B can be advanced to the Layer 2/3 transition, the proposed target for a scientific leg later in 1991.

This important success was tarnished by a frustrating inability to retrieve a much less serious piece of junk lost at the end of coring tests. This disappointment can be attributed to a defective fishing tool and a lack of time to procure and deploy any further appropriate tools, not to any difficult presentation of the junk itself. In fact, such tool losses and fishing jobs are not at all unusual in drilling any deep hole, and in this case it is virtually certain that the lost outer core barrel could readily be fished with the proper tool. Furthermore, Hole 504B has a history of being open to total depth on multiple revisits, so the fish can be expected to remain clean and in easily retrievable condition for a reasonable period of time. With appropriate fishing tools, it should pose little risk to a revisit in the near future.

The more serious dilemma facing future legs to Hole 504B is the inability of both the RCB and diamond coring systems to simultaneously cut core and make hole in this lithology. The RCB system can make hole with recovery on the order of 15%, whereas the diamond core barrel gives excellent recovery with very slow progress. Even with improved bit designs for these coring systems, trade-offs will have to be made between penetration and recovery. While Leg 137 has shown that the key scientific priorities for deepening and logging Hole 504B to the Layer 2/3 and/or dike/gabbro transition(s) can be achieved on a later leg, these objectives may require compromise strategies for drilling, coring, and logging.

BACKGROUND AND OBJECTIVES

Introduction

The principal objective of Leg 137 of the Ocean Drilling Program (ODP) was to revisit Hole 504B in the eastern equatorial Pacific (Fig. 1) to recondition the hole for future ODP operations. Hole 504B is by far the deepest penetration into the oceanic crust and perhaps our most important *in-situ* reference section for the structure of the upper oceanic crust (Fig. 2). However, its status had been jeopardized when a coring assembly was lost at the bottom of the hole near the end of Leg 111. Therefore, the highest priorities for Leg 137 involved engineering operations, including remedial measures to clean this junk from the hole and tests to prove the feasibility of continued coring on a subsequent expedition. If these objectives were successfully achieved during Leg 137, Leg 140 was committed to returning to the hole for a full scientific leg of coring and downhole measurements.

Leg 137 was the sixth expedition of the Deep Sea Drilling Project (DSDP) or ODP to occupy Hole 504B. The hole was originally spudded during Leg 69 in 274.5 m of sediments overlying 5.9-m.y.-old crust formed at the Costa Rica Rift, and was then deepened and/or logged during parts of four other DSDP/ODP legs, 70, 83, 92, and 111. These legs provided a wealth of scientific results, much of which are summarized by CRRUST (1982), Cann, Langseth, Honnorez, Von Herzen, White, et al. (1983), Anderson, Honnorez, et al. (1982, 1985), Leinen, Rea, et al. (1986), and Becker, Sakai, et al. (1988, 1989a, 1989b).

Although previous coring, logging, and geophysical programs at Hole 504B achieved unprecedented scientific success, the operational history of the hole was marred by repeated downhole hardware losses and by disappointing rates of core recovery (Fig. 3). These tendencies have become more pronounced with the depth of the hole and were a particular problem during Leg 111, which experienced four significant losses of hardware in the hole, a rash of premature bit failures, and an overall core recovery rate of less than 13%. During Leg 111, remedial work was successful in cleaning the hole on three occasions; however, when a diamond coring assembly was lost near the end of the leg, a lack of time and proper equipment forced temporary abandonment of the hole before the lost junk could be removed.

During its scheduled 22 days of operations at Hole 504B, Leg 137 was to focus upon removal of the existing junk, assessment of the condition of the hole and its casing and reentry cone, and development of more efficient coring and drilling techniques for the projected deepening of the hole on Leg 140. Additional objectives involved high-priority downhole measurements that could not be deferred to Leg 140, including temperature logging, borehole fluid sampling, and permeability measurements. Further logging was scheduled on the basis of time availability and as the primary contingency for the leg, in the event that the hole proved to be unsalvageable for future drilling.

Past Operational Difficulties in Hole 504B

Continued drilling in Hole 504B posed major technological challenges for ODP if the scientific successes already achieved at the site were to be continued. Prior to Leg 137, the basement section had been cored exclusively with the standard DSDP/ODP rotary core barrel system (RCB), but serious drilling problems had been encountered deep in the hole during Legs 83 and 111 (Fig. 3). Those problems included recurrent hardware losses as well as poor coring performance and bit life even after junk had been cleaned from the hole. Also, fishing operations at the end of Leg 111 hinted at the possibility of problems with the 276 m of casing that extends through the sediments. Those three aspects of drilling and engineering problems required distinctly focused efforts, and attacking those problems dominated the operational plan and decision-making processes of Leg 137.

Hardware Losses

During Leg 83, the drill pipe parted twice, each time leaving the bottom-hole assembly (BHA) in the hole. In each

Figure 1. Location of Hole 504B south of the Costa Rica Rift in the eastern equatorial Pacific Ocean (from Lonsdale and Klitgord, 1978).

case the lost BHA was successfully fished from the hole in about 3 days of operations, and Leg 83 was quite successful despite those interruptions. During Leg 111, the first two bits actually improved on the Leg 83 drilling performance, possibly because of the superior heave compensation of *JOIDES Resolution.* However, all eight roller cones were lost from the next two consecutive RCB bits, seriously disrupting operations and requiring extensive milling and fishing operations. After this junk was cleaned from the hole, an experimental diamond coring assembly was lost at the then total depth of the hole, 1562.3 mbsf, when the pin end of the bit sub failed due to a metallurgical deficiency (Fig. 4). Four fishing attempts at the end of Leg 111 succeeded in removing some of this assembly, but the diamond bit, float valve, and parts of the support bearing remained at the bottom of the hole. One obvious challenge facing Leg 137 was to clean this junk from the bottom of the hole using standard milling and/or fishing operations. That strategy was considered to be a conservative and straightforward approach to the junk problem, with good chances for success given sufficient time and a good stock of milling and fishing tools.

Possible Casing Problems

During the last two Leg 111 attempts to fish the lost diamond core assembly from the hole, an obstruction was

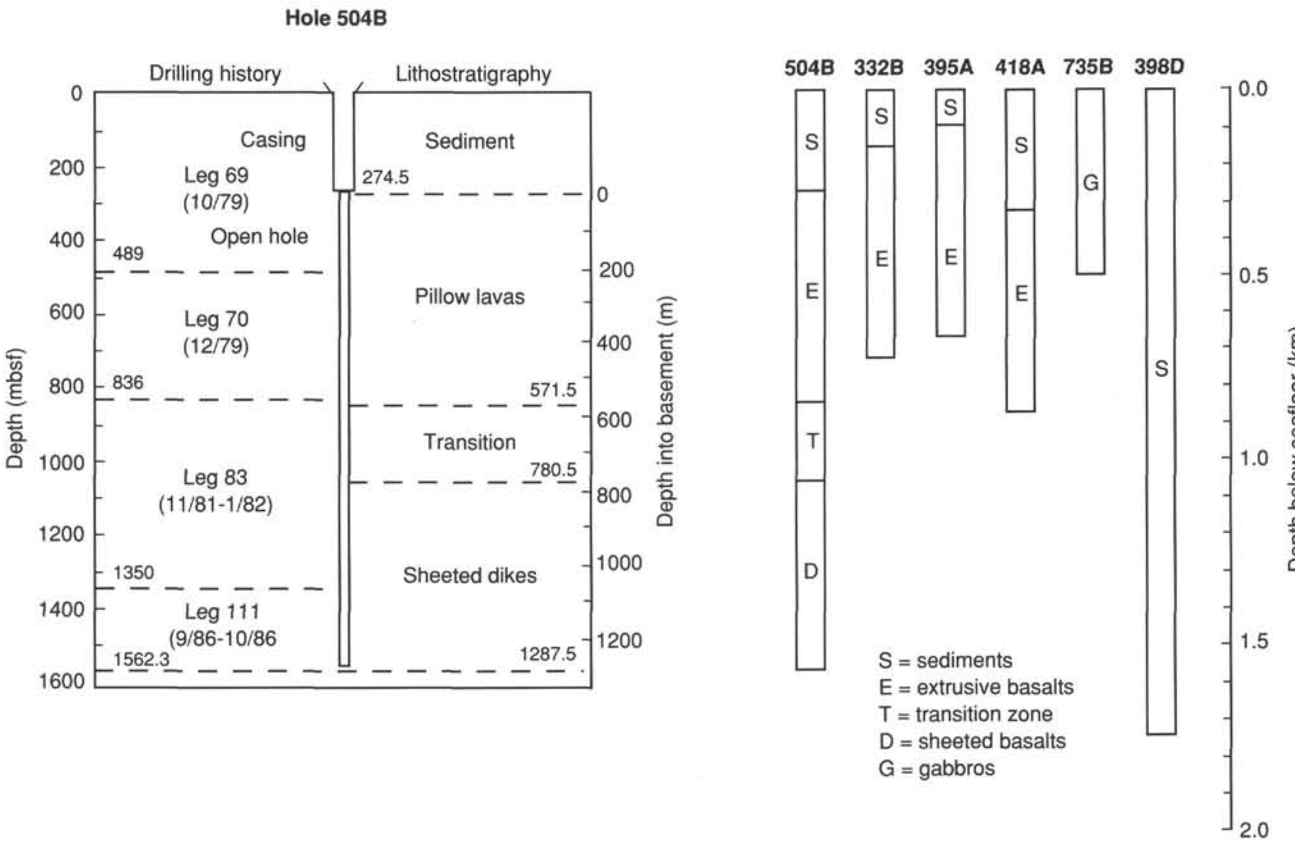

Figure 2. On the left, generalized drilling history and lithostratigraphy of Hole 504B prior to Leg 137. On the right, a comparison of this lithostratigraphy with (1) that encountered in the four other DSDP/ODP holes that penetrate at least 500 m into "normal" oceanic crust formed at a mid-ocean ridge, and (2) the deepest DSDP/ODP hole to date into any lithology, Hole 398D near the Galicia Bank.

encountered by the fishing overshot as it was lowered through the casing. It appeared quite likely that the obstruction was caused by an expansion joint in the casing within a few meters of the apparent drill-string depth to the obstruction. Such an expansion joint presents a slight internal shoulder that could have caught the square profile of the fishing overshot but would not have impeded a normal BHA terminated with a bit. However, it was also considered possible that the obstruction was caused by a flaw or hole in the casing that might have developed during Leg 111. Moreover, the reentry cone and casing had not been designed for such deep penetration and have been subjected to many more reentries and hours of pipe rotation than had been anticipated when the hole was originally spudded. Therefore, the casing required thorough inspection during Leg 137 prior to the projected deepening of Hole 504B during Leg 140. Possible remedial actions included minor casing repair during Leg 137 or the installation of a protective liner at the beginning of Leg 140.

Poor Drilling Performance

Perhaps the most challenging issue facing Leg 137 was improvement of the relatively poor drilling performance experienced deep in Hole 504B to demonstrate the feasibility of coring success during Leg 140. Past drilling problems in Hole 504B involved several unacceptable symptoms, including poor core recovery deep in the hole as well as several sudden failures of the drilling equipment. That poor performance may have resulted from a combination of several factors, including:

1. The recurring losses of steel junk in the hole during Legs 83 and 111, including parts of logging tools, bits, and coring assemblies;
2. Hole instabilities, probably caused by stress release in the formation, resulting in spalling of wall rocks into the hole and undue wear on the coring assemblies; and
3. Jammed and poorly recovered cores due to intense fracturing, probably also a result of stress-release phenomena but possibly related to lithology.

The extent of the contribution of junk in the hole to the catastrophic bit failures during Leg 111 could not be determined. Nevertheless, a successful solution to the junk problem during Leg 137 promised only to restore drilling performance comparable to that achieved by the first two bits employed during Leg 111 (15%–20% core recovery, 3 m/hr penetration) if standard RCB techniques were used. Leg 137 therefore was equipped to test another coring system (an oil-field diamond core barrel described below) that held promise for improved performance.

The effect of formation stress release and hole instabilities on past drilling experience is difficult to quantify. Ultrasonic borehole televiewer logs indicate numerous breakouts throughout the dike section, consistently oriented such that plate stresses were being relieved as or shortly after the hole was drilled (Newmark et al., 1985a; Morin et al., 1990; Moos and Zoback, 1990). The stress relief evidenced by these breakouts may have been aggravated by the thermal contrast between the cool circulating fluids and the hot formation. The bottom-hole temperature at the Leg 111 total depth is about

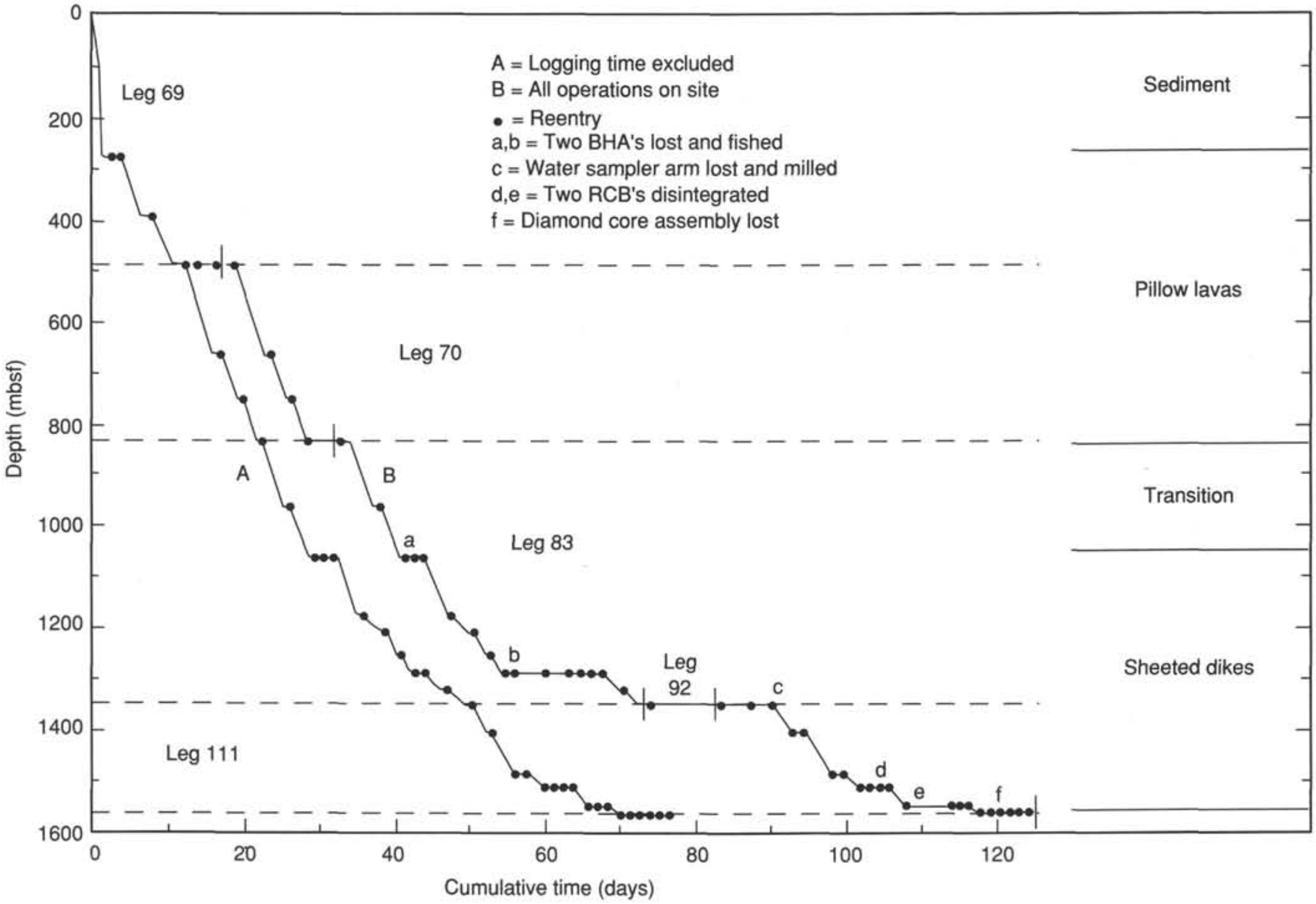

Figure 3. Detailed drilling history of Hole 504B prior to Leg 137.

165°C, and the thermal contrast between formation and circulating fluids can only increase as the hole is drilled deeper. Morin et al. (1990) suggested that the discontinuous nature of circulation and resultant cycling in borehole fluid temperatures may have been a key factor in inducing stress-release failure and attendant drilling difficulties. Therefore, vigorous and discontinuous circulation was to be minimized whenever possible during Leg 137, particularly when the drill string was not rotating.

Downhole Measurements Prior to Drilling Operations

In accordance with recommendations from JOIDES panels, an abbreviated suite of downhole measurements was to be conducted when Hole 504B was first reentered. A later phase also was planned toward the end of Leg 137 that could be expanded to utilize contingency time arising from drilling operations that were either very successful or very unsuccessful.

Two days were planned for temperature logging and borehole fluid sampling before any clean-out operations could disrupt the equilibrium of the borehole fluids necessary for these measurements. The hole had remained undisturbed for nearly 4-1/2 years since Leg 111, which provided excellent conditions for conducting an equilibrium temperature log and for sampling borehole fluids with the aim of deducing the composition of formation fluids. First, the temperature log was to be conducted with the French high-temperature tool that had been used successfully during Leg 111 (Gable et al., 1989). Next, about 1-1/2 days was to be devoted to sampling borehole fluids using high-temperature samplers from Los Alamos National Laboratory and Lawrence Berkeley Laboratory. The sampling program would also provide a moderately high-temperature test of these samplers prior to their possible use at even higher temperatures later during the Pacific drilling schedule.

Remedial and Drilling Operations

The operational plan for Hole 504B was structured with sufficient flexibility so that a variety of tools and techniques could be brought to bear on technical problems as the hole-salvage operation progressed. The overriding priority was to ensure that the hole would be available for future reentry, either from a drill ship or by wireline from a conventional oceanographic vessel.

Casing Assessment

By far the least likely and potentially most disappointing of the possible scenarios for Leg 137 would have involved serious casing failure or hole collapse to the extent that Hole 504B would not have been reenterable to total depth. If that were the case, it would probably have become apparent during the downhole measurements scheduled before the clean-out operations. The operating plan would have been altered at that point to concentrate efforts on opening the hole, delaying the fishing/milling work. Inability to reach total depth because of a serious casing problem would have necessitated termination of operations in Hole 504B without attempting to clean the junk from the bottom of the hole, tantamount to permanently abandoning the hole.

Given the more likely scenario that no fatal problems would be encountered during the downhole measurements,

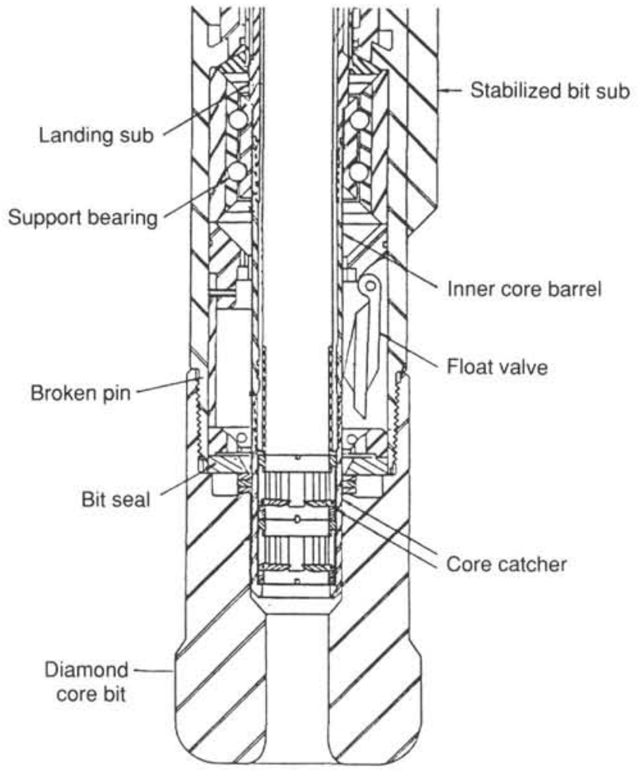

Figure 4. Schematic of the diamond coring assembly lost in Hole 504B at the end of Leg 111. The pin thread of the stabilized bit subassembly broke, leaving the inner core barrel, support bearing, float valve, and diamond core bit in the hole. The core barrel and outer race of the support bearing were recovered before Leg 111 ended.

the 11-3/4-in. surface casing in Hole 504B was to be carefully inspected to determine whether excessive wear or corrosion had occurred since the casing was set in 1979. If the casing proved troublesome during the initial phase of downhole measurements, this inspection was to be run immediately after the fluid sampling; otherwise, it was to be deferred to the phase of downhole measurements scheduled after the clean-out and coring tests.

The casing inspection was planned to be conducted with a digital borehole televiewer (BHTV), or the Schlumberger formation microscanner (FMS) if the BHTV were unavailable. The BHTV or FMS log was to be extended to the upper section of open hole, which was suspected to be the least stable section, possibly to the point of requiring the installation of a liner casing prior to future deepening of the hole. If the inspection revealed casing problems, minor repairs could probably have been accomplished during Leg 137, but major repairs or installation of a liner would have been deferred to Leg 140.

Hole 504B Clean-out

Upon completion of the initial suite of wireline investigations, the drill string was to be tripped to recover the logging BHA and to begin cleaning the junk from Hole 504B. Fishing tools were available, but the odds of removing all the junk by fishing were judged to be low, considering the nearly equidimensional profiles of the individual items and the possibility that they might have been covered with even a little rubble from higher in the hole. The primary approach planned to clean out the hole was reduction of the junk by means of tungsten carbide junk mills. The small bits of metal produced by the milling operations would be flushed from the hole by fluid circulation and some would be trapped in the pockets of "boot baskets" located in the BHA immediately above the mill.

As the logging and sampling operations described above would entail no circulation, the first "junk run" would initiate circulation in the hot, deeper section. To minimize the risk of additional damage to the hole through thermal shock, pump circulation was to be applied very gradually to the levels required for the initial milling or fishing operations.

Several round trips and reentries requiring several days were anticipated for the cleaning-out operations. Sufficient time was allocated for replacement of worn mills, emptying of junk baskets, and experimentation with alternative techniques of breaking up the junk, fishing, spotting cement to immobilize loose junk, etc.

Drilling and Coring Tests

After the completion of clean-out operations in Hole 504B, most of the remaining time on site (except for about 2 days reserved for permeability measurements and possible additional logging) was to be devoted to deepening the hole by coring and drilling. When milling parameters and recovered junk fragments indicated that the hole was clean, several meters of new hole were to be made with a rugged hard-formation drill bit (without coring). If drilling parameters with this bit verified that the hole had been successfully cleaned, RCB coring was to be attempted to confirm the feasibility of continued coring in Hole 504B.

Although the standard RCB system had yielded poor and declining recovery with depth during earlier coring operations in Hole 504B, RCB coring in the newly cleaned hole would provide a "control" basis against which to compare subsequent tests of alternative rotary coring systems. Of several possible alternatives, Leg 137 was equipped to test a conventional oilfield diamond core barrel (a different system than the small-diameter wireline diamond coring system under development at ODP). The conventional diamond coring system is known for excellent core recovery and quality, with cores of up to 100 mm in diameter and 18 m in length, although it requires a time-consuming round trip of the drill string to recover each core. This approach was considered to be a viable alternative for Hole 504B given that the last three RCB bit runs during Leg 111 averaged only 25 m penetration before bit distress dictated tripping the drill string. In addition, drilling with the conventional diamond core barrel requires lower circulation rates for effective coring and hole-cleaning than the RCB system, and it was hoped that the lower flow rates would alleviate fracturing and spalling problems initiated by thermal shock to the borehole wall and core.

Permeability Measurements and Additional Logging

About 2 days of the time available after cleaning the hole was to be devoted to permeability measurements and possible additional logging. A drill-string packer was to be inflated in the upper part of the hole to better document the rapid decrease of permeability with depth in that section, using conventional formation tests as well as a new flowmeter injection experiment (Morin et al., 1988). As discussed above, if there were no indications of possible casing problems, the digital BHTV log of casing and upper basement was to be deferred to this time. If all coring and permeability objectives had been met or if further coring operations were not deemed worthwhile, some time was to be devoted to logging the hole with the formation microscanner (FMS) and other tools that had not been run in the hole during previous legs. Such

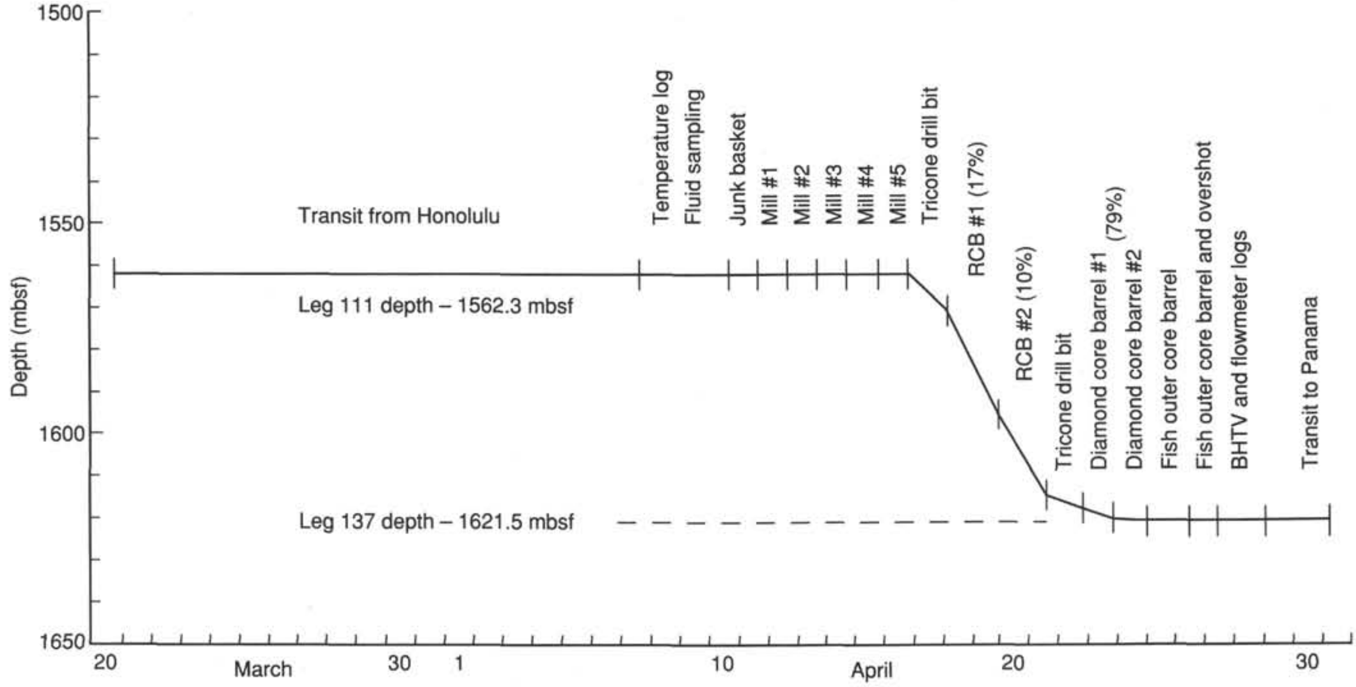

Figure 5. Summary of the sequence of operations conducted during Leg 137.

additional logging was the primary contingency for the site, should any time become available.

OPERATIONS

Introduction

Leg 137 spent about 21½ days at Site 504 and accomplished its primary objectives during this time. Figure 5 summarizes the sequence of operations conducted during Leg 137. Most important, the junk shown in Figure 4 was destroyed in good time, and Hole 504B was successfully reconditioned for future drilling. In addition, the initial downhole measurements were successfully conducted. The tests of coring equipment described in the "Background and Objectives" section (this chapter) were completed with mixed results and a frustrating loss of very fishable coring equipment near the end of the leg. Two fishing attempts with available tools did not succeed in retrieving this equipment, although it was left in condition to be readily fished with proper tools on a later leg.

The vessel departed 20 March 1991 after a very brief (6½ hr) port call in Honolulu, and began with a long transit to Site 504. Opposing trade winds and the North Equatorial Current limited the transit speed during the first 9 days, and the entire transit of 4533 nmi required nearly 18 days at an average speed of 10.7 kt. Time on site officially commenced when the positioning beacon was launched at 1315 hr, 7 April 1991.

Initial Downhole Measurements

A routine reentry was made with an abbreviated logging BHA consisting of seven drill collars terminated by a 9-in. reentry/cleanout bit. The end of the drill string was run to 3642 mbrf, about 5 m past the depth of the obstruction or shoulder that had been encountered by the fishing overshot run twice at the end of Leg 111. No obstruction was encountered and nothing was "felt" on the rig weight gauges, indicating that the casing was in reasonable condition and that speculation about serious casing damage was probably unfounded.

The French temperature logging tool was then run to seafloor depth on a 345-m section of high-temperature cable attached to the main logging cable. However, electrical problems were encountered in the cablehead "pigtail" and the high-temperature section of cable, resulting in a misrun and a delay of about 4 hr. While electrical troubleshooting was in progress, water samples were successfully collected with the Los Alamos National Laboratory (LANL) sampler (deployed on the coring wireline) from depths of 350 and 550 mbsf.

The logging cable problems were solved after the high-temperature section was removed, and the temperature log proceeded without further difficulty using the main logging cable. Temperatures were logged down from seafloor to a depth of 1545 mbsf as determined by the winch depth counter. The measured temperature at that depth (about 17 m above the total depth determined by the Leg 111 pipe length) was 164.6°C, which extrapolates to a bottom-hole temperature of 165°C.

Upon completion of the temperature log, the water-sampling program resumed. The solenoid-operated Lawrence Berkeley Laboratory (LBL) sampler had to be run on the electric logging cable and was alternated with the LANL (Leutert) sampler, which was deployed on the coring wireline. Samples were collected from wireline depths of 800, 950, 1100, 1250, 1400, 1500, and 1519 mbsf. All attempts were successful except those from 1100 and 1250 mbsf, in which the samples were lost or completely contaminated when the valve of the LANL instrument was prevented from closing by detritus (pipe rust?). Recovery of the final water sample concluded the initial phase of downhole measurements at 0300 hr on 10 April.

Remedial/Cleanout Operations

The reentry/cleanout bit was then run into the hole until resistance was met at about 5015 mbrf by drill string measurement. The top drive was picked up and circulation was slowly increased to avoid thermal shock to the hole. The hole fill yielded to circulation and rotation, and the hole was cleaned to 5031 mbrf before progress was halted by solid resistance. This depth was about 5 m short of the expected junk depth based on the Leg 111 drill string measurement. No serious attempt was made to clean the hole deeper because the BHA was not suitable. At that point, the hole was flushed with high-viscosity drilling mud, and the drill string was tripped.

Upon recovery, the reentry/cleanout bit showed fairly clear indications of contact with junk in the hole. It was therefore concluded that there was a discrepancy between the current drill pipe depth and that of Leg 111 and that the junk would be accessible to a fishing junk basket. A BHA featuring the Bowen full-flow reverse-circulating junk basket was assembled and the drill string was tripped. After reentry, the junk basket was lowered to 4800 mbrf (1325 mbsf), with pump circulation the remainder of the way to the fish to cool the hole gradually. Reverse circulation was established by pumping a steel ball into place, and the junk basket was "worked" on the fish for about 30 min. When it was brought to the surface, the basket contained the inner race of the lower support bearing and a considerable quantity of basalt cobbles and pebbles.

The second remedial run used a 9-5/8-in. ribbed "piranha" style junk mill in an attempt to machine the metal junk into flakes and cuttings that could be flushed from the hole with fluid circulation. Two "boot baskets" were located just above the mill to trap samples of the metal cuttings and also larger pieces of junk that were lifted into the annulus by circulation. The mill was rotated on the junk for 3 hr. When it was recovered, the boot baskets contained 40 of the 42 steel ball bearings from the lost lower support bearing as well as fragments representing about 10% of the float valve assembly.

A 9-5/8-in. concave junk mill was then deployed. Only 2-3/4 hr was spent in milling, as the mill tended either to spin free without "biting" or "to torque up" and stall the top drive with the application of any weight. Upon recovery, the mill was found to be severely worn and reduced in diameter around its leading edge, indicating that either junk was lodged in the side of the hole or the hole was undergauge. The contents of the boot baskets were somewhat disappointing in that the amount of metal was small and the few recognizable fragments were from the upper portion of the float valve assembly.

The mill was replaced with an identical concave junk mill for the fourth run. On the basis of the results of the previous run, more weight and higher rpm were used and the mill was "spudded" occasionally. Over 5 hr was spent on the fish before parameters indicated that the mill was probably worn out. The boot baskets produced a good assortment of metal fragments. Some were quite large and easily recognizable, while a considerable collection of thin flakes and shavings gave evidence of effective milling. Particularly significant were pieces of the float valve flapper (which had been expected to cause problems) and the 41st ball bearing, but the most exciting find was several pieces of matrix material from the diamond core bit. This indicated that the final and largest part of the fish was beginning to break up.

The fifth run was with a 9-3/8-in. ribbed or "castle" junk mill. Attempts to mill met with little success for the first 3 hr, as severe torquing and sticking occurred whenever the mill was lowered into contact with the fish. With a reduction in circulation and rotary speed, more normal parameters were achieved for milling. After an additional 4 hr, a drop in torque indicated that the mill probably was worn down. The junk mill was recovered in a completely worn-out condition. The contents of the boot baskets were again encouraging, with a reduced amount of metal and smaller pieces than on previous runs. Matrix material from the diamond bit was again recovered, but in smaller chunks.

The final mill run used a concave mill that had been redressed to full 9-7/8-in. diameter. After about 1 hr of fairly rough running, the milling parameters smoothed out with enough torque to indicate that progress was being made. The torque soon dropped further and indicated that the mill had worn down or that it was turning on solid rock at the bottom of the hole. The pipe was tripped after only 2-3/4 hr of milling. The mill was found to be worn smooth when recovered, but the lack of grooves or other junk marks on the steel surface of the mill's base was interpreted as a positive sign. The baskets yielded, in addition to the usual copious load of gravel-to-cobble-sized basalt, some disconcertingly large, flat steel pieces. However, the total load was again rather small, with very few mid-sized pieces and a fairly large proportion of fine and very fine shavings.

With the hole judged to be essentially clean, a hard-formation tricone Smith F7 bit was selected to drill ahead and prove that Hole 504B had been salvaged. As drilling commenced, some minor roughness was noted, but it was more typical of rocks than of junk. Weight was applied cautiously, but all parameters indicated normal hard-rock drilling in new hole. The hole was deepened to 5045 mbrf (1570 mbsf) and was swept with drilling mud. All indications were that Hole 504B had been cleaned adequately for coring operations, and the drill string was tripped. The bit was found to be in excellent condition when it was recovered, but there were a few large pieces of steel junk (showing drilling marks) in the boot baskets. The condition of the bit and review of drilling parameters led to the conclusion that the junk had been collected early in the bit run and that little or none remained in the hole. Accordingly, the decision was made to install a coring BHA, after not quite 1 week of remedial operations.

Coring Operations

The coring plan included a run with the conventional ODP wireline rotary coring (RCB) system before moving on to experiments with a standard oilfield-type diamond coring system. (The tungsten carbide roller-cone bits used with the RCB system are much less sensitive to the presence of junk in the hole than are the diamond coreheads of the oilfield system.) Coring results for Leg 137 are summarized in Table 1.

The RCB core bit chosen was a Rock Bit Industries model C-7, which features short conical cutting inserts and is designed for hard-formation drilling. When coring was initiated, the bit bounced and "ran rough" for a few minutes, although there was no excessive torque. Drilling then smoothed out for the remainder of the first core interval and the two ensuing cores. The rate of penetration varied between 1.5 and 2.0 m/hr, which was consistent with coring in Hole 504B during earlier legs. Core recovery ranged between 5% and 25%, which, unfortunately, also was consistent with past experi-

Table 1. Coring summary, Leg 137.

Core no.	Date (1991)	Time	Depth top bottom (mbsf)	Length cored (m)	Length recovered (m)	Recovery (%)
[a]171M	12	0023	274.5–1562.3	0.0	(3.52)	
[a]172M	18	0800	1562.3–1570.0	0.0	(0.65)	
173R	19	0430	1570.0–1576.3	6.3	1.65	26.2
174R	19	1215	1576.3–1585.8	9.5	2.13	22.4
175R	19	1945	1585.8–1595.3	9.5	0.44	4.6
176R	20	2015	1595.3–1604.5	9.2	1.15	12.5
177R	21	0245	1604.5–1613.8	9.3	0.78	8.4
178R	21	1100	1613.8–1615.5	1.7	0.17	10.0
[a]179M	22	2330	1615.5–1618.4	0.0	(0.57)	
[b]180M	24	0430	1618.4–1620.4	2.0	1.10	55.0
[b]181M	25	0630	1620.4–1621.5	1.1	1.35	123.0
			Coring totals	48.6	8.77	

[a]Drilled interval.
[b]4-in. diamond bit core.

ence. In consideration of the Leg 111 history of short bit life and the possibility that some junk remained in the hole, the bit was tripped after only 15-1/4 rotating hours, three cores, and 25.3 m penetration.

Upon recovery of the BHA, the bit was found to have surprisingly numerous broken inserts on three of the four roller cones. The bearings and seals were in good condition, and there were no junk marks or excessive wear on the bit body. As cutting-structure damage in hard-formation bits is virtually unknown in normal coring operations, it was suspected that some junk had remained in the hole, at least when coring had begun. The pockets of the boot basket/bit sub contained only a handful of thin flakes of steel in addition to the usual basalt pebbles and cuttings. There was no sign of anything that could damage a rugged C-7 bit.

Due to the possibility that steel junk still existed in the hole, the deployment of the oilfield coring system with its vulnerable and expensive diamond bit was postponed. A C-7 bit identical to the previous one was made up to the same BHA and sent back to the bottom of the hole. Two full cores were cut with all parameters essentially the same as with the previous bit; total core recovery was 1.9 m for 18.5 m cored. The rate of penetration fell to essentially zero after 1.7 m of the third core had been penetrated, so coring was terminated, the core was recovered, and the drill string was tripped. Although it had been used for only 11-1/2 rotating hours, the core bit was found have the drive rows totally destroyed on all cones—a more serious failure than on the previous bit. The pattern of failure was identical, however, and indicated bit failure as a result of interaction with very hard formation, not junk.

As there were again no junk marks on the bit and the boot basket contained only a handful of small junk flakes and tungsten carbide fragments from the bit, the presence of harmful steel junk remaining in the hole was all but ruled out. Conditions were considered acceptable to maintain the schedule and initiate the next phase—tests of conventional diamond coring. The 60-foot Eastman Christensen 250P core barrel assembly was picked up and predeployment checks began. It then was discovered that the required spacing between the lengths of the inner tube and outer barrel assemblies could not be achieved without a time-consuming modification of coring parts.

While these modifications were made, a quick "cleanup" run was made with a 9-7/8-in. tricone drill bit and boot baskets to crush and/or recover any tungsten carbide inserts remaining in the hole. The bit was rotated on bottom for 2-1/4 hr with essentially the same drilling parameters as had been used with the two previous core bits. Penetration was only 2.9 m, confirming the low drillability of the basalt with the available bits. Upon recovery, the bit was found to be in essentially new condition with absolutely no cutting-structure damage after a total of 11 rotating hours. The boot basket contained only a handful of steel and mill-matrix flakes, with no tungsten carbide fragments. All indications were that the hole was clean for diamond coring.

The spacing problem in the oilfield core barrel had been remedied, so the assembly was again made up and a 7-7/8-in. Hobic core bit was attached. Diamond coring began with very light weight and low rpm after the specified circulating rate had been established. The weight and rpm were increased slowly over the next 2 hr. During that period, the rate of penetration was extremely low, but about 2 m of apparent penetration was made. No further progress was made during the next 4-1/2 hr, despite gradual increases in weight and rpm. Circulating pressure had increased to a value that indicated bit failure, so the first diamond bit run was terminated after a disappointing 6-1/2 rotating hours and 2 m of (tide-assisted) penetration.

When the bit was recovered, the diamond-bearing matrix on the cutting surface was found to be severely worn, with the watercourses completely worn away to smooth steel on the lower shoulder of the bit. The core barrel contained 1.1 m of 4-in.-diameter core. The core was broken, but fractures appeared to be less numerous than in the earlier RCB cores. A few individual pieces about 10 cm in length were recovered.

The second diamond coring run with a 7-7/8-in. Christensen mining bit was similar to the first in most respects until near its end. Higher rotating speed and a slightly higher circulating rate were used on the advice of the bit manufacturer. About 1 m was penetrated within the first 30–40 min, but the rate of penetration dropped sharply after that. After 3-1/2 hr, the circulating pressure began to rise gradually, progressive bit failure was inferred, and preparations were made to trip the core barrel from the hole. A sudden drop in circulating pressure prior to the trip was difficult to interpret at the time, but was explained when the BHA was recovered missing the outer core barrel and bit. The inner tube assembly was intact, and 1.4 m of core was recovered, but the outer barrel had parted at the connection below the upper stabilizer, leaving the 60-ft outer barrel assembly and bit in the hole.

Remedial/Cleanout Operations, Second Phase

An overshot was dressed with a 6-3/4-in. basket grapple and mill control packer for an attempt to fish the outer barrel assembly, which was viewed as a fairly routine fishing operation. When the overshot had been run to the bottom of the hole, the top of the fish was contacted within 1 m of the anticipated depth. Only light weight and torque were applied to avoid damage to the grapple or fish. As the drill string was raised, some drag was noted and interpreted to indicate that the core bit was being pulled from the 7-7/8-in. hole. As the fish weighed only about 2500 lb, hanging weight could not be used as an indicator that the fish had been engaged. During the long pipe trip out of the hole, the reentry video camera was deployed above the cone. As the BHA was withdrawn from the cone, it could be seen clearly that no fish was attached.

The overshot was immediately lowered back to the fish for a second attempt to engage the core barrel. Contact was made 15 m higher in the hole, suggesting that the fish had been engaged on the first try, raised an unknown distance, and then dropped. The new calculated depth of the core bit corresponded within 2 m to a ledge that had been felt at 5079 m on two previous trips. The overshot was set down on the obstruction repeatedly with rotation, and some drag was noted each time the string was raised. When the BHA cleared the cone, the video again showed no fish present, and the overshot was lowered into the hole for a third fishing attempt.

The lack of success with such a seemingly straightforward fishing job was puzzling. The most plausible explanations seemed to be that the steel of the core barrel was too hard and smooth for the grapple to maintain its grip or that the end of the fish had become belled or otherwise deformed, preventing it from entering the grapple fully. On the third attempt, more rotation was used in an attempt to "dress" the top of the fish with the mill control of the overshot. Also, more weight was applied to force the fish into the grapple or to dislodge the fish and push it back to total depth. Unfortunately, the fish was again absent when the drill string cleared the cone.

The pipe was then tripped to the surface so that the overshot could be examined for signs of engagement with the fish, damage to the lip guide, or other indications. When the BHA arrived at the rig floor, the overshot assembly was missing. The threaded connection between the overshot bowl and top sub appeared simply to have stripped out. Markings on the lower surface of the recovered hardware appeared to have been made by contact with the top of the fish, so it was concluded that the fish had been engaged on the first attempt and then dropped when the overshot separated during the open-hole trip.

With operating time running out, the leg was faced with a fish in the hole that seemed to be easily fishable, but with a lack of suitable tools to recover it. The core barrel should have been accessible from above the overshot, but the only overshot and grapple of the right size were in the hole. The fish also was apparently well centralized and accessible for internal-catch fishing with a taper tap or spear. Unfortunately, because the dimensions of the oilfield core barrel differed from those of standard ODP equipment, no taps or spears of the right size were on board.

Without commercial fishing tools for the smaller fish, the choice was between rig-fabricated tools or modifying a large taper tap for engaging the 8-7/8-in. Bowen thread at the top of the overshot bowl. The maximum catch size of the largest available taper tap was 9 in., and there was a maximum of 4 in. of vertical bore to be engaged in the bowl before the taper tap would bottom out on the outer core barrel. Therefore the taper tap was shortened by all but about 4 in. of wickers, using a cutting torch. To avoid excessive embrittlement of the carburized surface, the tap was allowed to cool in air for about 4 hr before it was made up to the BHA and run into the hole.

The operating plan called for one brief fishing attempt, followed by a round trip/reentry for the logging/packer BHA and downhole measurements for the remainder of operating time. The recognized risk in the fishing operation was that relative motion between the overshot's basket grapple and the core barrel fish was possible with fairly little downward force on the overshot bowl. If such movement had already occurred downhole or if it resulted from contact with the taper tap, engagement of the threaded box would be prevented by contact of the tap with the top of the core barrel. Therefore, it was concluded that the fish would be engaged very quickly or not at all.

When the shortened taper tap was run into the hole, contact was made with a solid obstruction 6.5 m higher than on the previous fishing attempt. After initial "set-down" weight of 12,000–14,000 lb had been applied, light weight was put onto the fish while torque was applied. Considerable resistance was encountered while weight was applied, but very little as soon as the pipe was raised. The torque on the fish (presumably) was verified two or three times, and the string was raised. "Drag" of up to 20,000 lb was seen as the string was raised in the hole, and it appeared that the fish had been engaged.

To the intense disappointment of all concerned, the BHA again cleared the reentry cone with no fish attached. Fishing tools and time for the leg had run out, and the drill string was recovered to deploy a logging/packer BHA. Marks on the taper tap were few and inconclusive, but apparently the core barrel had been contacted before the box of the overshot.

Figure 6 shows a schematic diagram of the fish left in the hole at the end of Leg 137. The fish comprises the 60-ft Christensen outer core barrel and the overshot grapple. The grapple has probably slid down the outer surface of the core barrel some distance. It is impossible to tell for certain the position of the overshot grapple relative to the top of the core barrel, but ribs on the outside of the core barrel restrict the grapple's position to the top 8 m of the core barrel.

Downhole Measurements, Second Phase

The fishing effort left time for only an abbreviated set of the downhole measurements that had been planned for the end of the leg. The planned open-hole inflation of the packer was cancelled, as it posed the greatest risk of somehow disturbing or compounding the presentation of the fish. Lack of time and the presence of the fish at the bottom of the hole also did not allow the flushing of drilling fluids from the borehole and a NaBr-spiking experiment for the sake of future fluid sampling. There was time only for a digital BHTV log to assess the condition of the casing and a flowmeter experiment with the packer inflated in casing.

The BHTV performed well in casing, revealing that the supposed casing flaw suspected after Leg 111 can in fact be attributed to a casing expansion joint, but that there is some casing damage, apparently due to wear. The most severe degradation is in the lowermost 30–40 m, where the casing appears to have several small holes connected by some sort of vertical wear mark with high reflectivity. In some places this wear mark contained a thin vertical line of low reflectivity, which may denote a partial split or separation of the casing, although further analysis of the televiewer data is necessary to verify this.

The BHTV was then lowered to about 200 m below the casing, to the estimated maximum safe operating temperature, for a log of the open hole section. About 100 m was logged with good results, but the tool then failed and was pulled out of the hole.

Just enough operating time remained for a slightly abbreviated flowmeter/packer experiment. Additional drill pipe was picked up to run the packer to 112 mbsf, for inflation in the casing. The flowmeter/sinker-bar/go-devil assembly was run on the logging line to the packer, and the first-ever operation of the flowmeter go-devil proceeded per design. The packer inflated normally with 750 psi and held pressure. Pressure was then raised to 1300 psi to shear the internal pins and free the logging line from the go-devil. When the pressure was bled off, the packer remained seated and holding 12,000–15,000 lb of drill-collar weight. Initial calibrations and pre-circulation readings were taken in preparation for the injection experiment, when the packer then abruptly slid free after being firmly seated for 2 hr. The packer deflation was noted to coincide with an unusually large set of swells, but the cause of the deflation was unknown.

Time allowed a second attempt before operations on site were terminated. The flowmeter and go-devil were retrieved, the go-devil was redressed, and the entire assembly was redeployed to the packer. The second actuation of the go-devil and packer inflation were apparently normal. To avoid accidental deflation, 20,000 lb of collar weight was set down on the packer. The flowmeter was again lowered below the drill string—and after only 10 min the packer gradually slid down the casing and deflated again.

Time did not allow another attempt, and the flowmeter assembly was recovered. The go-devil was found to be packed with fine rust flakes, although it had been clean on the first retrieval. When the BHA was recovered, the packer arrived on deck in apparently good condition. Heavy equipment was then secured for sea and the vessel departed for Panama at 0215 hr on 29 April 1991.

IGNEOUS PETROLOGY AND ALTERATION

Lithostratigraphy

Hole 504B was drilled on previous Legs 69, 70, 83, and 111 to a total depth of 1562.3 mbsf. This includes 274.5 m of

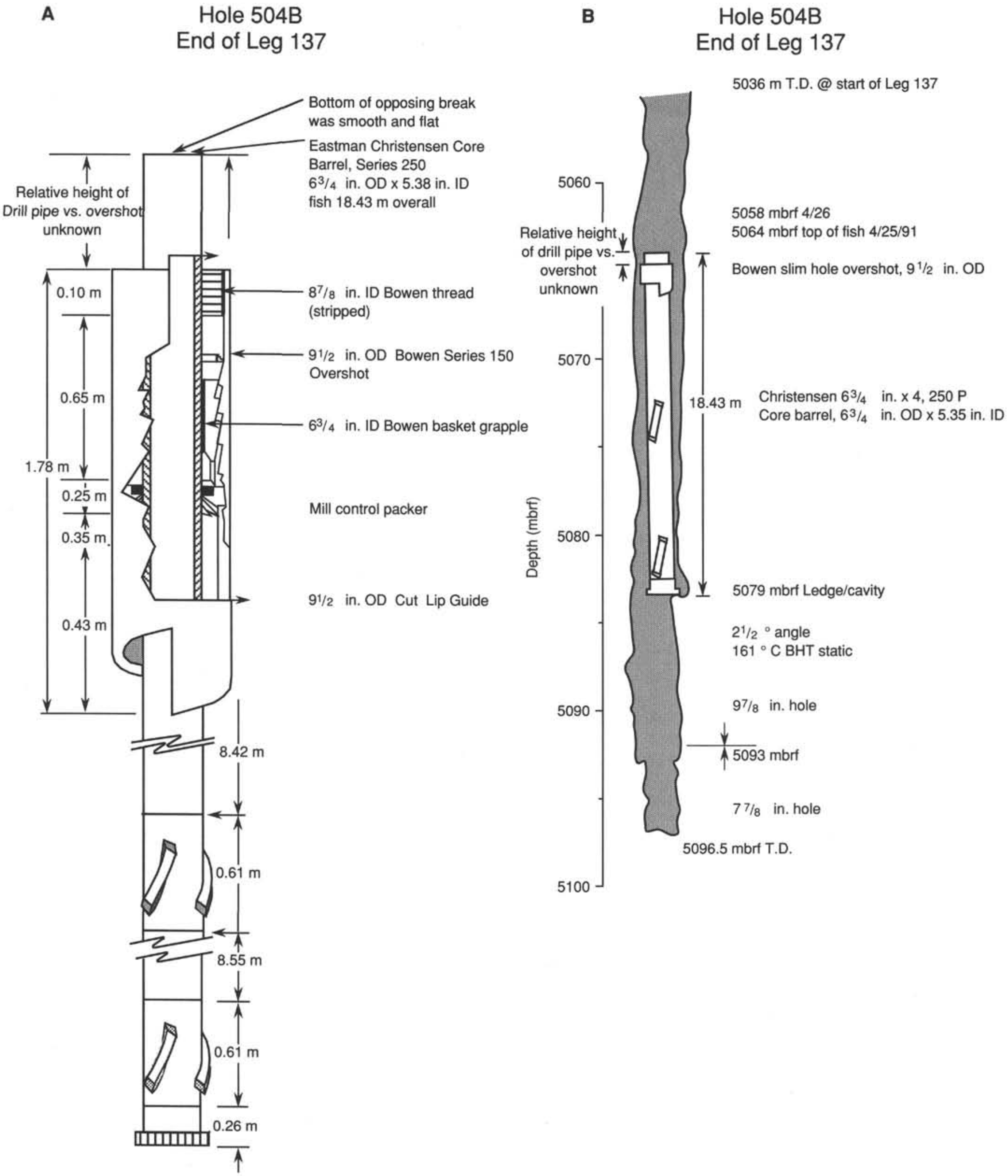

Figure 6. Schematic of tools lost in Hole 504B at end of Leg 137. **A.** Diagram of the Christensen core barrel and Bowen overshot bowl assembly. **B.** Inferred position of the fish in the hole.

sediments and 1287.8 m into oceanic basement. Drilling on Leg 137 penetrated an additional 59.2 m into basement to 1621.5 mbsf, for a total basement penetration at the site of 1347.0 m. Cores 137-504B-180M and -181M are 4-in. diameter cores, 1–2 m long, taken with a diamond core bit, whereas other cores were taken with the standard RCB system. Overall core recovery on Leg 137 averaged 18%, 79% for the diamond bit and 14% for the RCB.

Included in the 59.2 m basement penetration is 7.7 m from 1562.3 to 1570 mbsf (Core 137-504B-172M), and 2.9 m from 1615.5 to 1618.4 mbsf (Core 137-504B-179M), which were drilled without coring. Rocks recovered from the boot baskets on these drill runs were curated and briefly described, but were not examined in detail because the depth of their origin is unknown. Rocks could easily have fallen into the hole as drilling was proceeding and could have been scraped from the sides of the hole as the drill bit was being withdrawn. The depth sequence of the material in these curated sections is purely arbitrary, having no relationship to their stratigraphy in the hole. Material was also recovered in the junk basket run initially (Section 137-504B-171M-1) and in boot baskets on subsequent milling runs (Sections 137-504B-171M-2 through -6). The larger fragments of this material were curated and briefly described, but were not examined in detail for the above reasons.

The lithostratigraphy of the upper 1287.8 m of basement at Site 504 is described in detail by Adamson (1985) and the Leg 111 Shipboard Scientific Party (1988). Basement can be divided into three zones at Site 504 (Fig. 7): an upper 571.5-m volcanic section; a 209-m transition zone consisting of volcanics, dikes, and massive units; and a lower 507.5 m of intrusive dikes and massive units, interpreted to be the upper part of a sheeted dike complex.

Fifteen massive basalt units have been recognized in basement recovered on Leg 137. Determination of lithologic unit boundaries was complicated somewhat because of the low recovery in the rotary cored section (Cores 137-504B-173R through -179R). The rocks recovered on this leg are interpreted as a continuation of the sheeted dike complex drilled on previous legs. No intrusive dike margins were recovered on Leg 137, in contrast to Legs 83 and 111 (Shipboard Scientific Party, 1985, 1988). Because intrusive contacts with chilled margins that would unequivocally define dikes were not recovered, all units are referred to as massive.

As outlined in the "Introduction and Explanatory Notes" chapter (this volume), lithologic units were distinguished on the basis of phenocryst phases present and their total and relative abundances, plus the presence of contacts between units. In accordance with previous results from Hole 504B, however, lithologic units are classified only on the basis of the phenocryst assemblages or individual phases present, without regard to the total phenocryst content or the relative abundances of the different phases (Shipboard Scientific Party, 1985, 1988). Five lithologic types have been recognized in this classification, four of which are porphyritic:

OPC: Olivine, plagioclase, clinopyroxene phyric basalt, including those with minor accessory chromian spinel (= SV group of Leg 83).
OP: Olivine, plagioclase phyric basalt.
OC: Olivine, clinopyroxene phyric basalt.
PC: Plagioclase, clinopyroxene phyric basalt.
A: Aphyric basalt.

The lithostratigraphy of Leg 137 rocks using this classification is shown in Figure 8, and depths to the top of each unit are given in Table 2. Although no intrusive dike contacts were recovered, a very fine-grained rock, interpreted as a chilled margin of a dike, was recovered at the top of Unit 199 (Sample 137-504B-176R-1, 0–6 cm). Fine-grained pieces in Section 137-504B-177R-1 (Pieces 1 and 6) define the top and bottom of Unit 201 and are interpreted to be the fining of grain size toward the margins of a dike. Unit 204 (Section 137-504B-180M-1, Piece 1) is very fine grained, and is likely close to a dike chilled margin. Piece 5 in Section 137-504B-176R-1 is a breccia composed of 1–5-cm fragments of highly altered basalt cemented by dark blue-green chlorite and cut by later white prismatic laumontite. This material is not fine grained enough to be a brecciated chilled dike margin, such as was identified on Legs 83 and 111 (Shipboard Scientific Party, 1985, 1988). This breccia, which fell apart upon splitting, originally had a horizontally layered structure, in contrast to the generally high-angle breccia zones at dike margins recovered on previous legs.

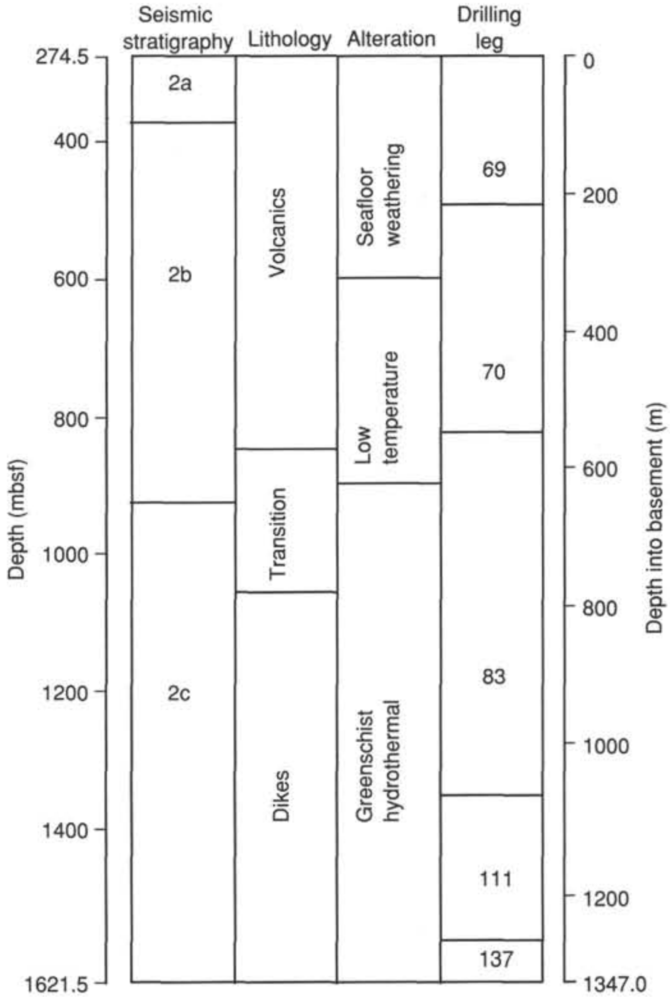

Figure 7. Summary diagram for the basement section of Hole 504B, showing seismic stratigraphy, lithology, alteration, and penetration for drilling legs to date.

Igneous Petrology

Nearly all the rocks recovered on Leg 137 are sparsely to moderately phyric (1%–10% phenocrysts), with 13 out of the 15 units falling in the OPC classification (Fig. 7). Only one aphyric unit and one PC unit (Units 197 and 199, respectively) were identified. OP and OC lithologies were not observed, nor was any Cr-spinel detected in any Leg 137 thin section. The

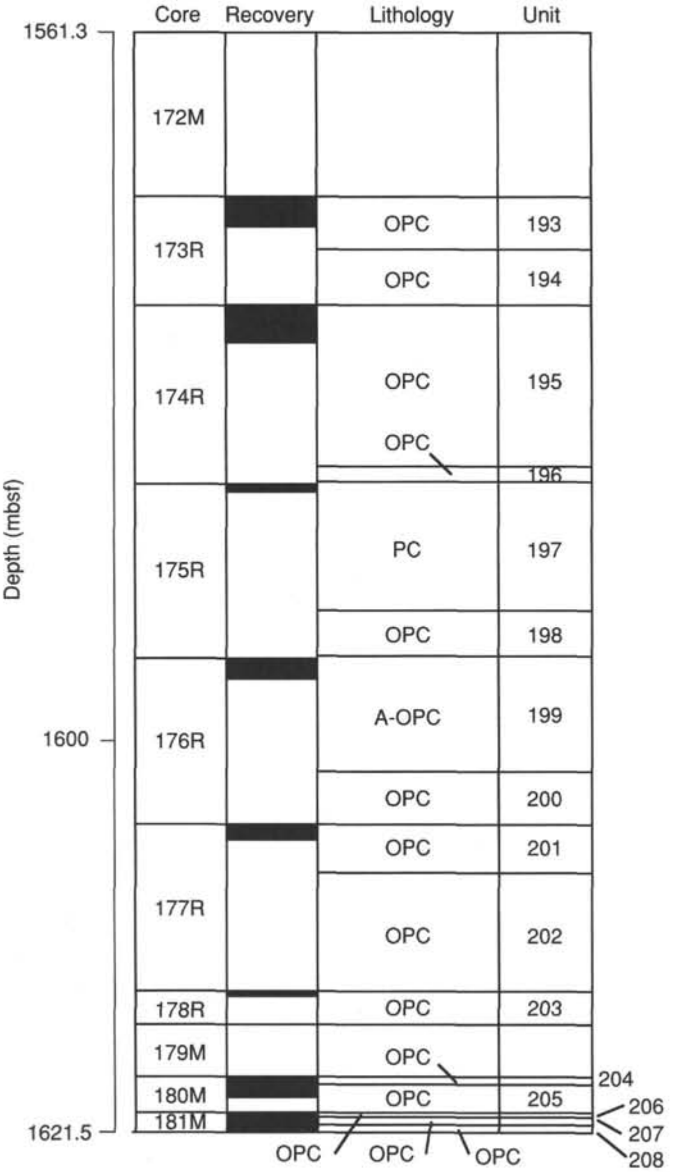

Figure 8. Lithostratigraphy of rocks recovered on Leg 137. Lithologic classification described in text. Depth to the top of each unit was calculated by stretching out the material recovered in each core over the entire cored interval for that core.

descriptions below are based mainly on thin section observations.

Plagioclase phenocrysts make up 1%–5% of the porphyritic rocks. The subhedral to euhedral tabular prisms range from 0.4 to 2.0 mm in size. Some have rounded cores containing abundant glass inclusions. Plagioclase occurs both as individual phenocrysts and as glomero-crysts, in some cases together with olivine or clinopyroxene. Plagioclase phenocrysts are generally unaltered to slightly altered to chlorite and albite.

Clinopyroxene phenocrysts range from 0.5 to 2.8 mm in size, and comprise <1%–5% of the mode. The crystals are generally anhedral, occurring mostly as phenocrysts, but also as glomerocrysts with plagioclase. Large (5–10 mm) glomerocrysts of plagioclase and clinopyroxene occur in Unit 208 (Sections 137-504B-181M-1 and -2). The outer rim of clinopyroxene phenocrysts is commonly intergrown with groundmass plagioclase, indicating continued phenocryst growth during groundmass crystallization.

Table 2. List of lithologic units from Leg 137 coring. Classification explained in text.

Lithologic unit	Type	Core, section (depth in section, cm)
193	OPC	173R-1, 0
194	OPC	173R-1,80
195	OPC	174R-1, 0
196	OPC	174R-2,75
197	PC	175R-1, 0
198	OPC	175R-1,32
199	A-OPC	176R-1, 0
200	OPC	176R-1,94
201	OPC	177R-1, 0
202	OPC	177R-1,22
203	OPC	178R-1, 0
204	OPC	180M-1, 0
205	OPC	180M-1,15
206	OPC	181M-1, 0
207	OPC	181M-1,62
208	OPC	181M-1,82

Olivine phenocrysts, now totally replaced, originally made up from <1% up to 6% of the mode. The rounded to euhedral crystals ranged from 0.5 to 4 mm in size. In some cases, skeletal crystal outlines are observed. Olivine occurs mostly as single phenocrysts, but also in clusters (glomerocrysts) of 2–3 olivine crystals, and in some cases as glomerocrysts with plagioclase.

The groundmass of the rocks is fine grained, with silicates ranging in size from 0.1 to 1.0 mm. Plagioclase comprises 49%–53% of the matrix, and consists of 0.1–1.0 mm blocky to tabular prismatic crystals. Equant to elongate clinopyroxene crystals, 0.1–1.0 mm in size, make up 30%–40% of the groundmass. The clinopyroxene is partly altered to actinolite. Rounded to euhedral crystals of olivine originally made up 2%–5% of the groundmass. The 0.1–0.4 mm crystals are now totally replaced by chlorite and magnetite. Igneous titanomagnetite comprises 4%–5% of the groundmass. Skeletal to euhedral magnetite crystals range from 0.01 to 0.25 mm in size, and occur interstitial to the silicates. Sphene partly replaces the magnetite. Pyrite and chalcopyrite are ubiquitous in small amounts (<1%) disseminated in the groundmass. These minerals occur as 0.01–0.05 mm rounded globules and irregular grains replacing igneous sulfides and silicates, and as secondary interstitial grains.

The overall texture of the rocks is subophitic, with groundmass plagioclase partly enclosed within clinopyroxene. Clusters of radiating plagioclase crystals impart a "palmate" texture locally. Aligned phenocrysts in some Unit 205 samples (e.g., 137-504B-180M-1, Piece 7) may be due to flow within the massive dike.

Geochemistry

Five samples were analyzed by XRF for major and trace elements, and results are listed in Table 3. The compositions of the rocks analyzed on Leg 137 are identical to those from shallower in the dike complex sampled during Leg 111. All the Leg 137 samples have high MgO contents (>7.5%) and very low K_2O contents (none detected). The Fe number (100 × FeO^T/FeO^T + MgO) ranges from 52 to 55 and falls within the range of Leg 111 rocks (48–58; Shipboard Scientific Party, 1988). Trace-element abundances of Leg 137 rocks fall in the Group D basalt type of Autio and Rhodes (1983; Fig. 9). The Group D basalts are similar to normal I-type mid-ocean ridge basalt (Bryan et al., 1976), but exhibit extreme depletion of highly and moderately incompatible elements: Nb, ≤1 ppm; Zr, 42–46 ppm; Zr/Nb, 42–45. It has been suggested that such

Table 3. Whole-rock chemical analyses of Leg 137 samples. Major element oxides in weight percent, trace elements in ppm. Major elements are averages of duplicate analyses.

Core, section interval (cm) Depth (mbsf)	173R-1 4–6 1570.04	173R-1 105–107 1571.05	174R-1 50–53 1576.8	174R-2 86–88 1578.63	176R-1 124–126 1596.54
SiO_2	50.77	49.87	50.68	50.08	49.17
TiO_2	0.96	0.84	0.91	0.88	0.85
Al_2O_3	15.27	15.38	15.36	15.17	15.04
Fe_2O_3T	10.82	9.93	10.63	10.30	9.90
MnO	0.18	0.17	0.17	0.16	0.15
MgO	8.04	8.11	7.83	7.74	8.38
CaO	13.13	13.09	13.14	12.85	13.03
Na_2O	1.43	1.32	1.56	1.55	1.40
K_2O	0	0	0	0	0
P_2O_5	0.07	0.07	0.07	0.06	0.07
Total	100.67	98.78	100.35	98.79	97.99
LOI	0.89	0.77	6.71	1.05	1.05
Nb	0	0	1	1	1
Zr	46	42	45	43	42
Y	24	23	24	23	23
Sr	47	49	48	46	46
Rb	0	0	0	0	1
Zn	53	59	49	51	45
Cu	82	88	70	81	65
Ni	86	89	93	94	98
Cr	203	228	231	259	264
V	262	266	281	270	262
Ba	9	13	7	5	0

extreme depletion may be due to melting of a previously melted mantle source (Autio and Rhodes, 1983).

One of the analyzed samples had a high loss on ignition, 6.71% (Sample 137-504B-174R-1, 50–53 cm; Table 3). This sample contains vugs, up to 3 mm in size, that are filled with chlorite and actinolite and surrounded by extensively altered rock for up to 5–10 mm (see "Alteration" section below). Sample 137-504B-174R-2, 86–88 cm, also contains similar vugs, but does not exhibit the high LOI of Sample 137-504B-174R-1, 50–53 cm. Neither of these rocks is enriched in Mg compared to the others. Both have slightly higher Na_2O and Sample 137-504B-174R-2, 86–88 cm, has slightly lower CaO than the other samples, which can be attributed to albitization

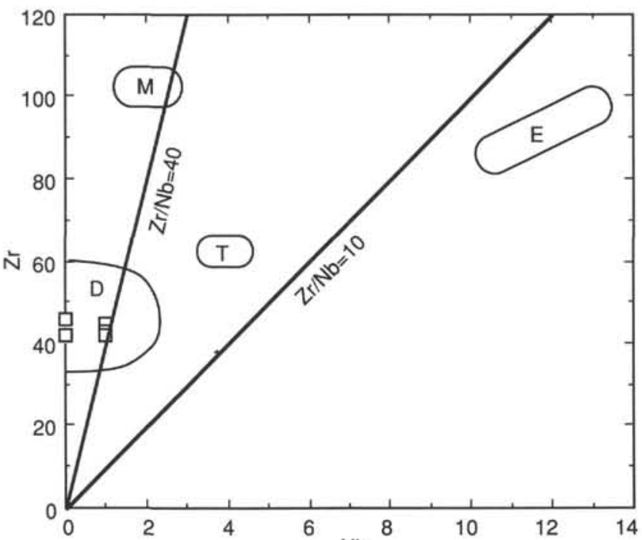

Figure 9. Trace element abundance of Leg 137 samples in ppm. Fields for different basalt groups identified from Hole 504B (Autio and Rhodes, 1983) also shown.

of plagioclase. The lack of Mg-enrichment of the rocks and the uptake of Na suggests alteration at low water/rock ratios.

Alteration

Alteration of basement recovered from previous drilling legs at Hole 504B has been documented in detail by Alt et al. (1986, 1989). The core can be divided into three zones (Fig. 7): the upper 320 m of the volcanic section affected by "seafloor weathering" at low temperatures (0°–100°C); the lower portion of the volcanic section affected by low-temperature (<150°C), reducing alteration; and the transition zone and dikes, which were hydrothermally altered under greenschist and superimposed zeolite conditions. A sequence of hydrothermal alteration in the transition zone and dikes was established on the basis of cross-cutting vein relationships. This sequence can be briefly summarized in three basic stages. First, chlorite and actinolite formed in veins, and greenschist minerals formed in the rocks during axial hydrothermal alteration at temperatures of 250°–350°C. Later, as the crust moved off-axis into a recharge zone, penetration of seawater into still-warm rocks resulted in precipitation of anhydrite in cracks. Finally, zeolites formed in fractures and rocks during later off-axis alteration at lower temperatures (less than about 150°C).

Some variations in proportions of secondary minerals with depth in the dike section became apparent on Leg 111. The abundance of actinolite replacing clinopyroxene generally increases with depth in the dikes, whereas calcic plagioclase is less extensively altered to albite as depth increases. This increase in actinolite and decrease in alteration of plagioclase was interpreted to reflect higher temperatures at depth, with conditions approaching the actinolite facies of Elthon (1981) where calcic plagioclase and actinolite are stable.

The rocks recovered on Leg 137 are generally slightly altered (5%–15%) and dark gray in color. Olivine is completely replaced by chlorite, talc, magnetite, and pyrite. Traces of red ferric oxides are also present in some samples (e.g., in Section 137-504B-174R-2). Mixed-layer chlorite-smectite, which was identified in Leg 83 and 111 samples (Alt et al., 1986, 1989) is also likely present in Leg 137 samples. This is indicated by the greenish color in plane polarized light and the first-order interference colors of clay minerals, rather than the anomalous blue of chlorite. Plagioclase is slightly altered to chlorite and albite. Clinopyroxene phenocrysts are unaltered, but groundmass clinopyroxene is partly (about 5%–10%) replaced by actinolite and fine magnetite "dust." Igneous titanomagnetite in the groundmass is generally 10%–20% replaced by sphene. The alteration is identical to that observed in Leg 111 rocks. Based on analogy with previous analyses of Leg 111 samples (Alt et al., 1989), alteration of Leg 137 rocks occurred at temperatures of around 300°–350°C and low water/rock ratios.

Locally the rocks are very highly to totally altered, in 5–10 mm light gray alteration halos around veins and vugs. Vugs of 5–10 mm are filled with chlorite and actinolite, and in one case a vug is zoned with both quartz and interstitial zeolite at the center of the vug (137-504B-174R-2, 85–88 cm, Piece 14). Minerals in the light gray alteration halos around the vugs are nearly completely recrystallized to the assemblages described above. Similar features were observed in Leg 83 and 111 samples. They are likely areas of enhanced primary porosity that would allow locally higher water/rock ratios or areas of abundant interstitial glass, which is readily altered.

Fractures make up less than 1% of the core and are nearly all less than 1 mm wide. Many are open cracks, perhaps formed during drilling and concomitant stress release. Some apparently contain a white mineral (albite?, zeolite?), although the whitish color may be due to fracturing of igneous minerals along an open hairline fracture. Chlorite is present in several fractures, in some cases with 5 mm wide light gray alteration halos (e.g., 137-504B-174R-2, Piece 1; -176R-1, Piece 3). In addition to the light gray zone, Sample 137-504B-177R-1, Piece 5, has a 1-mm dark green chloritized zone adjacent to the chlorite vein. A platy, white prismatic mineral coats a fracture in Sample 137-504B-174R-1, 13–20 cm, and cuts across the chlorite cement of a breccia in 137-504B-176R-1, Piece 5. This mineral was originally described as anhydrite on the barrel sheets but was later identified as laumontite by X-ray diffraction of both of these samples. A pale green mineral (prehnite?) occurs at the center of a reopened chlorite vein in Sample 137-504B-174R-1, 49–52 cm. These occurrences are consistent with the alteration sequence for Legs 83 and 111, from initial axial hydrothermal alteration to later off-axis zeolite formation (Alt et al., 1986, 1989).

Cores 137-504B-180M and -181M are the first diamond-cut cores from deep within oceanic crust sampled by DSDP/ODP. The excellent recovery (55%–100%) during coring and the large diameter of the cores (4 in.) aided in observation of alteration features (as well as igneous and structural features). In particular, these cores appear to contain fewer open fractures and more abundant chlorite + actinolite veins than the RCB cores. This can be attributed to the good recovery, in contrast to the RCB cores where the rocks may commonly be broken along previous veins, and the altered material along fractures ground away during drilling. It would appear from the diamond cores that the trend of increasing proportion of actinolite in the secondary mineral assemblage recognized on Leg 111 continues with depth.

PHYSICAL PROPERTIES

Physical properties investigations can provide data that complete the description and classification of a rock. Properties like bulk or grain density and porosity are related directly to the fabric of the rock. Ultrasonic velocity is related to the mechanical behavior and the deformation as well as the weathering condition of the rock (Dearman, 1976; Christaras, 1989).

Basalt samples recovered from Hole 504B during Leg 137 were studied regarding their index properties, ultrasonic velocity, thermal conductivity, and magnetic susceptibility. Because coring activities were performed in a limited depth range between 1570.0 and 1621.5 mbsf, only 11 representative samples were used for physical properties measurements. All tests, except thermal conductivity, were performed on minicores of 24.67 mm diameter and ~20 mm height. Two-minute discrete GRAPE and discrete magnetic susceptibility measurements were taken using a multisensor track scanner. Analytical techniques are described in the "Introduction and Explanatory Notes" chapter (this volume).

Index Properties

Measurements for index properties were taken on 11 samples. One or two minicores from each core section, depending on the lithology, were used for this purpose. Sample volumes were measured using a Quantachrome Penta-Pycnometer helium displacement pycnometer. The samples were weighed on a programmed dual pan Scientech balance. Wet/dry weight and volume measurements were used to determine the parameters of wet/dry bulk density (WBD, DBD), porosity (n), wet/dry water content (WWC, DWC), and grain density (GD). Test results are given in Table 4.

The average wet bulk density of the samples measured was 2.96 g/cm^3 with a standard deviation of σ_{n-1} = 0.017 g/cm^3. The grain density determinations gave a mean value of 2.99 g/cm^3 with a standard deviation of σ_{n-1} = 0.015 g/cm^3. Dry bulk density measurements having a mean value of 2.95 g/cm^3 with a standard deviation of σ_{n-1} = 0.019 g/cm^3 do not differ significantly from those of the wet bulk density. This may be related to the low porosity (average = 0.64%, σ_{n-1} = 0.111%) and water content (average = 0.22%, σ_{n-1} = 0.041%) values observed. The water content obviously presents a significant dependence on the porosity (r^2 = 0.995, Fig. 10). Wet bulk density is related linearly with the dry bulk density, presenting a significant critical correlation coefficient of r^2 = 0.921 (Fig. 11). However, water content and porosity changes do not show a significant correlation with either wet or dry bulk density, or with grain density. Excluding the data from the deepest sample (137-504B-181M-2, 147–150 cm), dry bulk density is related more or less linearly with the grain density, as is shown in Figure 12.

Wet bulk density was also measured using the Gamma Radiation Attenuation Porosity Evaluation (GRAPE) technique. Discrete measurements of the corrected and the true wet bulk density (CWBD, TWBD), taken using the above method, are given in Table 5. Small sample size may have been the reason that GRAPE density measurements were lower than gravimetric ones on the same samples.

As a general observation, index properties data remain more or less constant with depth. The very small range of depth in relation to the number of samples offers an explanation for this observation. Test results related to the depth are given in Figures 13 and 14. Leg 137 values are generally a little higher than those from Leg 111, but they are similar to the values of the deepest samples recovered during that leg.

Ultrasonic Velocity

Ultrasonic velocity measurements were made on the same 11 minicores that were used for index properties measurements. Samples were tested in both wet and dry states. The traveltime of a 500-kHz source pulse was measured using an oscilloscope. Both compressional (vp) and shear (vs) wave

Table 4. Index properties of basalts from Hole 504B, Leg 137.

Core, section, interval (cm)	Depth (mbsf)	WBD (g/cm^3)	DBD (g/cm^3)	GD (g/cm^3)	n (%)	WWC (%)	DWC (%)
173R-1, 6–8	1570.06	2.95	2.94	2.98	0.85	0.30	0.30
173R-1, 105–108	1571.05	2.97	2.96	2.98	0.77	0.27	0.27
174R-1, 53–56	1576.83	2.97	2.96	2.99	0.61	0.21	0.21
174R-2, 96–99	1578.73	2.97	2.97	2.99	0.69	0.24	0.24
175R-1, 13–16	1585.93	2.98	2.98	2.99	0.50	0.17	0.17
176R-1, 106–112	1596.36	2.98	2.98	2.99	0.57	0.19	0.20
178R-1, 20–24	1614.00	2.95	2.94	2.97	0.74	0.26	0.26
180M-1, 72–82	1618.13	2.95	2.95	2.96	0.55	0.19	0.19
180M-2, 67–78	1619.03	2.95	2.94	2.95	0.51	0.18	0.18
181M-1, 26–29	1619.37	2.96	2.95	2.97	0.61	0.21	0.21
181M-2, 147–150	1621.50	2.92	2.92	2.99	0.63	0.22	0.22

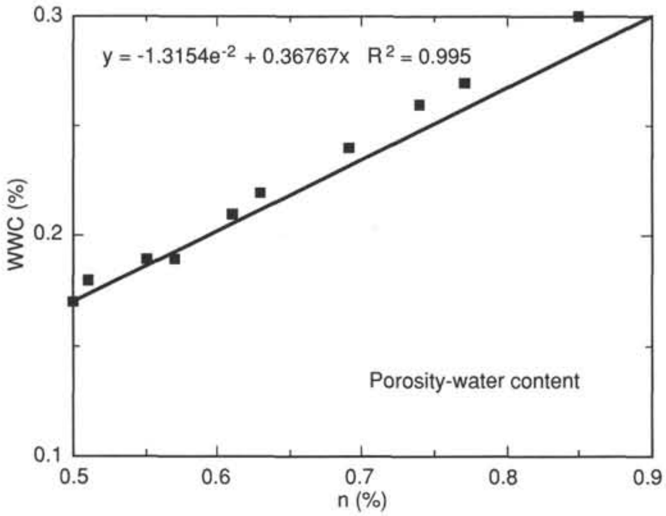

Figure 10. Correlation between porosity (n) and wet water content (WWC) of basalts from Hole 504B, Leg 137.

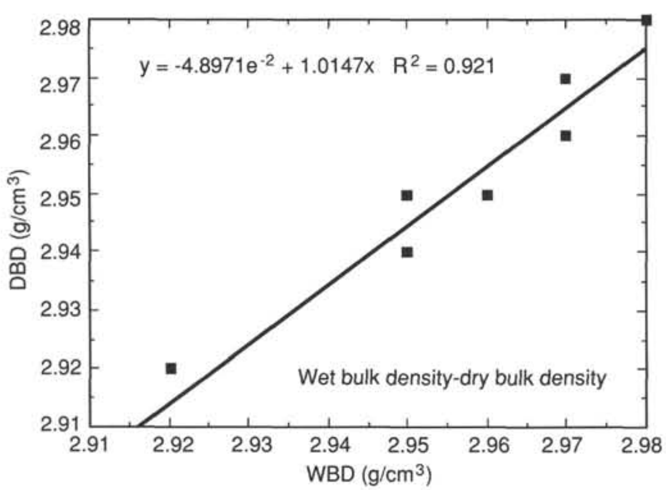

Figure 11. Correlation diagram between wet bulk density (WBD) and dry bulk density (DBD) of basalts from Hole 504B, Leg 137.

velocity measurements were taken and their results are given in Table 6 and Figure 15.

Measured values do not differ significantly from each other and only a slight decrease with depth is observed. Velocity data corresponding to deeper samples from Leg 111 compare better with our measurements than the data corresponding to samples from the upper part of the section cored during that leg. Velocity measurements made on dry specimens provided data that vary independently with depth. The small depth range cored might explain this. The slight decrease in compressional velocity with respect to depth observed in wet velocity measurements might relate to the influence of water on the stress-strain changes of the rock mass in relation to the existing stress field. *S*-wave measurements on wet samples show a more constant distribution with depth than those of *P*-wave measurements, resulting in a slight increase in the compressional/shear velocity ratio with the depth. This observation of anisotropic change could be related to changes in the stress field with depth. The small depth range of sampling (only 59 m) and the small number of samples make it difficult to confirm this possibility. A study of the strain behavior of the rock under stress could clarify the phenomenon. The average compressional ultrasonic velocity for the wet test material is 6029 m/s with a standard deviation of 78 m/s, while for the dry material it is 5723 m/s with a standard deviation of 114 m/s. The average ultrasonic velocity for the wet samples is 3727 m/s with a standard deviation of 112 m/s, while for the dry samples it is 3602 m/s with a standard deviation of 91 m/s. The small range of velocity measurements could be related to the similarly small range of index properties changes (Fig. 16). Some relationship between wet and dry shear velocities is also observed (Fig. 17).

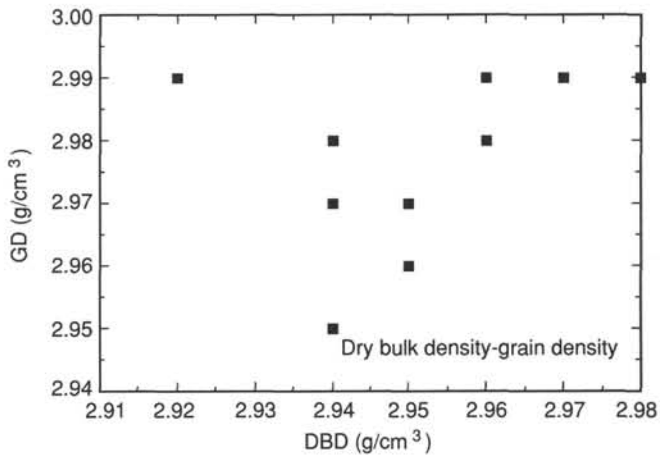

Figure 12. Relationship between dry bulk density (DBD) and grain density (GD) of basalts from Hole 504B, Leg 137.

Magnetic Susceptibility

Magnetic susceptibility (X_0) is primarily a function of the concentration and grain size of magnetic minerals. Data were collected on minicores using a Bartington Magnetic Susceptibility Meter (Model MS1). The X_0 for the investigated samples is given in Table 7 and Figure 18.

The average magnetic susceptibility measured during Leg 137 (excluding the data from Sample 137-504B-181M-2, 147–150 cm, which give a value of 296 μG/Oe) is 1827 μG/Oe with a standard deviation of 391 μG/Oe. This value is not far from those that were measured in Leg 111, which are in the range of 1500–3500 μG/Oe. Section 137-504B-181M-2, corresponding to the bottom of the hole, presents a significantly low magnetic susceptibility, in relation to the values measured on the other samples. Repeated measurements made on this sample confirm these data. A thorough study of the material from this depth should explain

Table 5. GRAPE bulk densities of basalts from Hole 504B, Leg 137.

Core, section, interval (cm)	Depth (mbsf)	CWBD (g/cm^3)	TWBD (g/cm^3)	Thickness (cm)
173R-1, 8–9	1570.80	2.846	2.839	5.65
173R-1, 106–107	1571.06	2.819	2.810	5.68
173R-1, 118–119	1571.18	2.850	2.843	5.68
173R-1, 134–135	1571.34	2.829	2.821	5.71
173R-2, 23–24	1571.63	2.828	2.820	5.68
174R-1, 16–17	1576.46	2.906	2.901	5.68
176R-1, 17–18	1595.47	2.160	2.115	3.01
176R-1, 74–75	1596.04	1.220	1.125	2.98
176R-1, 107–108	1596.37	2.906	2.901	5.63
177R-1, 13–14	1604.63	2.223	2.182	6.18
177R-1, 64–65	1605.14	1.991	1.397	6.28
180M-1, 76–78	1618.17	1.340	1.034	6.28
180M-2, 68–72	1619.04	2.579	2.558	2.46
181M-1, 26–29	1619.37	2.978	2.978	2.48
181M-2, 147–150	1621.50	2.904	2.905	2.47

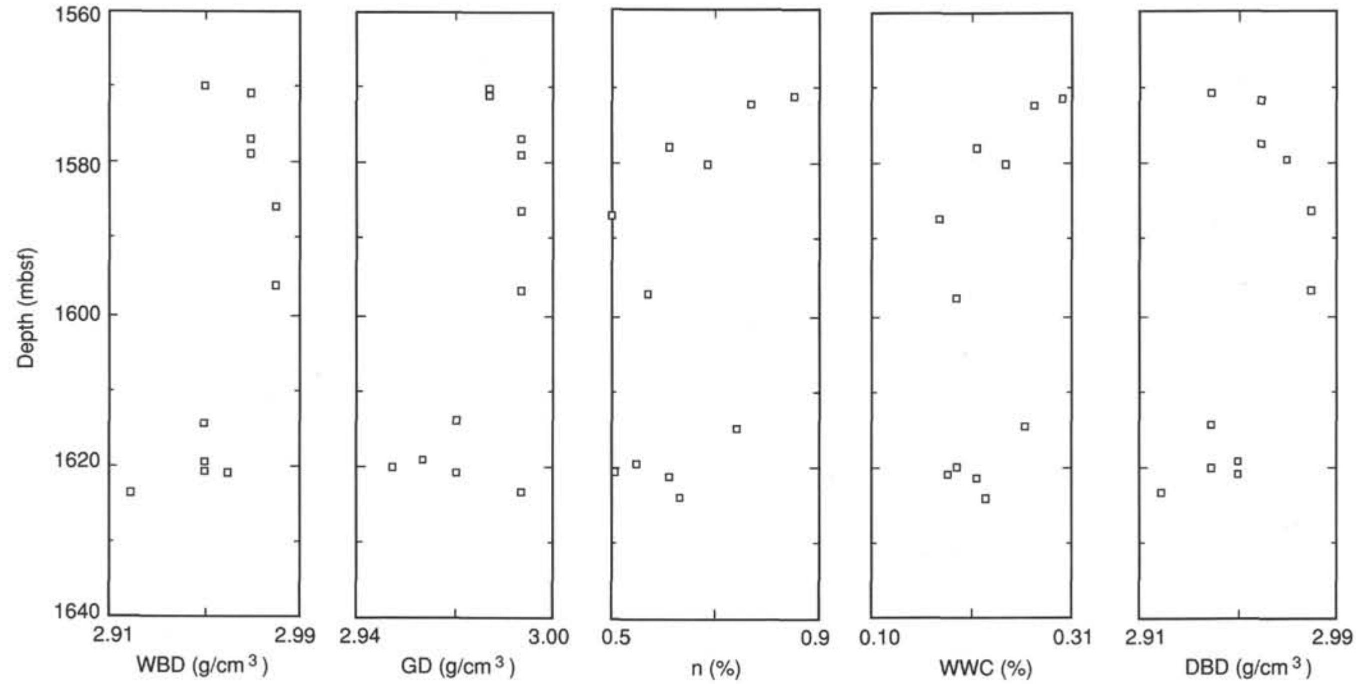

Figure 13. Variation with depth of index properties of basalts from Hole 504B, Leg 137.

whether this anomalously low value is related to the nature of the rock, or whether it was only a measurement error. Magnetic susceptibility values do not show a significant correlation with the previously described properties. Disregarding the sample from the bottom of the hole, a slight positive increase with grain density can be observed (Fig. 19).

Thermal Conductivity

Thermal conductivity (K) measurements were made on the same rock pieces from which minicores were cut. Measurements were made by the half-space method and measured values are given in Table 7. The average value of our measurements is 2.156 W/m·K with a standard deviation of 0.137 W/mo significant relationship is observed between this and the previous properties (Fig. 18).

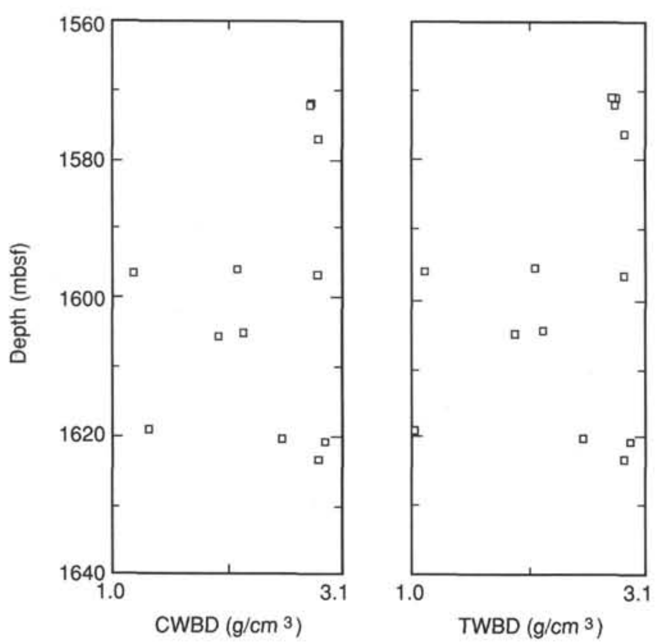

Figure 14. Variation with depth of GRAPE bulk densities of basalts from Hole 504B, Leg 137.

FLUID SAMPLING AND CHEMISTRY

Fluids sampled from within reentered DSDP/ODP boreholes provide a unique opportunity to observe the effects of water-rock interaction within the oceanic crust. During Leg 137, eight borehole fluid samples were obtained from separate depths in Hole 504B. The goals of the water sampling program during this leg were to investigate the geochemistry of basement fluids, further define hydrological processes occurring in the borehole itself, and test two flow-through sampler designs for applicability to high-temperature oceanic borehole sampling. The samples obtained reveal an integrated chemical signal of a number of processes, possibly including: (1) mixing and displacement of surface seawater (originally pumped into the hole) by oceanic bottom water flowing down into the borehole, (2) reaction of these components under elevated temperatures, (3) mixing and displacement of the borehole water by true formation fluid, and (4) contamination or dilution as a result of the sampling process.

Introduction

Oceanic basalts altered by seawater have been observed throughout the history of the DSDP/ODP. Secondary phases observed indicate alteration of rocks by high, moderate, and low temperature fluids (cf. Mottl, 1983). The magnitude of alteration suggests that the seafloor weathering of oceanic rocks could influence the composition of seawater. Definitive estimation of the fluxes resulting from the reaction of seawater and the oceanic basement can be obtained from a knowledge of both the mass flux of seawater through the crust as well as the chemical composition of the reacted fluids. While the mass flux of circulating fluid can be estimated by anomalies in the measured heat flow from the theoretical values, the chemical composition of this fluid is more elusive. Sampling fluids from within oceanic boreholes may provide the information necessary to quantify the composition of these fluids. Mottl and

Table 6. *P*-wave velocities measured in basalts from Hole 504B, Leg 137.

Core, section, interval (cm)	Depth (mbsf)	wvp (km/s)	wvs (km/s)	dvp (km/s)	dvs (km/s)	vp/vs (wet)	vp/vs (dry)
173R-1, 6–8	1570.06	6.015	3.660	5.651	3.534	1.557	1.691
173R-1, 105–108	1571.05	6.037	3.744	5.758	3.628	1.564	1.688
174R-1, 53–56	1576.83	6.043	3.808	5.822	3.622	1.569	1.590
174R-2, 96–99	1578.73	6.100	3.869	5.856	3.718	1.575	1.577
175R-1, 13–16	1585.93	6.100	3.820	5.867	3.700	1.586	1.597
176R-1, 106–112	1596.36	6.094	3.833	5.828	3.714	1.587	1.612
178R-1, 20–024	1614.00	5.936	3.661	5.726	3.578	1.599	1.643
180M-1, 78–82	1618.13	6.073	3.658	5.528	3.551	1.660	1.557
180M-2, 67–78	1619.03	6.082	3.662	5.700	3.644	1.660	1.677
181M-1, 26–29	1619.37	6.057	3.799	5.608	3.436	1.607	1.587
181M-1, 147–150	1621.50	5.853	3.491	5.609	3.502	1.632	1.594

Gieskes (1990) have reviewed the progress of the borehole water sampling program. To date, borehole fluids have been obtained in only four oceanic wells, with Hole 504B receiving the greatest attention both in terms of downhole sampling intervals as well as repeated visits.

Leg 137 was the sixth time borehole water samples have been taken from Hole 504B. The borehole was left undisturbed for 1633 days since flushing it with surface seawater at the end of operations during Leg 111. This compares with 1233 days, 470 days, 710 days, and 39 days for samples collected on ODP/DSDP Legs 111, 92, 83, and 70, respectively.

Fluid samples from past visits to Hole 504B have revealed chemistries substantially different from seawater. However, the composition of the formation fluid end-member remains elusive (Mottl and Gieskes, 1990). In preparation for future reentry, boreholes are flushed with surface seawater to remove drilling mud and debris. Temperature measurements indicate that oceanic bottom water flows down into the relatively porous upper few hundred meters of Hole 504B (Gable et al., 1989). The contribution of surface seawater remaining in the borehole can be estimated using tritium measurements, as discussed in Mottl et al. (1985). Tritium is a radioactive fallout product resulting from atmospheric testing of nuclear devices in the 1950's and 1960's. Due to its short half life (12.5 years) tritium is not found deeper than the surface waters in the Pacific Ocean. Tritium profiles from Hole 504B reveal increasing tritium with depth, and therefore increasing surface water component (Mottl and Gieskes, 1990). This has been interpreted to be a result of slow downward mixing of bottom seawater into the borehole.

While displacement of the surface water placed in the borehole with bottom seawater is evident from the tritium measurements, this process can not explain the observed changes in fluid chemistry. Magnesium, potassium, sodium, and sulfate are removed in the borehole fluids while calcium and silicon are increased relative to seawater. Two possible processes have been suggested for the observed changes in chemistry: (1) The possibility of reaction of the seawater components while in contact with the wall rocks, and (2) diffusive exchange with formation fluids. Reaction with the

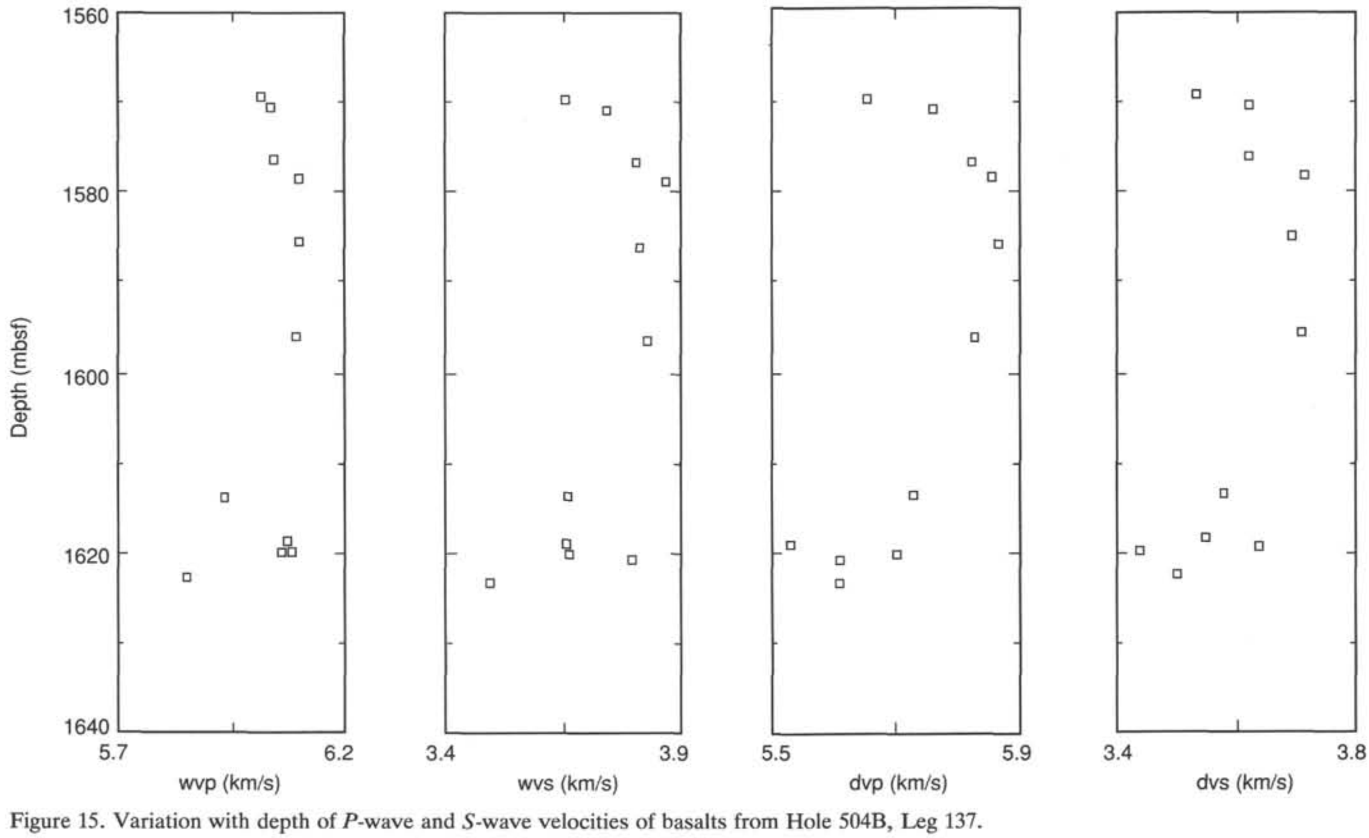

Figure 15. Variation with depth of *P*-wave and *S*-wave velocities of basalts from Hole 504B, Leg 137.

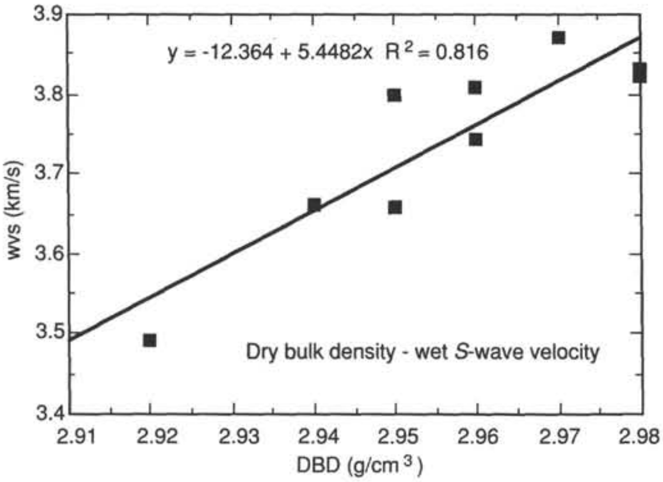

Figure 16. Correlation diagram between dry bulk density (DBD) and wet *S*-wave velocity (wvs) of basalts from Hole 504B, Leg 137.

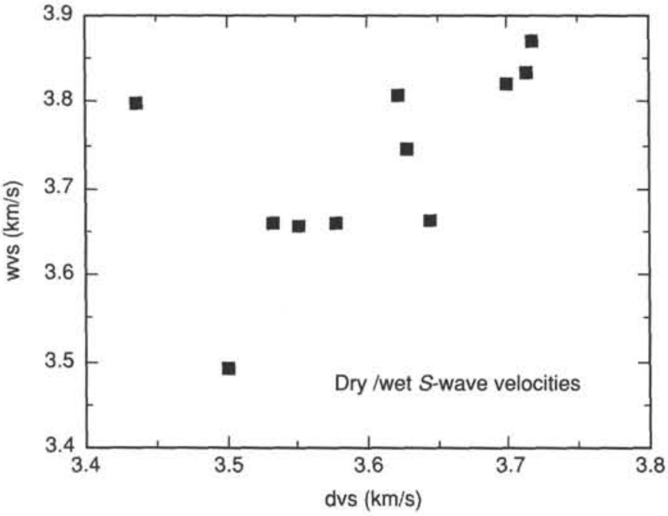

Figure 17. Relationship between dry (dvs) and wet (wvs) *S*-wave velocities of basalts from Hole 504B, Leg 137.

Table 7. Thermal conductivities and magnetic susceptibilities of basalts from Hole 504B, Leg 137.

Core, section, interval (cm)	Depth (mbsf)	K (W/m·K)	X_0 (μG/Oe)
173R-1, 6–8	1570.06	2.279	1461
173R-1, 105–108	1571.05	2.102	1469
174R-1, 53–56	1576.83	2.325	2227
174R-2, 96–99	1578.73	2.045	2229
175R-1, 13–16	1585.93	2.118	2270
176R-1, 106–112	1596.36	2.005	1801
178R-1, 20–24	1614.00	2.441	1466
180M-1, 72–82	1618.13	2.117	2023
180M-2, 67–78	1619.03	2.065	1233
181M-1, 26–29	1619.37	2.183	2097
181M-2, 147–150	1621.50	2.036	296

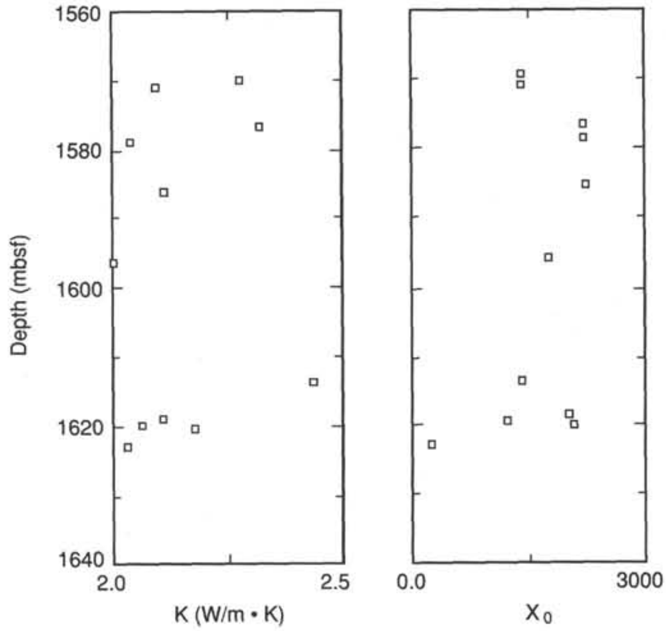

Figure 18. Variation with depth of magnetic susceptibility (X_0) and thermal conductivity (K) of basalts from Hole 504B, Leg 137.

wall rocks is possible, but experimental water-rock studies suggest that the temperatures are too low and the water-rock ratio in the borehole is much too high to account for the observed chemical signal (Seyfried and Bischoff, 1979). Lower temperature reactions such as the precipitation of anhydrite from the borehole fluids have been suggested from past studies (Gieskes et al., 1986; Shipboard Scientific Party, 1988). Chemical diffusive exchange with fluids in the wall rocks appears to be possible. Mottl and Gieskes (1990) calculated a diffusive path length up to 35 cm into the wall rock between DSDP Leg 92 and ODP Leg 111 (1233 days), based on temperature and porosity measurements.

Sampling difficulties have been encountered during all previous attempts to sample Hole 504B fluids. The overall success rate of retrieving borehole fluid samples for all borehole sampling attempts during DSDP and ODP has been near 50%. Mottl et al. (1985) defined two modes of sampling: the active mode in which fluids are actually withdrawn from the formation under negative pressure, and the passive mode in which fluids are collected from the ambient borehole. During previous legs active mode sampling was largely unsuccessful, due to the low permeabilities of the formation. The fluids collected were ambient borehole fluids, in many cases largely diluted with seawater pushed down the hole with the sampling tools. Passive mode sampling has been most successful upon reentering holes some time after drilling. Almost all sampling attempts have resulted in some dilution effects either by pushing seawater down the borehole with large diameter samplers such as the Lynes go-devil or the Schlumberger RFT, or with leaking valves on the trip through the water column. One problem previously not considered was the possibility of sample shrinkage due to cooling during retrieval (Lysne, in press). As the samples are moved up from the hot borehole into seawater, thermal contraction should occur. This could lead to failure of the sealing valves, particularly in samplers which rely on positive internal pressure to maintain a seal (e.g., Gearhart Owen and Kuster samplers). During DSDP Leg 92, additional problems were encountered with large quantities of drilling mud left in the hole from DSDP Leg 83.

During Leg 137, two high-temperature geothermal well samplers, from Los Alamos National Laboratory (LANL) and Lawrence Berkeley Laboratory (LBL), were tested for their applicability to oceanic borehole fluid sampling. These sam-

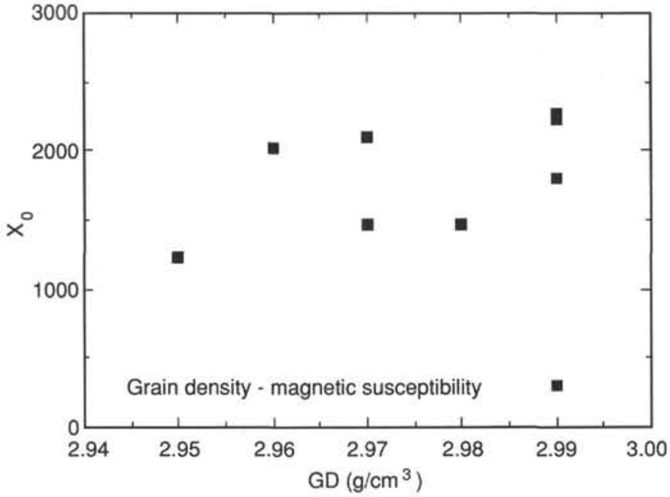

Figure 19. Relationship between magnetic susceptibility (X_0) and grain density (GD) of basalts from Hole 504B, Leg 137.

plers and their operations are described in the section "Borehole Fluid Samplers Tested during Leg 137" below. Both samplers employ a flow-through design which allows flushing of the samplers as they are lowered to depth. This design prevents flash boiling of the fluids as they enter evacuated spaces, a technique used in other sampler designs. The samplers use valves which are designed to be shut using springs and internal hydrostatic and gas pressure as the samplers are withdrawn from isothermal wells. Recent attempts to sample very hot geothermal wells (>300°C) have resulted in substantial sample dilution due to shrinkage of the samples and failure of the internally seated valves (Goff et al., 1990). Attempts to overcome these problems are discussed in the section "Borehole Fluid Samplers Tested during Leg 137" below. The LANL approach to the sample shrinkage problem was to attach a catch on the valve so that it could not open after initially triggering. This approach apparently did not work adequately, as the sampler returned to the surface with an overpressure, indicating that the valves had opened at some point below the ocean surface. The LBL sampler successfully overcame the sample shrinkage problem with the installation of an expandable bellows pressure compensator. However, this apparatus had the disadvantage of restricting flow through the tool and probably resulted in entraining water within the sampler.

Sampling Logistics

Fluid sampling was attempted at nine depths in Hole 504B during Leg 137. Sampling began at 0350 hr on 8 April after a section of the high-temperature logging cable was found to be faulty and prevented the successful completion of the temperature profile. Two sampling attempts were made with the LANL sampling tool deployed on the coring line. Sampling was resumed at 0800 hr on 9 April after the completion of the temperature profile. The LBL and LANL sampling tools were deployed in alternating sequence on the logging cable and coring line, respectively. The LBL tool was lowered at a maximum rate of 50 m/min until 50 m above the desired sampling depth, at which point its descent was slowed and stopped at the desired position to prevent disturbing the water within the borehole. During the first two runs the logging speed of the LANL tool was kept below 50 m/min to prevent any disturbance of the water column for the temperature profile. In subsequent runs, the LANL tool was run at maximum speed of near 90 m/min in the drill pipe, 50 m/min in the open borehole to 50–100 m above the desired sampling depth, tapering to a stop. Details of the fluid sampling runs are given in Table 8.

Methods

Sample Extraction Procedures

When taking fluid samples from reducing/oxygen-free environments such as exist in Hole 504B, it is desirable to limit exposure of the samples to the atmosphere. During previous DSDP/ODP legs to Hole 504B, precipitation of iron oxyhydroxides was observed immediately upon exposure of the sample to the atmosphere. To limit this problem the following extraction protocol was followed to either trap samples immediately upon removing them from the sampler, or process them in such a way as to minimize atmospheric exposure for rapid chemical preservation.

Samples were intended to be removed from the LANL samplers through extraction manifolds which were attached to each end of the sampler. The extraction manifolds are designed to push the valve springs open, allowing fluid to be withdrawn through the valve/manifold assembly. Due to high hydrostatic pressure built up inside the LANL tool (see discussion below) it was not possible to open the valves in this manner. During sample retrieval from the first run (Sample BS-1, 350 mbsf), attempts to open the valves resulted in bending the valve stems to such an extent that the only option for recovering the sample was to completely unscrew the valves and recover the fluid by pouring it into a sample bottle. On subsequent runs the threads connecting the valve assembly to the sampler were partially unscrewed to bleed off the high internal fluid pressure, and reassembled allowing extraction through the manifolds as planned. This allowed minimal exposure of the sample to the atmosphere prior to extraction. However, due to the release of pressure, gas samples may have been compromised.

Samples were removed from the LBL sampler through gold-plated rupture discs located at both ends of the sample chamber. Low-volume valves with specially designed puncture fittings were used to pierce a hole in the rupture disc allowing samples to be withdrawn without exposure to air.

All subsequent extraction description applies to both the LANL and LBL samplers. The samplers were placed upright, and a gas sampling manifold was attached to the upper extraction port. The gas manifold and sample bottles were evacuated with an attached vacuum pump. The vacuum was then shut off, and the samples bottles closed. The extraction valve on the sampler port was opened. The gas sample bottles were then opened and closed separately, and the pressure was recorded to allow calculation of the volume of gas retrieved in each sample.

After gas sampling, the fluid extraction was performed through the bottom sampling port while pushing nitrogen through the top. The sampling port was connected to a stainless steel valve with 0.25 cm teflon tubing to allow control of the sample flow. The first tens of milliliters were muddy (from settling solids) and were decanted into a polyethylene bottle through a piece of tygon tubing attached to the flow control valve. Next, a 20 cm piece of 1/4-in.-i.d. copper tubing was attached for collecting dissolved gases and helium isotope samples. Fifty to 100 mL of water was passed through the tubing (into the next aliquot) to make sure no bubbles were trapped, and the tubes were clamped shut. The copper tubes were removed and 500 or 1000 mL was collected for tritium analysis in glass bottles. The tygon tubing was removed and an in-line filter assembly was placed directly onto the flow

Table 8. Summary of fluid sampling operations.

Run no.	Tool	Date (1991)	Depth (mbrf)	Depth (mbsf)	Sampling times In hole	Collection	Out of hole	Volume (mL)	Temperature (°C)
BS-1	LANL	8April	3924	350	0455	0635	0730	>>1000	56
BS-2	LANL	9April	4124	550	0755	0915	1045	1010	90
BB-3	LBL	9April	4274	800	0000	0225	0405	1930	115
BS-4	LANL	9April	4424	950	0440	0600	0710	1000	130
BB-5	LBL	9April	4574	1100	0730	0930	1146	1990	134
BT-6	LANL	9April	4724	1250	1235	1320	1430	0	—
BB-7	LBL	9April	4874	1400	1445	1718	1900	1970	155
BS-8	LANL	9April	4974	1500	2030	2115	2200	1020	158
BB-9	LBL	10April	5020	1537	2215	0015	0230	1930	162

[a]On run 1, approximately 200 mL of fluid was lost due to internal overpressure and failure of the LANL extraction valves. On sample runs BS-2, BS-4, and BS-8, a small amount of fluid was lost due to cracking the valve fitting to relieve the overpressure (see text). Volumes were estimated to be ±20 mL.

control valve. Prewashed 0.45 μm cellulose millipore acetate membrane filters were used to remove suspended particulates from the remainder of the sample. The remaining sample was extracted into a 500 or 1000 mL polyethylene sample bottle. All sample containers were prewashed and flushed with nitrogen prior to sample extraction. All sample bottles, containers, and filters were weighed before and after filling to estimate the volume of recovered fluid at depth. The filtered sample was immediately divided into aliquots as described in Table 9.

Use of the in-line filter was particularly effective for avoiding atmospheric contamination. This was evident during the processing of sample BS-1. In this run it was necessary to filter the sample using a standard vacuum filtration apparatus due to the destruction of the sampler valves (see above). Precipitation of bright orange iron oxyhydroxides was evident within minutes of filtration. On subsequent runs the in-line filtering apparatus prevented this problem, and precipitation of iron oxyhydroxides in the unacidified samples was evident only after many hours to days.

Analytical Techniques

The methods for estimation of the dissolved constituents determined on board are described in the "Introduction and Explanatory Notes" chapter (this volume). Alkalinity and pH were determined immediately. A failure of the pH electrode during the alkalinity titration did not allow for the estimation of alkalinity for the final sample (BB-9). Hydrogen sulfide was fixed immediately by precipitation with $CdNO_3$ as CdS for later determination. An immediate dilution of 1 mL sample in 3 mL 0.1N HCl was made to prevent amorphous silica from precipitating out of solution. Chloride, magnesium, calcium, and nitrate were analyzed on unacidified aliquots in a period from hours to days after sampling.

Results

Chemical Composition of Borehole Fluid Samples

The results of shipboard analyses from Hole 504B borehole fluid samples are given in Table 10. The composition of surface seawater collected from Hole 504B during Leg 137 and surface and bottom seawater from the region as reported during Leg 111 (Shipboard Scientific Party, 1988) are provided as reference.

Of the eight samples obtained, seven appear to contain a large component of borehole fluid from the intended depths. Sample BS-4, intended to be taken from 950 mbsf, shows composition nearly identical to surface seawater. Rust scale flakes were observed on the inside of the filter screen located at the bottom of the LANL sampler subsequent to this sample run. This evidence suggests that the valves did not close properly, and seawater from very near the ocean surface was retrieved.

The depth profiles for major species are given in Figure 20. The chemistry reveals that oceanic bottom seawater is present to at least 350 mbsf, confirming results of the temperature profile indicating renewed downward flow into the upper section of Hole 504B. Calcium and dissolved silica increase

Table 9. Division of borehole fluid samples (listed in chronological order). All fluid samples from aliquot 5 were filtered through an in-line 0.45 μm cellulose acetate filter.

Aliquot no.	Function	Quantity/Container
1	1–3 10 mL/stainless gas bottles	Gas analysis, He isotopes
2	10–50 mL muddy H_2O/poly bottle	Mineralogical observations
3	15–30 mL/Cu tubing	Dissolved He isotopes
4	500–1000 mL/glass	Tritium
5	400–900 mL/poly	Filtered Sample
	5 mL unacidified/poly	Alkalinity
	1 mL diluted 1:4 (0.1N HCl)	Dissolved Si
	5 mL fixed with $CdNO_3$/poly	Sulfur isotopes
	100 mL with 1% 6N HCl/poly	Shipboard analyses/Sr, B isotopes
	4 each 5mL/glass ampules	O, C, and H isotopes, halides, and archive
	5 mL/poly tube	Archive
	10 mL/plastic	Shipboard analyses
	Remainder 1% HNO_3/poly	IC, ICP-MS, rare earths, and intercalibration of shipboard results.
6	In-line filter	Mineralogical/chemical examination.

Table 10. Chemical composition of borehole fluid samples.

Sample	Depth (mbsf)	pH	Alk (mM)	Salinity (‰)	Cl^- (mM)	Mg^{2+} (mM)	Ca^{2+} (mM)	SO_4^{2-} (mM)	H_4SiO_4 (μm)	Na^+ (mM)	K^+ (mM)	Sr^{2+} (μM)	Li^+ (μM)	H_2S (μM)	H_4^+ (μM)	$NOH_3^-+NO_2^-$ (μM)	NO_2 (μM)	PO_4^{3-} (μM)	Solids (mg/L)
BL-1	350	6.87	2.32	34.2	555	54.02	10.70	29.6	19	481	10.5	86	38	<2	23.8	23.5	1.38	0.0	62.5
BL-2	520	7.2	2.50	34.8	556	50.74	13.50	27.0	395	473	10.1	88	34	<2	4.5	22.5	2.49	0.3	104.3
BB-3	800	7.13	2.10	34.8	537	45.29	19.75	23.1	951	462	9.6	82	34	<2	16.1	6.25	3.45	0.5	56.3
BL-4	950	7.27	2.03	35.2	544	53.67	10.33	28.0	27	473	10.1	86	32	<2	5.8	38.8	0.23	0.0	68.8
BB-5	1100	6.82	1.90	34.1	554	42.32	22.80	19.9	1213	449	9.4	75	40	<2	16.1	8.59	2.82	0.7	27.9
BB-7	1400	7.08	1.90	34.0	553	43.92	21.93	20.2	1066	455	9.5	79	38	<2	17.4	8.07	1.44	0.3	14.9
BL-8	1500	5.66	1.74	33.4	556	26.88	42.99	6.1	1802	409	8.4	66	53	<2	35.4	1.06	0.33	0.7	41
BB-9	1550	5.84		33.5	559	35.91	31.23	14.4	1728	433	8.9	72	47	<2	23.8	2.75	0.25	0.7	25.2
SURF		8.03	2.36	33.5	549	53.75	10.33	27.7	2	473	10.3	86	29		0.0	8.02	0.38	0.7	
[a]DEEP		7.62	2.50	34.8	554	53.41	10.45	28.6	165	475	10.4					39.1		2.3	
[a]SURF		8.17	2.33	32.5	540	52.03	9.82	27.4		463	10.1					0.09			

[a]Surface and deep water from Leg 111 for comparison (Shipboard Scientific Party, 1988).

with depth and temperature, while magnesium, sodium, potassium, and sulfate decrease with depth. These trends are in agreement with past observations (cf. Mottl and Gieskes, 1990). Chloride concentrations are relatively constant throughout the borehole. Salinity, determined by refractive index, shows a slight decrease with depth.

Anoxic conditions in the borehole were inferred from the precipitation of large quantities of orange iron oxyhydroxides in the solids aliquots upon exposure to air. Alkalinity and pH decreased with depth. Hydrogen sulfide was below detection limits of 2 μM. Ammonium increased gradually with depth. Nitrate and nitrite were present in variable quantities, presumably as a result of contamination from pipe greases (see discussion below).

It appears that some contamination of samples BB-7 and BB-9 resulted in decreases in the compositional changes relative to seawater in comparison to the next shallowest sample. This could be a result of pushing fluid down the borehole from previous runs, entrainment of fluid in the sampler, or opening the sampler valves on ascent as discussed above. Entrainment of fluids within the LBL sampler is a likely possibility since the internal area of the sampler was significantly reduced by the presence of the pressure compensating bellows.

A complete review of the sources of contamination is given in Mottl and Gieskes (1990). The presence of rust debris on the sampler screens and ubiquitous grease on the samplers are obvious sources for contamination. In one case, sample BS-4, the presence of rust scale prevented complete closure of the valve, resulting in obtaining a sample of predominantly surface seawater. Large flakes of rust scale were also found in the valves of the LANL sampler during sample run BT-6, resulting in no sample recovery. The solids aliquots often smelled of burnt petroleum. Grease was observed in the solids and on the filters from all samples (see section "Particulates from Borehole Water Samples" below).

In past studies, the concentration of dissolved nitrate + nitrite has been used to correct for bottom water contamination during sampling (cf. DSDP Leg 83, Mottl et al., 1985). Since conditions in Hole 504B are reducing, with abundant dissolved iron, it is believed that nitrate + nitrite cannot be present for any sustained amount of time. Thus, any measured nitrate + nitrite was assumed present as a result of oceanic bottom water contamination.

This correction may not always apply. The correction would not account for nitrate-free fluids pushed down from shallower depth in the borehole. Experiments with bentonite drilling mud during Leg 111 show that NO_3– is released upon reaction with seawater at elevated temperatures. The large amount of drilling mud recovered in DSDP Leg 92 samples may have contributed nitrate + nitrite to the samples as suggested during Leg 111 (Shipboard Scientific Party, 1988). Other possible sources of nitrate + nitrite are the various greases used on the drill pipe. As mentioned earlier, the sampling tools came to the surface covered with grease, and the solids aliquot smelled of burnt petroleum from samples taken deep in the borehole (samples BB-5, BB-7, BS-8, and BB-9).

The effect that pipe greases may have on the nitrate + nitrite concentrations of the samples was the subject of a shipboard laboratory experiment. Two lubricants used on the drill pipe prior to the sampling run were collected for investigation. DP Sedco Forex ZN-50 is a petroleum-based drill pipe compound composed of 50% zinc. DP Sedco Forex L-60 is a petroleum-based drill collar compound composed of 60% lead. One gram of each lubricant was placed in 200 mL of 3% NaCl solution in a 500 mL beaker. The covered mixture was placed on a hot plate and heated to 100°C for 3 hr to simulate the average time for the sampler in the borehole. The solutions were cooled, filtered with a 0.45 μm filter, and stored in the refrigerator until analyzed for $NO_3^- + NO_2^-$ 6 hr later. The $NO_3^- + NO_2^-$ concentrations of the solutions were determined to be 6.1 μM and 11.5 μM for the ZN-50 and L-60 grease experiments, respectively. These values correspond to 1.2 μmole and 2.3 μmole $NO_3^- + NO_2^-$ released per gram of lubricant, respectively. Thus, it would take only 20 g of L-60 grease per 1-L sample to yield a $NO_3^- + NO_2^-$ equivalent to bottom seawater concentrations.

Thus, the release of $NO_3^- + NO_2^-$ from the greases during sampling could easily account for the variable nitrate concentrations. For this reason, no correction for bottom water contamination based on $NO_3^- + NO_2^-$ was applied.

Sampling Tool Evaluation

The quantity of recovered fluids can yield some insight to performance of the samplers (Goff et al., 1990). The contraction of the samples during cooling during ascent through the cold water column was a concern prior to sampling. The volume of water recovered at the surface should be less than the total volume of the sampler at atmospheric pressure if the sampler did not leak upon ascent. Table 11 shows the percentage volume change based on the sampler volume at the surface ($\%\Delta V_s$, 25°C, and 1 bar). The theoretical percent volume change (from Kennedy and Hosler, 1966) for pure water between the borehole and the seafloor ($\%\Delta V_1$) and between the seafloor and the surface ($\%\Delta V_2$) are also included. The sum of these quantities ($\%\Delta V_t$) is the net expected percentage volume change. It is important to note that our volume calculations are based on the weight of sample in each aliquot, not accounting for fluid lost during gas sampling, or as a result of minor spills, and are thus minimum values. The volumes were calculated using 1.025 g/mL as the density of

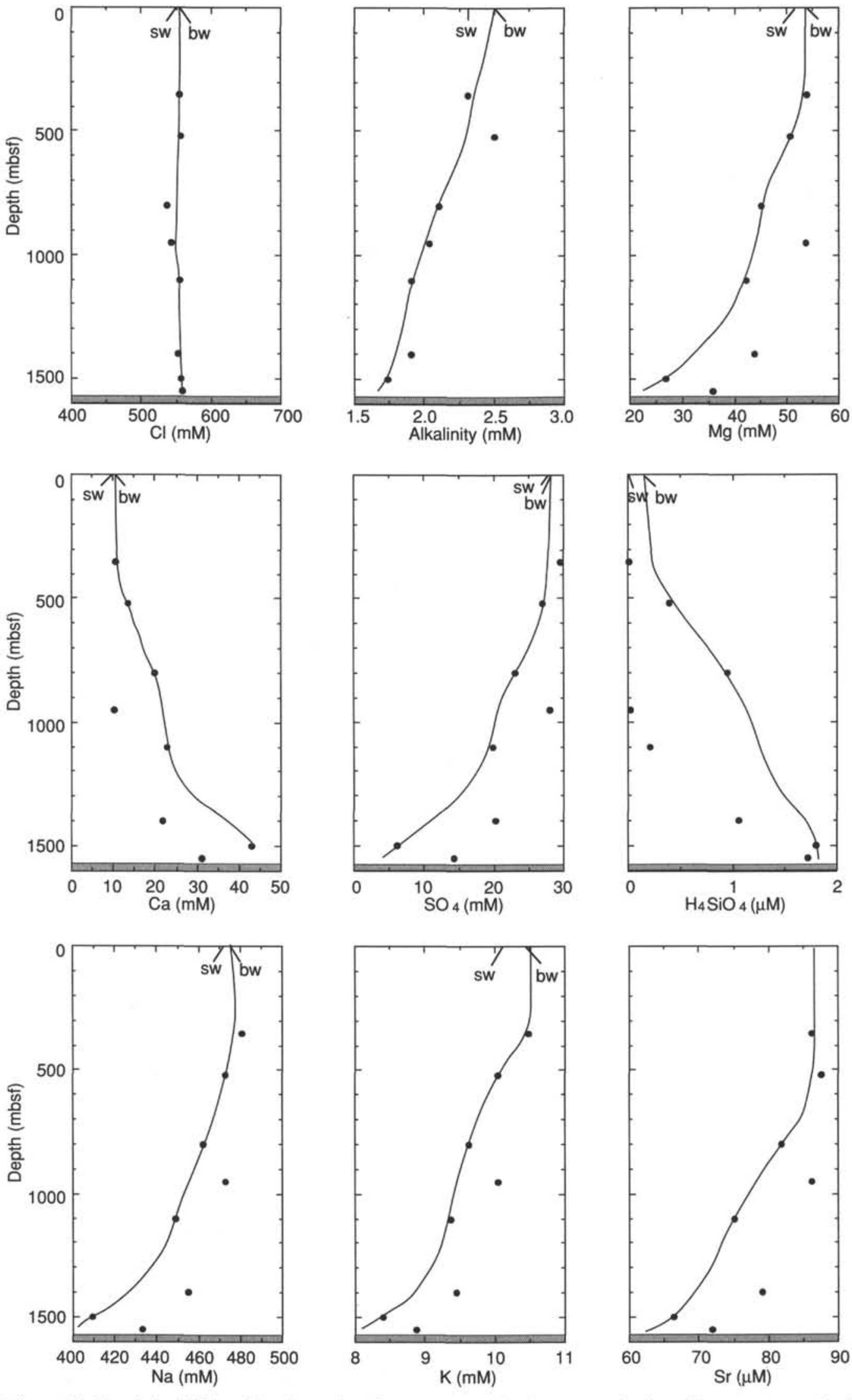

Figure 20. Borehole fluid profiles for selected components. Surface water (sw) and bottom water (bw) concentrations are shown for comparison.

Table 11. Comparison of recovered fluid sample volume with theoretical values.[a]

Sample	Temperature (°C)	Pressure (bar)	$\%\Delta V_1$	$\%\Delta V_2$	$\%\Delta V_t$	$\%\Delta V_s$
BL-1	56	394	−1.0	+2.9	+1.9	[b]>0
BL-2	90	414	−3.6	+2.9	+0.7	[c]+1.2
BB-3	115	429	−4.7	+2.9	−1.8	[c]−4.9
BL-4	130	445	−5.8	+2.9	−2.9	−0.6
BB-5	134	460	−6.1	+2.9	−3.2	−6.4
BB-7	155	490	−7.8	+2.9	−4.9	−6.7
BL-8	158	500	−8.1	+2.9	−5.2	+2.9
BL-9	162	504	−8.3	+2.9	−6.2	−9.1

[a]$\%\Delta V_1$ is the volume change expected when moving pure water from the ambient temperature and pressure in the borehole to 2°C and 359 bars at the seafloor. $\%\Delta V_2$ is the volume change expected when moving a parcel of pure water from the seafloor to the surface at 20°C and 1 bar. $\%\Delta V_t$ is the sum of these effects. $\%\Delta V_s$ is the difference between the volume of recovered fluid and the sampler volume at 20°C and 1 bar. Information on the specific volume of pure water at varying pressures and temperature was obtained from Kennedy and Hosler (1966).

[b]Approximately 200 mL lost upon extraction. Volume was greater than at atmospheric pressure as evidenced by high internal hydrostatic pressure.

[c]Some sample was spilled (10–25 mL) during sample extraction.

seawater at 20°C. Thus, we feel the estimates are good only to a few percent.

The pressure-compensating bellows on the LBL sampler performed their function. Upon retrieval of the sample the bellows were expanded in compensation for the contraction of the samples. The volume changes appear greater than what is expected for pure water. This could be the result of a number of factors, including variations in the compressibility and/or thermal expansion between pure water and seawater, loss of fluid during gas extraction, or decreased volume of the sampler due to incomplete retraction of the pressure-compensating bellows from subsequent runs. In general the direction and magnitude of the volume changes matches the expected deviations. On the two final runs of the LBL sampler, the volume of fluid expelled from the bellows when recompressing them to their original volume was measured, yielding 150 mL and 160 mL for samples BB7 and BB9, respectively. These measurements correspond to sample shrinkages of 7.1% and 7.6% and are in agreement with the percentage volume change expected (Table 11).

The overpressure which prevented proper extraction of samples from the LANL tools is direct evidence indicating the opening of the samplers during ascent. Hydrostatic expansion would account for the observed internal overpressure within the LANL tools. At some point the volume shrinkage during cooling forced the valves to open, filling the sampler to capacity. The valves probably reseated as the tool was raised through the water column and were held shut by building internal hydrostatic pressure upon ascent. The measured volumes for all samples (excluding sample BS-4 which contained surface seawater, see above) indicated that the volume of seawater recovered was greater than the volume of the sampler at one atmosphere. The recovered volume for sample BS-8 matched the hydrostatic expansion ($\%\Delta V_2$, Table 11) for bringing the sample from the seafloor to the surface.

Each sampler appears to have advantages and drawbacks. The sample with the greatest change from seawater composition (BS-8) was obtained with the LANL tool. The LANL tool also has the apparent advantage of rapid deployment on the coring wireline. However, this rapid descent may have contributed to the dilution of the samples taken on the following runs (with the LBL tool). The deepest sample (BB-9) shows less change from seawater than the sample immediately above it (BS-8). The large diameter sinker weight attached above the LANL tool could have created significant turbulence in the borehole, causing fluids to be mixed as it was lowered and withdrawn at high speeds. The lack of a pressure-compensating device on the LANL tool accounted for its opening upon ascent, as evidenced by its excess sample volume and hydrostatic overpressure. The extraction manifolds for this sampler were inadequate to handle the hydrostatic overpressure. Rupture discs similar to the LBL design would be an improvement.

The positive identification of the depth of closure, and temperature measurement are definite advantages to the LBL tool. While the logging cable speeds are limited compared with the freefall of the coring line, this may be insignificant as faster speeds will mix more fluid in the borehole, and coring line sampler deployment speed should be much slower than was used during Leg 137. However, as higher temperature boreholes are encountered, the logging cable may prove to be inoperable, and a mechanical clock firing mechanism would be necessary. The pressure-compensating bellows of the LBL tool appears to have performed its primary function quite well, as samples of expected volumes were recovered. However, the bellows must have greatly reduced the flushing effect produced by lowering the tools down the borehole. This counteracts the advantages of using a flow-through sampler, by creating areas to entrain fluid from shallower depths. Further development of a pressure-compensated sampler is needed.

Particulates from Borehole Water Samples

The total quantity of recovered particles was between 14 and 105 mg/L (Table 10). This indicates that flushing of the borehole at the end of Leg 111, with approximately 6.5 hole volumes of surface seawater, was adequate to remove the bentonite drilling muds. The estimate of total recovered solids does not include the suspended particulates from the unfiltered aliquots, but solids in these fractions would only increase recovery by a factor of 2 at the most.

The solids aliquots were filtered with 0.45 μm millipore filters, and were air-dried for 24 hr. These filters and the filters from in-line filtration were examined under a binocular microscope to identify the particles present. Generally the same type of material appeared on all the filters, although the grain size and amounts of material varied. The particulates mainly consist of fine- to coarse-grained (<10–600 mm) orange to red Fe-oxides plus lesser amounts of similar-sized particles of black grease. The Fe-oxides are likely rust fragments from the casing in the sediment section, plus some very fine-grained material that precipitated from solution prior to filtering. Also present are deep red colored, shiny, curved fragments of Fe-oxide, 50–200 mm in size, which appear to be replacements of diatoms or foraminifers.

X-ray diffraction identified goethite in all samples analyzed (BB-3, BB-5, BB-7, and BS-8), but material amorphous on X-ray may also be present. Round and globular white foraminifers/diatoms also occur in trace amounts in samples BB-5 and BB-7. Shiny steel metal shavings were observed in samples BS-4 and BB-5, and brassy yellow metal shavings occur in samples BB-3 and BB-5. Clear, flat, prismatic grains, 50–200 mm in size, are rare in samples BB-3 and BB-7, but are common in samples BB-5, BS-8, and BB-9. X-ray diffractograms of smear slides from samples BB-5 and BS-8 exhibit the major peak for anhydrite, consistent with prior tentative visual identification of these crystals as anhydrite. Anhydrite probably did not show up in all the diffractograms because it is a minor to trace constituent, and very small amounts of

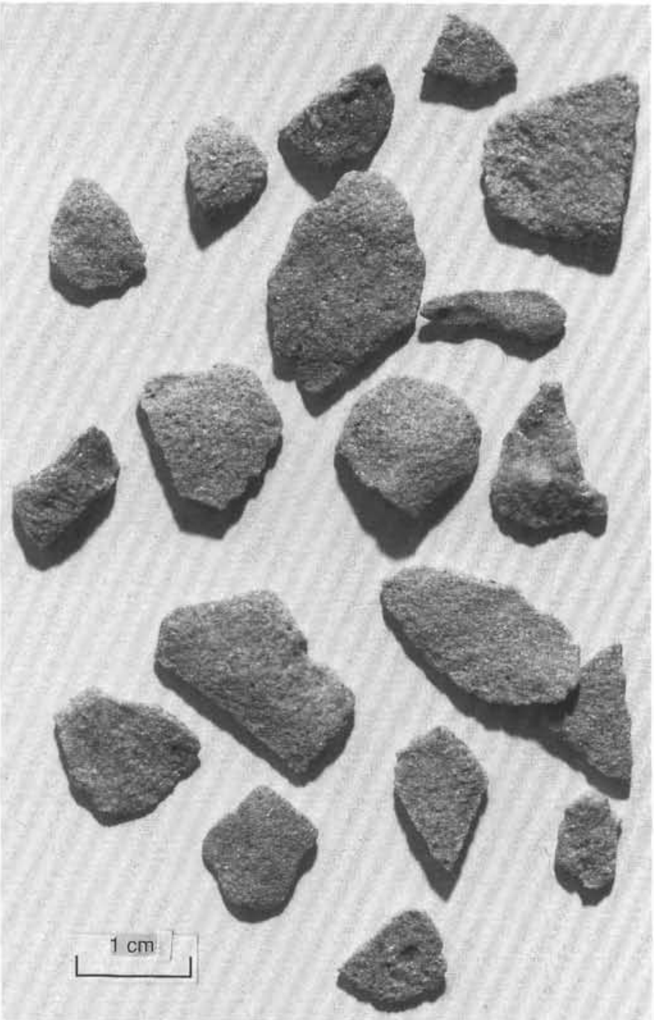

Figure 21. Close-up photograph of anhydrite crusts recovered from the first junk basket.

material were X-rayed. White and rare dark gray grains of plagioclase(?) and basalt(?) occur in small amounts in samples BB-3, BB-7, and BB-9.

Small red filaments, <10 mm in diameter and ≤ 200 mm long, are present in samples BB-4 and BB-8. Similar filaments were observed in borehole water samples from Leg 111 (Shipboard Scientific Party, 1988), and were suggested to be bacterial in origin. These were only observed in the Leg 137 samples that had very small amounts of material on the filters, suggesting that such filaments may be present on filters from other samples, but that they are covered by other material. Traces of a bluish-green granular material, which appears similar to a copper salt, were observed in sample BB-7. A fragment of green clays, apparently broken from the wallrock somewhere, is present in sample BB-5.

The first junk basket run in the hole recovered several pieces of a white to tan colored crust, 1–4 cm across and a few mm up to 1 cm thick (Fig. 21). The pieces range from nearly flat to slightly curved. These crusts are made up of intergrown, clear, flat prismatic grains, 50–200 μm across. X-ray diffraction confirmed that the crusts are composed of 100% anhydrite. The presence of anhydrite in particulates from water samples from 800 mbsf and below suggests that anhydrite is precipitating from fluids in the borehole at these depths. The pieces of anhydrite crust from the bottom of the hole probably represent the thicker and more durable fragments of an anhydrite crust that may continuously coat much of the lower portion of the hole. The crust is likely made up of anhydrite crystals precipitated *in situ* along the borehole walls as well as grains that precipitated within the borehole fluids and settled to the bottom.

Borehole Fluid Samplers Tested during Leg 137

The borehole fluid sampling problems encountered on previous legs to Hole 504B reviewed by Mottl and Gieskes (1990) and problems anticipated in the future suggested a need for developing new sampling techniques for oceanic borehole sampling. During Leg 137, two samplers used for downhole fluid sampling in the Continental Science Drilling Project (CSDP) wells, one from Lawrence Berkeley Laboratory (LBL) and one from Los Alamos National Laboratory (LANL), were tested for their applicability in deep ocean environments. The following describes the design and performance of these samplers in Hole 504B on Leg 137. Also included is a general discussion of the difficulties in obtaining samples from high temperature boreholes.

Los Alamos National Laboratory (LANL)/Leutert Borehole Samplers

A commercially available fluid sampler made by Leutert Inc. and a modified version constructed of titanium were used to sample Hole 504B (Fig. 22). The LANL/Leutert samplers are flow-through samplers, meaning that borehole fluids continuously flow through the sampler until the sampler valves are closed. The sample enters through the bottom nose cone of the sampler and exits just past the upper valve through exit ports. The sampler valves are held open on each end by springs that are compressed and held in place by a trigger mechanism. The triggering mechanism is controlled by a mechanical clock that can be set for up to 10 hr. The clock chamber is isolated from the outside environment by O-ring seals. When the clock allows the trigger to fire, springs push the valves closed. The closing of the valves isolates the sample in the sample chamber. The flow-through design eliminates the problem of the sample flashing into a steam phase, which is possible if the sample is flowing from a high-pressure to an evacuated sample chamber at high temperatures.

The original sampler was constructed of 316 stainless steel with seals and O-rings made of Viton. A titanium version of the original stainless sampler was fabricated for work at high temperatures and corrosive conditions. All the parts including the sample chamber were made from Beta-C titanium. Since the original O-rings and seals were of a lower temperature polymer, they were replaced by the high temperature O-ring material EPDM (ethylene propylene diene monomer).

The stainless steel sampler has an outside diameter of 1.50 in., is 108 in. long, and weighs 40 lb. The titanium sampler is also 108 in. long, but is slightly wider at 1.625 in., and weighs approximately 30 lb. The volumes of the samplers are 990 mL for the titanium version and 1000 mL for the standard sampler.

The sampler is triggered by a mechanical clock, thus avoiding the need for any electrical input. This eliminates problems seen with electrical and logging cables that occur when temperatures are above 250°C. When the clock reaches its preset time, the triggering mechanism allows springs to close the valves. To avoid binding caused by dissimilar material expansions as seen in the standard clocks at high temperature, hardened clocks made entirely of stainless steel were fabricated for use at high temperatures.

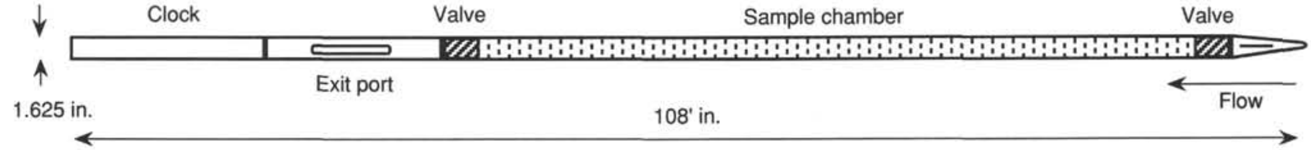

Figure 22. Diagram of the LANL/Leutert fluid sampler.

To guard against accidental spring opening due to thermal contraction of the sample, a positive lock collet was developed. The collets hold the valves in place after firing so that sealing is not compromised due to reversal of pressure that can occur when hot samples are cooled and contract.

Sampler Performance during Leg 137

Good samples were obtained at 350, 550, and 1500 mbsf. Poor samples or no sample were obtained at 950 and 1250 mbsf. Table 8 gives details of the sampling of Hole 504B. Both the stainless steel and the titanium sampler were tested. Also, several valve configurations were used to evaluate the best valving for further sampling of deep ocean drill holes.

Several problems with these samplers were discovered during the sampling of Hole 504B. Problems during runs BS-4 and BT-6 (950 and 1250 mbsf) were attributed to large rust flakes that back-flowed into the samplers resulting in valve sealing failures. This problem was eliminated on run BS-8 (1500 mbsf) with a screen added to prevent material from entering the top exit ports.

Another difficulty encountered was reopening the samplers with the standard valve opener to extract the sampled fluids. This was caused by the inability of the opener to overcome the excessive hydrostatic pressure of the samples when brought to the surface from depth. This problem could be overcome in two ways. The first option would be to strengthen the valve opener and valve stems to accommodate greater hydrostatic pressures. Another way would be to have a puncture disk arrangement incorporated into the sample chamber that would allow retrieval of sample without reopening the valves.

One serious problem to contend with in very hot wells is the contraction of the sample on cooling. This causes the valves to open briefly as the contraction overcomes the spring tension of the valves. This force is counteracted by the decrease in outside hydrostatic pressure as the sampler is brought to the surface. This can allow fluids to leak in until the hydrostatic pressure differences overcome the contraction of cooling sample. To overcome this problem, collets that do not allow movement of the valve springs once the sampler closes were tested on sample BS-2. This arrangement seemed to work well for this run, but unfortunately the collets were not tested in the hottest part of the well (BS-8, 1500 mbsf) because the addition of a screen to prevent rust from entering valves did not allow placement of the collet on the upper valve. This collet arrangement can be improved on and may prevent valve leakage.

One advantage of the Leutert sampler is that it does not need an electric logging type cable to operate. This is an advantage because coring lines generally can be run in and out at faster speeds. Since the reliability of logging cables decreases with higher temperatures, the dependence of electrical inputs is eliminated. The one problem with using the mechanical clock is that there are no records of temperature or exact time of sampler firing.

Lawrence Berkeley Laboratory (LBL) High-temperature Borehole Fluid Sampler

Under contract to the U.S. Department of Energy, Division of Geothermal Technology, LBL designed and fabricated a flow-through downhole sampler. The sampler is rugged, simple to operate and maintain, and can operate in high temperatures and corrosive environments. The sampler is fabricated of MP35N alloy, which is chemically inert to wellbore fluids and gases. Table 12 lists the specifications for the sampler.

The sampler (Fig. 23) is of the flow-through type; that is, while the instrument is lowered down the wellbore, the upper and lower valves are in the open position and fluid is free to enter at the bottom and exit at the top of the sample chamber.

The mechanism used for holding the valves open until closure is required consists of two primary components: an electromagnet assembly and a lock-ball arrangement. When the magnet is energized with current, the lock balls hold the valves open. After the current is removed from the magnet, the lock balls disengage the valves from their open position and they are driven into a shut position by heavy spring pressure.

Operating Procedure

The sampler is attached to a single or multiconductor cable with an appropriate cablehead. The interior of the magnet housing is filled with high-temperature insulating oil to protect electrical components from the adverse effects of downhole fluid. Even though these parts are in pressure equilibrium with the downhole fluid during a sampling run, the high density of the injected oil prevents fluid from entering. This technique eliminates the need for differential pressure seals on the tool, except as required for sealing the sample chamber.

Before lowering the sampler into a well, the upper and lower sampler valves are opened with the help of cocking tools and held in that position by supplying the required current through a single conductor of the logging cable. The sampler is then lowered downhole. After the appropriate sampling depth is reached, the sampler valves are closed by decreasing the current supplied to the electromagnet. A sudden drop in the current readout at the surface indicates that the valves have closed.

Table 12. LBL fluid sampler specifications.

Sampler type:	Downhole flow-through
Length:	110 in. (279 cm)
Diameter:	2.25 in. (5.72 cm)
Weight:	75 lb (3.4 kg)
Sample volume:	2,000 mL
Material:	MP35N alloy (all parts in contact with well fluid)
Sampler pressure: (internal) at 350°C)	20,000 psi (pending hydrostatic proof test
Temperature limit:	350°C
Power requirement:	40 ma DC

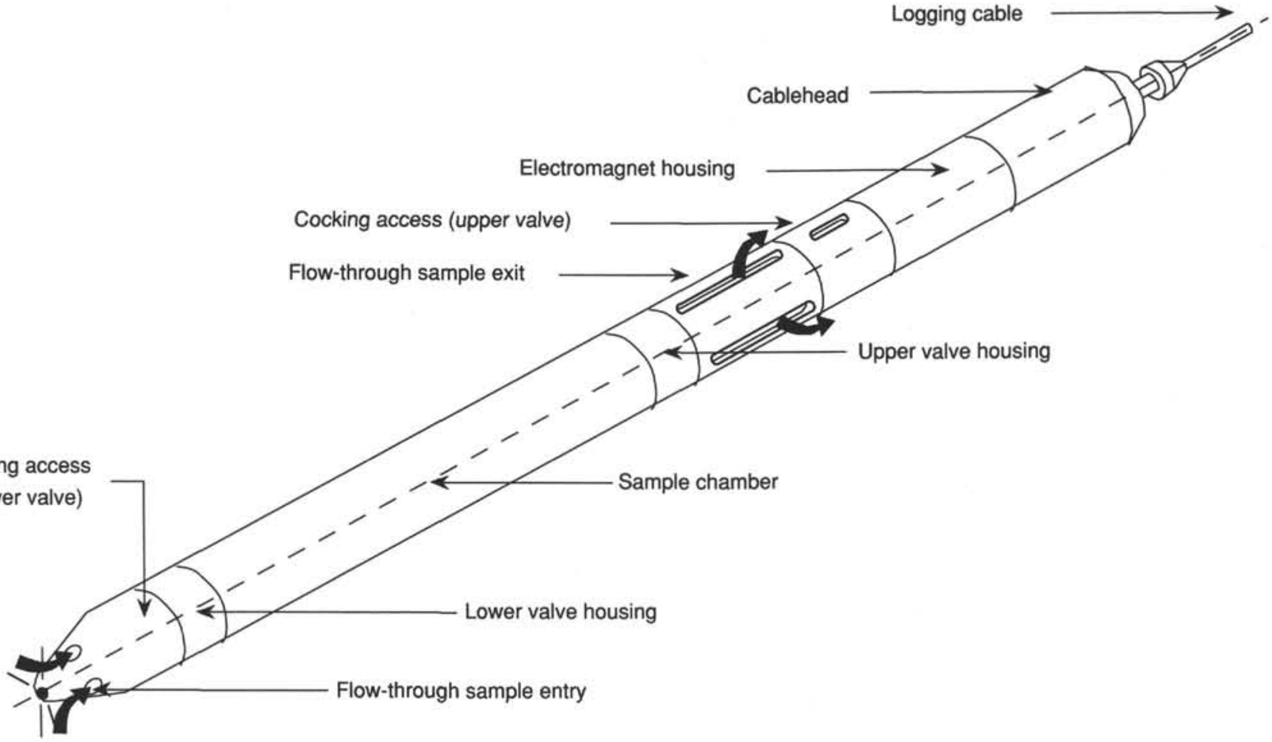

Figure 23. The LBL fluid sampler with its major components and the fluid flow path during sampling.

After retrieving the sampler, small piercing valves are attached to rupture disks located on each end of the sampler chamber. A sample extraction system is then attached to remove gas and fluid from the sampler without exposing them to air.

After the sampler valves are closed, they are designed to be held in the closed position by heavy spring pressure. As the sampler is brought up from depth, they seat even better than during the initial closure, since they were designed to take advantage of the ever-increasing pressure differential between the sample chamber and the constantly lowering hydrostatic pressure surrounding the sampler.

This system works perfectly if there is no pronounced cooling of the sample during retrieval from depth, but severe cooling of the sample does occur when it is brought up from the elevated temperatures found in Hole 504B and exposed to the relatively low temperatures in the drill string through the oceanic water column. This cooling shrinks the volume of the sample and drops the pressure inside the sample chamber. The high hydrostatic pressure surrounding the sampler can then force the valves inward and let fluid leak in and mix with the sample.

To resolve this problem, the LBL sampler was fitted with an internal bellows system (volume compensators) which was intended to make up the volume the sample lost during cooling and provide internal pressure within approximately 125 psi of the actual hydrostatic pressure. Using this technique, the 350-lb spring pressure used to hold the valves shut was more than sufficient to prevent leakage of fluid into the sampler. The bellows system adversely affects the flow-through characteristics of the sampler. Due to internal obstructions, it may take longer for fluid to flush through the sampler as it moves downhole.

Sampler Performance during Leg 137

The LBL sampler successfully retrieved samples from various depths in Hole 504B. The sampling and sample extraction process were carried out without any problems. Some contamination of the fluids was indicated by the chemical analyses. This contamination was probably the result of entrainment of fluid within the sampler due to the presence of the internal bellows.

Suggested Modification to the LBL Sampler.

The LBL fluid sampler was able to retrieve samples from Hole 504B during Leg 137, with some contamination. The shrinkage of the sample during retrieval from depth will most certainly cause more of a problem in higher temperature boreholes. One relatively simple solution to the problem would be to make the lower valve assembly into a moveable piston. As the sample cools, and begins to shrink, an O-ringed piston which is part of the lower valve assembly is forced upward into the sample chamber by hydrostatic pressure occupying the volume vacated by the shrinking fluid sample. This will keep the hydrostatic pressure in equilibrium with the sample pressure except for the friction and weight involved in moving the piston. Sampler valve springs of sufficient strength would certainly be able to compensate for that small amount of pressure differential. The bellows used in the LBL sampler work on the same principle as the sliding piston but can only compensate for small amounts of shrinkage. The moveable piston modification will also allow unobstructed flow through the sampler.

Discussion

The data from Leg 137 borehole fluid samples appear to agree with past studies of the hole suggesting removal of magnesium, potassium, sodium, and sulfate, in exchange for increasing concentrations of calcium with depth (Fig. 20). Figure 24 shows a comparison of the magnesium profile of Leg 137 to the non-nitrate corrected data from Legs 83, 92, and 111 (Mottl and Gieskes, 1990). Samples which appear to be contaminated by fluids from above are omitted from Figure 24

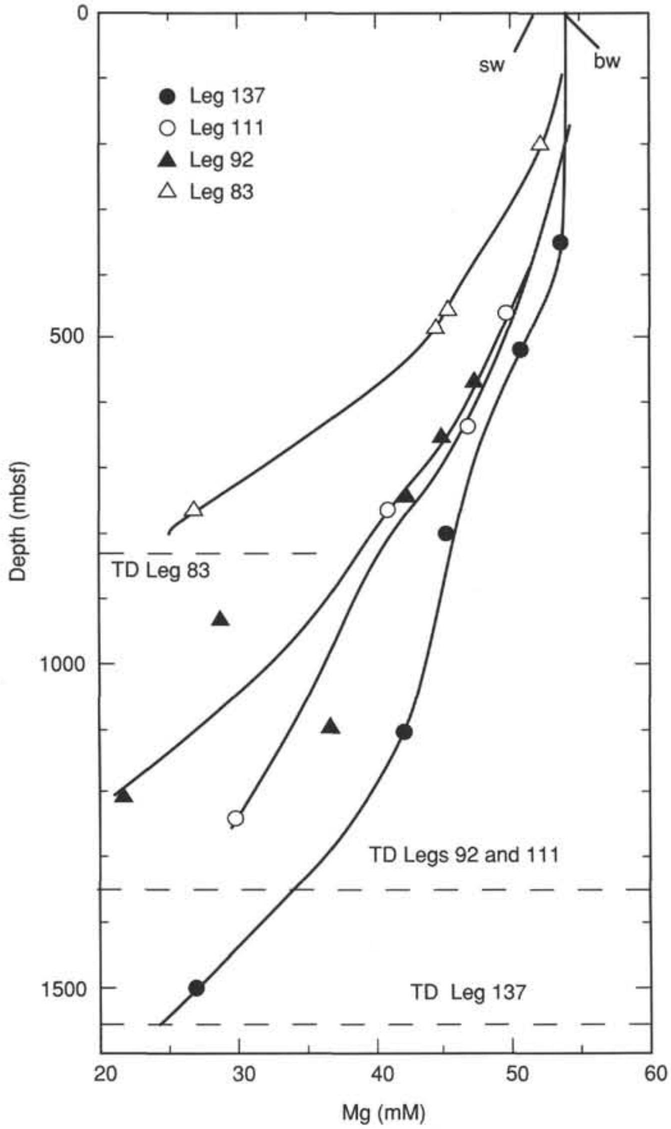

Figure 24. Comparison of magnesium profiles from Legs 83, 92, 111, and 137. Surface water (sw) and bottom water (bw) concentrations are shown for comparison.

for clarity. Two factors must be considered when this comparison is made: (1) only Legs 92 and 111 represent sampling of Hole 504B when it was the same depth, and (2) different time intervals had elapsed between previous disturbance due to drilling and sampling on each leg. The profiles show that the change of borehole fluid composition from seawater composition appears to decrease at a given depth from Leg 83 through Leg 137. The concentration of magnesium at the bottom of the hole for each respective leg appears constant. Profiles such as these could arise from slow downhole mixing of bottom seawater with a component of reacted fluid.

Element vs. element correlation plots for Leg 137 borehole fluid are shown in Figure 25. The linear relationships are quite good for all correlations. This suggests linear mixing of two components. One end-member is bottom seawater (the mixing line passes through this point), and the other lies along the mixing line past the data point furthest away from bottom seawater. Any deviations from the mixing line can be interpreted as reaction occurring in the borehole water column or during sampling. For example the silica vs. magnesium graph reveals linear mixing trends, except for sample BL-8. The silica concentration for BL-8 falls below the mixing line suggesting removal of H_4SiO_4 from the sample. This probably occurred during ascent through the water column as the sample cooled and amorphous silica was precipitated from solution.

Mottl and Gieskes (1990) suggest that the other end-member lies at the point where the concentration of magnesium is equal to zero. While a complete removal of magnesium in the borehole by reaction with the wall rocks appears unlikely due to the high water/rock ratio (water/rock = 10^4–10^5), magnesium may be close to zero in the formation fluids themselves. Table 13 provides a comparison of the extrapolated zero Mg "end-member" from Leg 137 with the calculated end-member values reported in Mottl and Gieskes (1990).

The sulfate vs. magnesium graph (Fig. 25) reveals that sulfate is removed before complete removal of magnesium. This suggests removal of sulfate from within the borehole. The presence of anhydrite ($CaSO_4$) on the filters from the borehole fluid samples confirms that removal of SO_4 does occur. The precipitation of anhydrite from seawater was predicted in experimental studies at temperatures between 100°C and 150°C by Seyfried and Bischoff (1979). Observations of relatively large anhydrite crusts recovered while cleaning junk from Hole 504B, and apparent undergauged hole diameter are strong evidence that anhydrite is precipitating along the borehole walls at least in the bottom few hundred meters. Further examination of the anhydrite recovered in the fluid samples and from the junk baskets will be performed in shore-based laboratories.

Summary

Seven samples were recovered from the basement section of Hole 504B. Two of these samples, BB-7 and BB-9, were determined to have been diluted with waters from depths shallower than the intended sampling depths. Adopting corrections for bottom water contamination based on the dissolve nitrate + nitrite concentrations was deemed unsupportable given the confirmed release of nitrate from the drill pipe compounds.

The chemical analyses suggest that the loss of magnesium, sodium, and potassium is roughly balanced by increases in calcium. Relatively undiluted bottom seawater is present in the borehole to a depth of at least 350 mbsf, supporting the results of the temperature profile suggesting that the formation has not reached hydrostatic equilibrium almost 15 years after first drilling. Initial comparison of this data set to past studies of borehole fluids from Hole 504B suggests that mixing of bottom water entering the top of the borehole with a basalt reacted "end-member" does occur. While the shapes of downhole profiles have changed as Hole 504B has been deepened, the "end-member" composition has remained relatively constant. The discovery of anhydrite crusts apparently precipitating on the walls of the borehole confirms predictions that anhydrite is saturated in the deeper, higher temperature Hole 504B borehole fluids.

TEMPERATURE LOGGING

Introduction

Leg 137 represented an outstanding opportunity to log equilibrium temperatures in Hole 504B, given that nearly 5 years had passed since the last thermal disturbance to the hole during Leg 111. After the first reentry of the hole during Leg 137, the pipe was held within the casing, and temperatures were logged and borehole fluids sampled before any circulation or drilling operations. Similar undisturbed temperature

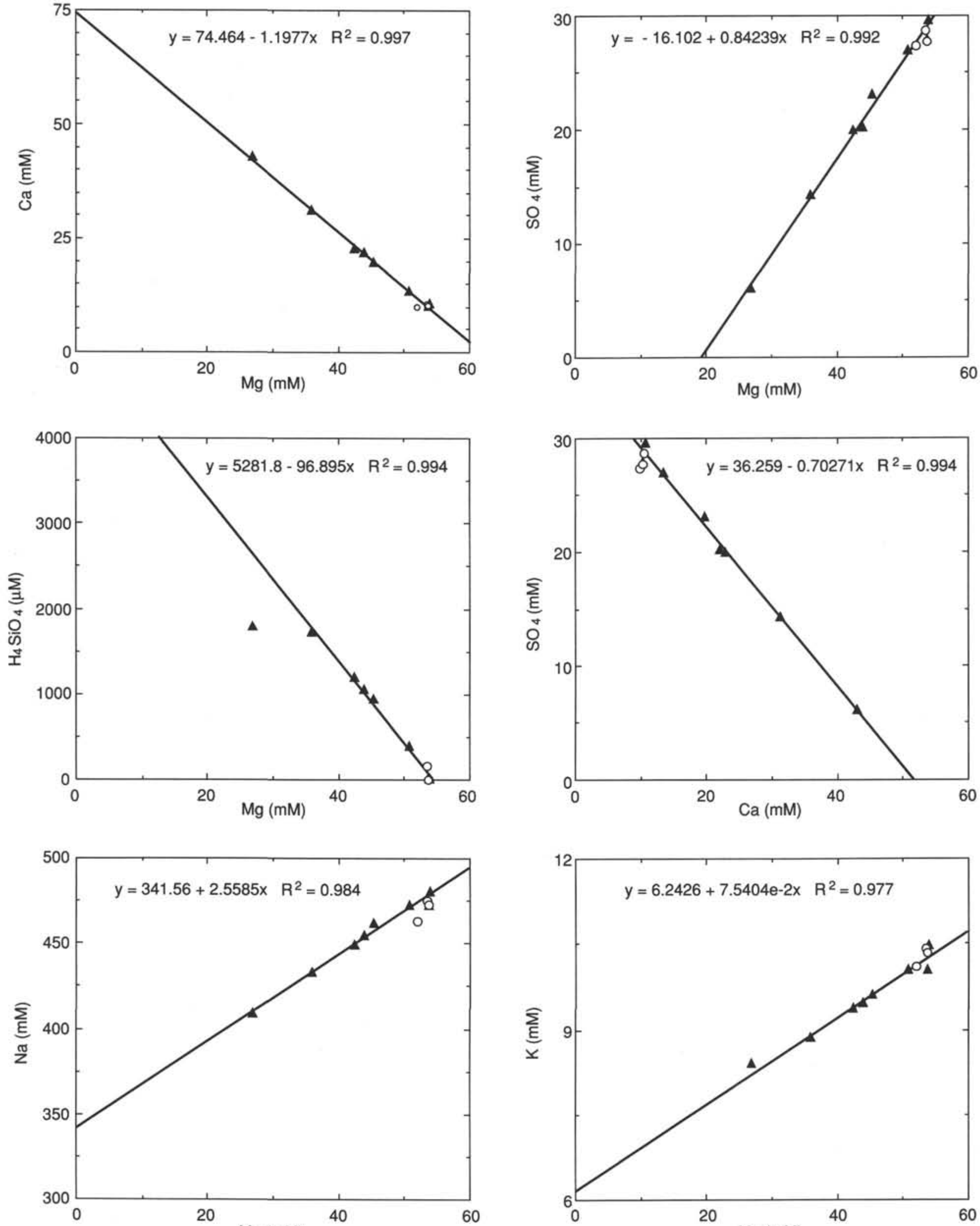

Figure 25. Element vs. element correlations. Lines are the linear regression of the sample data. For H_4SiO_4, sample BL-8 was omitted from the regression (see text). Bottom seawater composition (circle) is provided for comparison.

Table 13. Calculated "end-members" for borehole fluids from Leg 137. End-member concentrations are calculated by extrapolation of element vs. magnesium graphs to zero magnesium. End-members from Mottl and Gieskes (1990) are supplied for comparison.

Component	Leg 137	Previous legs
Mg (mM)	0	0
Ca (mM)	74	70 ± 5
K (mM)	6.2	4.5 ± 1
Na (mM)	342	400 ± 20
SO_4 (mM)	0	0

profiles had been obtained after the initial reentries of Legs 70, 83, 92, and 111 (Becker et al., 1983a, 1983b, 1985; Gable et al., 1989); thus, the Leg 137 temperature log represented the latest in a series of studies extending to greater and greater depths over a period of 12 years.

Temperature-Logging Equipment

The equipment used to obtain a temperature profile in Hole 504B during Leg 137 was essentially the same as that used by Gable et al. (1989) to log temperature during Leg 111 nearly 5 years earlier. However, the temperature sensors used in the earlier deployment were replaced by others having a greater measurement precision at the anticipated higher temperature range. This adjustment improved the resolution capability of the temperature probe for the Leg 137 deployment.

Probe

The downhole probe is a cylinder made of stainless steel, 60 mm in diameter and 3 m in length, weighing 50 kg. The temperature sensors are accurately calibrated thermistors housed in a 5-mm-diameter tube at the lower end of the probe. Temperatures are determined from the resistance of two thermistors that can be monitored separately or in combination for maximum sensitivity across the entire logged interval.

Measuring and Recording Equipment

The control unit, monitored with a personal computer, acquires data being transmitted through the seven-conductor logging cable and records and displays thermistor resistance values. The unit includes a DC current calibrator and a digital voltmeter. The validity of the recorded thermistor values can be verified by substituting a 10-kohm precision resistor for the cable and probe.

Calibration

The entire system, including simulated cable resistance, was calibrated at the Laboratoire National de Mesures in Paris, which issued a calibration certificate. Calibrated resistance data for the entire system are given in Table 14. The temperature-resistance calibration data were fit to the standard function for thermistor resistance (R),

$$1/T(K) = A + B\ln(R) + C[\ln(R)]^3$$

and the appropriate calibration constants were used to convert measured resistance values to temperature values. An example of typical resistance values that correspond to temperature variations of 0.1°C is presented in Table 15, illustrating the sensitivity of the measurement system. For comparison, the total cable resistance was on the order of 300 ohms.

Table 14. Temperature-resistance calibration values of temperature probe thermistors.

Temperature (°C)	Thermistor #1 (ohms)	Thermistor #2 (ohms)
0.0	314947.5	321935.8
[a]29.7646	72787.0	73425.0
79.70	10088.42	10034.50
[b]156.5985	1059.49	1128.61
199.28	403.61	461.75

[a] Fusion point of gallium.
[b] Fusion point of indium.

Table 15. Resistance-temperature table extracted for temperatures of 145°–150°C for thermistors used during Leg 137. Resistances are measured in ohms.

°C	145	146	147	148	149	150
0.0	1517.9	1480.8	1444.7	1409.8	1375.8	1342.7
0.1	1514.1	1477.1	1441.2	1406.3	1372.4	1339.4
0.2	1510.4	1473.5	1437.6	1402.9	1369.1	1336.2
0.3	1506.6	1469.8	1434.1	1399.5	1365.8	1333.0
0.4	1502.9	1466.3	1430.6	1396.0	1362.5	1329.8
0.5	1499.9	1462.6	1427.1	1392.6	1359.1	1326.5
0.6	1495.5	1459.0	1423.6	1389.2	1355.8	1323.3
0.7	1491.8	1455.4	1420.2	1385.8	1352.5	1320.2
0.8	1488.1	1451.9	1416.7	1382.5	1349.2	1317.0
0.9	1484.4	1448.3	1413.2	1379.1	1346.0	1313.8

Results

Logging Procedure

On 8 April 1991, the temperature tool was slowly run downward into the borehole at a logging speed of 4 m/min. The sampling frequency was selected such that a temperature measurement was taken every 10 cm. Temperatures were logged continuously until the cable depth counter registered 5020 mbrf, without the probe encountering any obstruction or touching down on the bottom of the hole. This cable length nominally equates to a final logged depth of 1545 mbsf, although there were no calibration points to tie the cable length to depths below seafloor normally determined from drill string length.

Prior to the log, some technical difficulties arose due to a poor connection between the main logging cable and a 345-m-long leader of high-temperature cable. The resulting delay reduced our allocated logging time and eliminated the stationary measurements that had been scheduled at the bottom of the hole. During the delay, fluid samplers were run to depths of 350 and 550 mbsf prior to the temperature log. However, these deployments did not appear to significantly disturb equilibrium temperatures measured a few hours later.

Temperature Profile and Geothermal Gradient

The temperature profile recorded during Leg 137 is illustrated in the composite log of Figure 26, which includes the previous temperature logs measured in Hole 504B during DSDP Legs 69, 70, 83, 92, and ODP Leg 111. Unexpectedly low temperatures were observed from the seafloor to a depth of 310 mbsf, at which point the temperature increased rapidly by more than 10°C over 50 m. This pattern is remarkably similar to the temperature profiles obtained after the hole first penetrated basement and a vigorous downflow of ocean bottom water was initiated (Becker et al., 1983a, 1983b).

Below 400 mbsf, the temperature values closely resemble those measured during Leg 111 (Fig. 27). The difference

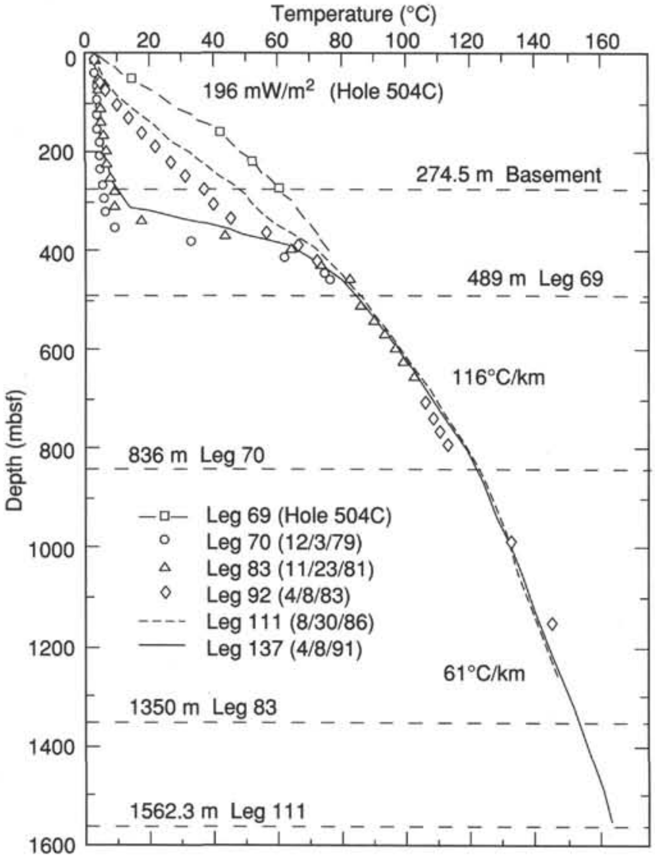

Figure 26. Composite of temperature logs obtained in Hole 504B during Legs 69, 70, 83, 92, 111, and 137.

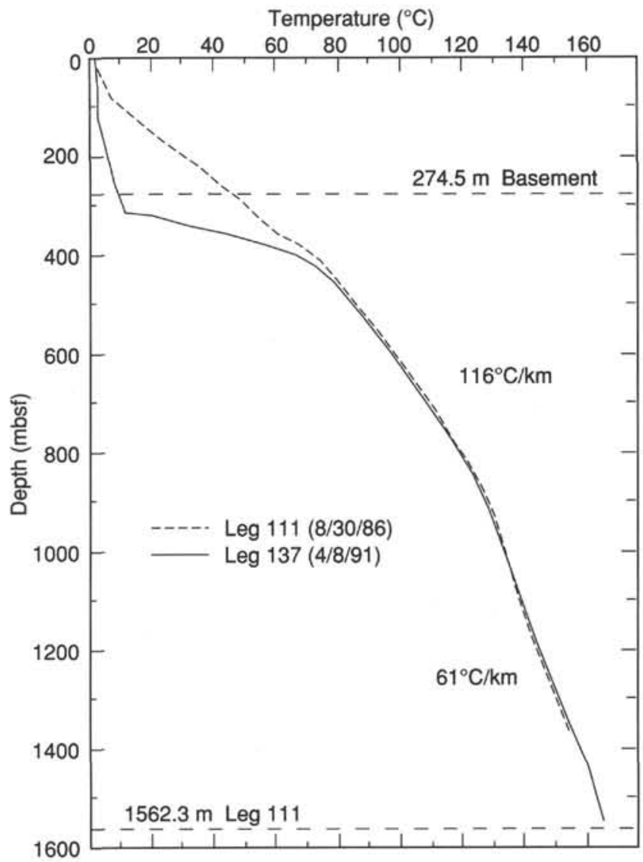

Figure 27. Comparison of temperature profiles measured in Hole 504B during Legs 111 and 137.

between Leg 111 and Leg 137 temperatures at any given depth is generally less than 1°C. Near the bottom of the hole, the recorded temperature reaches a value of 164.6°C at the maximum logged depth of 1545 mbsf.

The profile of geothermal gradient, computed directly from the logged temperatures, is presented in Figure 28. Low gradient values are observed in the shallow part of the hole, gradually increasing from a value of 30°C/km near the seafloor to a value of about 55°C/km at 310 mbsf. The gradients are highly variable between 310 and 360 mbsf, where values reach 600°C/km. Deeper into the well, the observed gradients decrease rapidly down to 525 mbsf, then more gradually down to 945 mbsf. Below this depth, the geothermal gradient continues to decrease slightly, but settles around an average value of 55°–60°C/km.

Discussion

Variations in the Temperature and Gradient Profiles

Variations in both the temperature and the gradient profiles (Figs. 27 and 28) delineate three distinct thermal regimes in the hole:

1. The upper section (0–~450 mbsf), in which the thermal state is dominated by the effects of the downhole flow (Fig. 29). This zone can be subdivided into two parts: (a) the nearly isothermal section to about 310 mbsf, which results from the flow of ocean bottom water through the casing and into the permeable, uppermost basement; and (b) the zone below 310 mbsf with very high gradients that mark the lower section of the permeable reservoir into which the downhole flow is directed and also may be associated with the transition to the more conductive zone below.
2. The lower pillow lavas (~500–900 mbsf), which are thought to be partly sealed and much less permeable, and where the nearly linear profile and moderate variations in gradient suggest a largely conductive regime. The moderate gradient variations in this zone may be due to some combination of thermal conductivity variations and the effects of residual downhole flow or convection of borehole fluids.
3. The deepest interval (915–1545 mbsf), corresponding to the impermeable transition zone and sheeted dikes, in which a quasi-linear temperature profile and stable but slightly decreasing gradient are indicative of a conductive heat transfer regime. The slightly decreasing geothermal gradient observed in this section is probably a response to the gradual increase in the thermal conductivity of the formation vs. depth.

Renewed Downhole Flow in the Upper Section

When Hole 504B was first drilled, measured temperatures in the upper 300 m were nearly isothermal (Fig. 26), indicating a vigorous flow of cold ocean bottom water down through the casing and into the upper levels of basement (Becker et al., 1983a). Through the time of Leg 111, temperatures in this section slowly rebounded toward the gradient in the sediments before the hole was drilled, indicating that the rate of downhole flow had decayed to less than 1% of the original rate (Becker et al., 1983b, 1985; Gable et al., 1989). Based on this trend and on numerical simulations (Williams et al., 1986), we expected that the downhole flow would have decayed even further or ceased and that temperatures in this section would be very close to the sediment gradient.

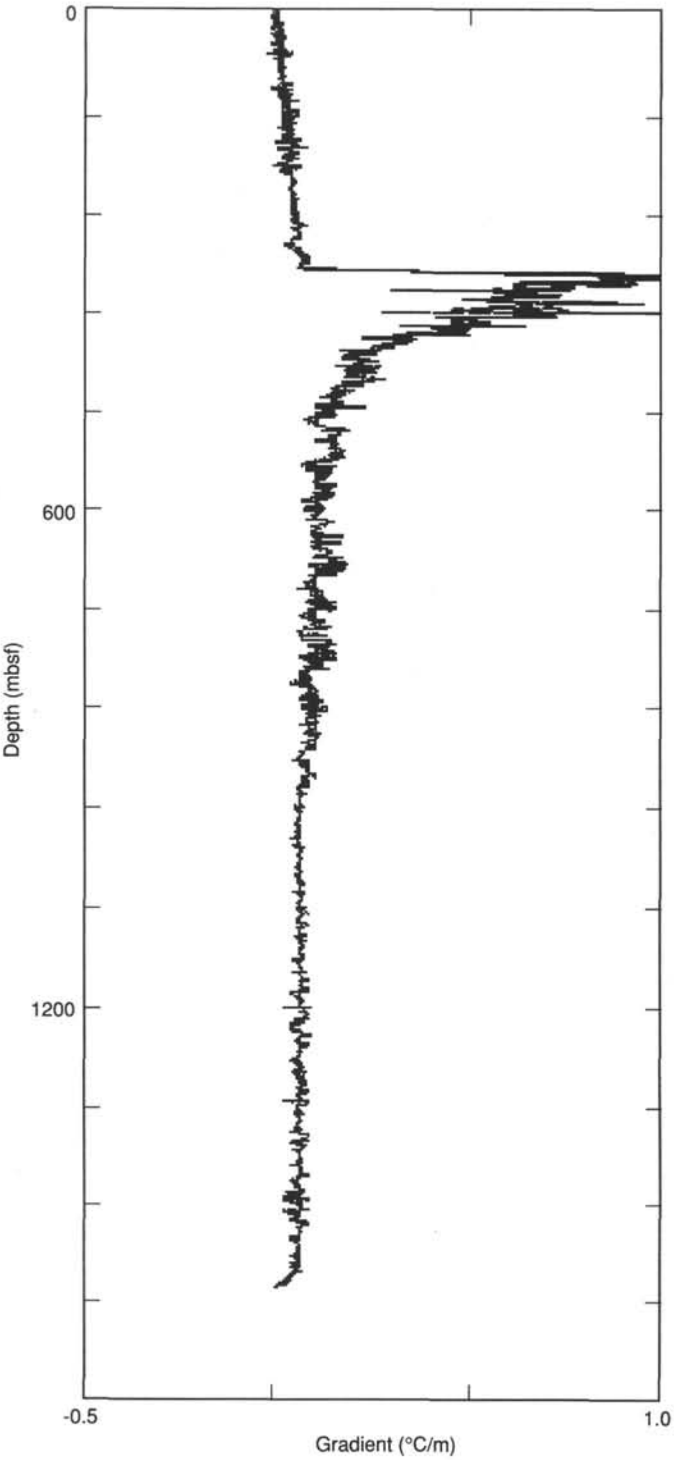

Figure 28. Geothermal gradient profile measured in Hole 504B during Leg 137.

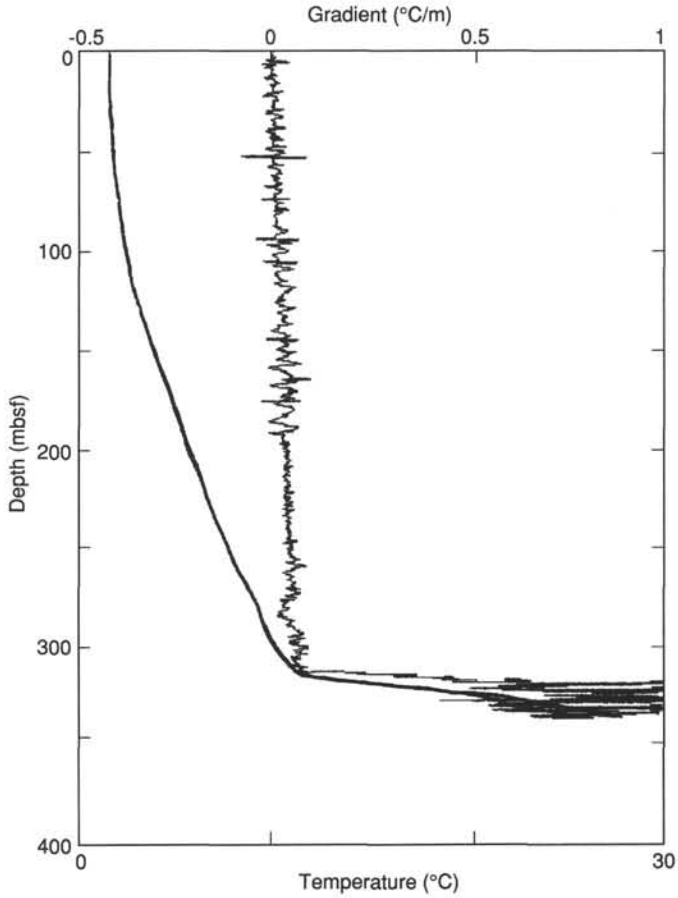

Figure 29. Detailed profiles of the temperature and the geothermal gradient in the upper section of the hole.

However, temperatures measured during Leg 137 are similar to those measured nearly 10 years ago during Leg 83, indicating a remarkable renewal of the downhole flow. This inference was corroborated by the composition of the fluid sample collected from 350 mbsf, which proved to be ocean bottom water (see "Fluid Sampling and Chemistry" section, this chapter). The rate of downhole flow was estimated by matching temperatures measured in the cased section (where the rate of flow must remain uniform with depth) to profiles predicted for various constant downhole flow rates using the transient model of Becker et al. (1983a). The comparison of temperatures measured during Leg 137 with those predicted using this model (Fig. 30) indicates that the rate of downhole flow was about 15 m/hr, or about 1000 L/hr, at the time of Leg 137. This estimate (and those for previous legs) must be considered a first approximation, because the model rests on the assumption of a constant rate—but the Leg 137 result indicates that the downhole flow rate is clearly not constant, nor even monotonically decreasing with time as was previously thought.

Heat Transfer in the Deeper Part of the Hole

The geothermal gradient decreases with depth in the deepest part of the hole and attains a value of about 60°C/km at the bottom. Assuming a constant heat flow of 120 mW/m^2, Gable et al. (1989) extrapolated temperatures as a function of depth and predicted a borehole temperature of 165°C at 1563 mbsf. The maximum temperature recorded during Leg 137 was 164.5°C at 1545 mbsf. The close agreement between the Leg 111 extrapolated temperatures and Leg 137 measured temperatures in the deepest part of Hole 504B confirms that this interval is a predominantly conductive heat transfer regime.

The Leg 137 temperature log also confirms previous observations of a puzzling reduction in the apparent heat flow with depth, from about 200 mW/m^2 in the sediments to about 180 mW/m^2 in the lower pillow lavas to 120 mW/m^2 deep in the hole (Becker et al., 1983b; Gable et al., 1989). The strong decrease in gradient with depth can only partly be explained

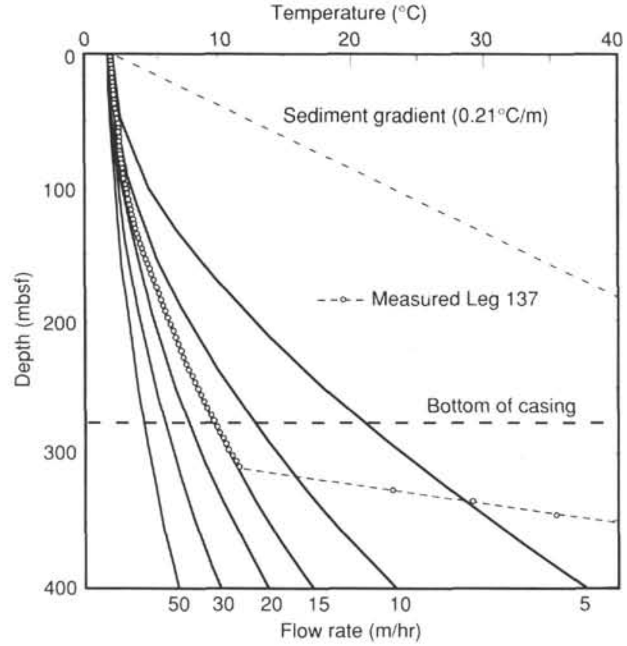

Figure 30. Comparison of temperatures measured in the upper section of Hole 504B during Leg 137 with profiles predicted under conditions of constant downhole flow since the hole first penetrated into basement.

by the documented increase in thermal conductivity with depth. Gable et al. (1989) discuss several other hypotheses, including the possibility of slow convection of the borehole fluids (see also Fisher and Becker, 1991), but this is not supported by the stability of the gradient in the deepest 600–700 m of the hole. Thus, the reduction in heat flow with depth still lacks a satisfactory explanation.

BOREHOLE TELEVIEWER

Introduction

The Borehole Televiewer (BHTV) is an ultrasonic tool that produces an acoustic image of the borehole wall. A transducer emits ultrasonic pulses which are reflected at the borehole wall. The same transducer also records the reflected signal. Then the BHTV electronically analyzes the incoming signal. Amplitude and traveltime of the reflected signals are stored onto mass storage in the logging computer. While the transducer rotates and the tool moves upward, information on the entire borehole wall and borehole shape are recorded pointwise, leading finally to an unwrapped image of the borehole wall both in amplitude and time (Fig. 31).

The amplitude of the reflected signal depends on the reflection coefficient of the borehole fluid-rock interface, the position of the BHTV tool in the borehole, the shape of the borehole, and the roughness of the borehole wall. Especially, changes in the borehole wall's roughness (e.g., at fractures intersecting the borehole) are responsible for the modulation of the reflected signal. Fractures or changes of the drilled rocks can easily be recognized in the amplitude image. On the other hand, the recorded traveltime image gives detailed information about the shape of the borehole; as typically 128 signals are recorded per revolution, the BHTV can be considered to be a "multi-arm caliper log."

Amplitude and traveltime are recorded together with a pointer to magnetic north, so it is possible to display the oriented data and to get a complete image of the borehole wall. This feature can be used to reorient cores.

The digital BHTV used on this leg for open hole measurements and casing inspection differs from the "old" analog BHTV which was used in previous downhole measurements in Hole 504B as follows:

1. The received signal reflected from the borehole wall is digitized downhole in the tool itself (digital BHTV).
2. The transducer does not rotate, but is fixed in the tool axis. Instead, a rotating mirror focuses and reflects the emitted and reflected signals to and from the transducer.
3. A broadband signal (600–1300 kHz) instead of the usual monofrequency signal (500 kHz or 1.2 MHz) is used for scanning the borehole wall.

The BHTV was set up in the following configuration (Fig. 32) starting from top to bottom: upper centralizer with Gearhart Owen connector, orientation tool, electronic tool, lower centralizer, and transducer.

The upper and lower centralizers are necessary to keep the tool and therefore the transducer in the center of the borehole. This is to avoid amplitude effects due to the off-center position of the tool. The orientation tool consists of three fluxgate magnetometers, which allow orientation of the data with respect to the Earth's magnetic field. Implemented in the electronic tool is the software for running the transducer and analyzing and digitizing the incoming data. Also included is the software for the data transfer to the shipboard registering computer. The final transducer part consists of transceiver, mirror, and depth compensator.

On Leg 137, the BHTV was run without the upper centralizer bow springs to avoid uneven travel due to sticking of the tool. Earlier ODP measurements have shown that data quality could be considerably increased if the BHTV was run without the upper centralizer bow springs (Shipboard Scientific Party, in press).

Onboard processing of the data was made possible by data transfer via Ethernet and fileserver from the logging PC to one of the Macintosh units. Processing and display software were installed which allow a first analysis of the data already onboard.

Method

As described by other authors (e.g., Zemanek et al., 1970; Bell and Gough, 1979; Plumb and Hickman, 1985; Zoback et al., 1985), the borehole televiewer can be used to locate fractures and formation changes, to reorient cores, and to detect and distinguish between stress- and nonstress-induced borehole elongations.

Stress-induced borehole elongations or breakouts occur due to spalling of the borehole wall. They occur on opposite sites of the borehole in the direction of minimum horizontal stress, S_h (Kirsch, 1898; Jaeger and Cook, 1979), when the circumferential stress $\sigma_{\theta\theta}$ acting on the borehole wall exceeds the compressional strength of the rock C (Fig. 33).

$$\sigma_{\theta\theta} = S_{H,eff} + S_{h,eff} - 2(S_{H,eff} - S_{h,eff}) \times \cos(2\theta) - \Delta P \geq C \quad (1)$$

where $S_{H,eff}$ is the maximum effective horizontal stress component, $S_{h,eff}$ is the minimum effective horizontal stress component, ΔP is the difference in pressure between the borehole fluid (P_o) and the formation pore pressure (P_p), and θ is the angle with respect to the direction of S_h, while

$$S_{i,eff} = S_i - P_o;\ i = H,h \text{ with } P_o = P_p \text{ and therefore } \Delta P = 0. \quad (2)$$

Thermal stresses ($\sigma_{\theta\theta}(\Delta T)$) acting on the surface of the borehole may result in an increase or decrease of the circum-

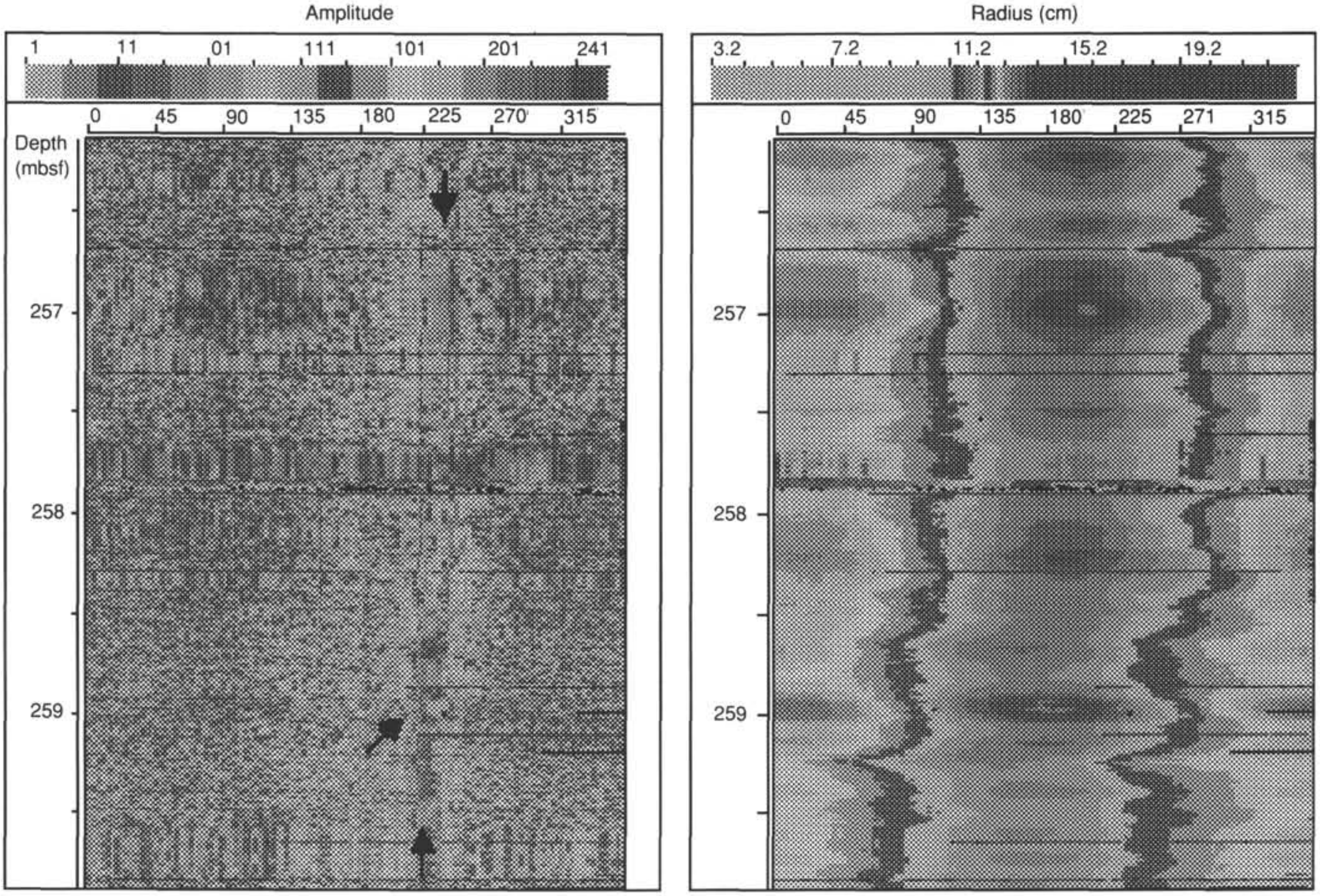

Figure 31. Unprocessed unwrapped amplitude and traveltime gray-scale image of a section of the casing in Hole 504B. Vertical arrows indicate the groove in the lower section of the casing; the tilted arrow points toward a circular structure which might be a hole.

ferential stresses $\sigma_{\theta\theta}$ if the temperature contrast (ΔT) between borehole fluid and rock is positive or negative, respectively (Fig. 33). Under these conditions, formula (1) becomes:

$$\sigma\theta = S_{H,\mathrm{eff}} + S_{\mathrm{h,eff}} - 2(S_{H,\mathrm{eff}} - S_{\mathrm{h,eff}}) \times \cos(2\theta) - \Delta P + \sigma_{\theta\theta(\Delta T)}. \quad (3)$$

In the case that a positive temperature difference between borehole fluid and rock is high enough, breakouts might occur, while in the opposite case, tensile cracks might occur if the borehole fluid is cooling the borehole wall and the tensile strength, T, of the rock is exceeded. Both breakouts as well as tensile cracks are reliable stress indicators and can be detected by the borehole televiewer (e.g., Bell and Gough, 1979; Zoback et al., 1985).

If the borehole televiewer is used for investigating stresses and borehole stability, breakouts are represented by two broad bands of low amplitude in two orthogonal directions and by two bands of increased traveltime at the same azimuths. Both bands are aligned in the direction of minimum horizontal stress component S_h. Tensile cracks are normally indicated by two narrow vertical bands of low amplitude, 180° apart in the direction of the maximum horizontal stress component S_H. However, broad tensile cracks have been reported from deep in Hole 504B (Morin et al., 1990).

Logging

Logging Hole 504B with the digital BHTV was one of four downhole measurements (temperature, fluid sampling, flowmeter, and BHTV) scheduled for Leg 137.

The BHTV was scheduled to complete the following measurements: (1) investigation of the casing of Hole 504B, (2) completing BHTV records of Hole 504B, and (3) overlapping measurements with BHTV records from previous legs.

BHTV logging started at 1845 hr on 27 April 1991 with the downhole trip. Logging operations ended at 0045 hr on 28 April 1991, and the BHTV was rigged down at 0315 hr on 28 April 1991.

Casing Inspection

The casing inspection was required to assure that no prior damage to the casing will jeopardize future operations. Upward logging of the casing started as soon as the televiewer reached the open hole at 276 mbsf. In order to avoid jerking the tool, the tool was run at a vertical speed of 1000 ft/hr. As the upper 100 m of casing was being logged, the pipe was pulled up to allow a complete casing inspection. After a minimum depth of 12 mbsf was reached, the inspection was finished.

Logging of the casing revealed no major damage to the casing. In the lower 50 m of the casing a groove (dark color

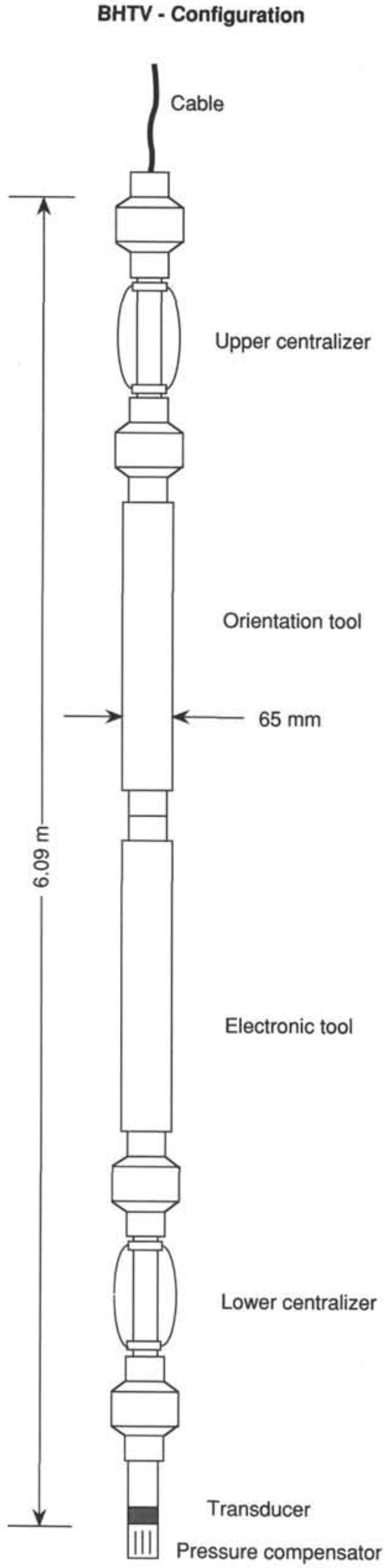

Figure 32. General tool setup of the digital borehole televiewer.

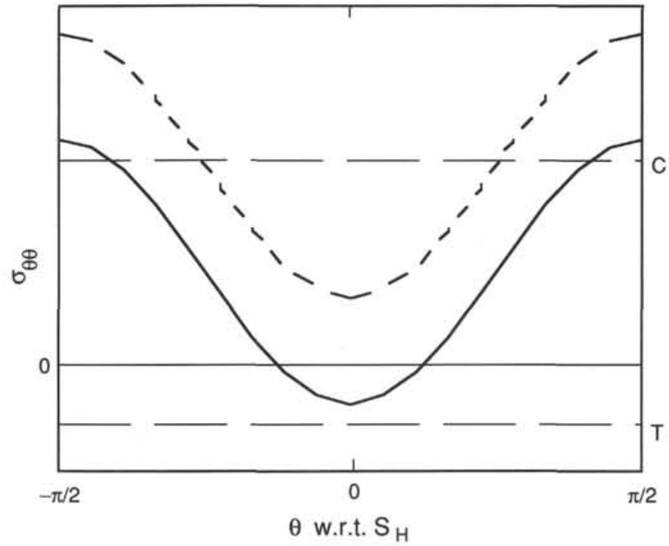

Figure 33. Distribution of circumferential stress($\sigma_{\theta\theta}$) around the borehole wall. Horizontal lines indicate compressional (C) and tensional strength (T) of the rock. Where these lines are exceeded by the circumferential stress breakouts, respectively, tensile cracks occur. The dashed line shows the increase in circumferential stress due to positive temperature difference between borehole fluid and surrounding rock.

band within light color band) is obvious which is occasionally interrupted by spots low in amplitude (dark color, Fig. 31). The circular structure and the low amplitudes in a high amplitude azimuth interval indicate that the casing is corroding in a few spots.

Open Hole Logging

Although there were three BHTV logs during previous legs (DSDP Leg 69, DSDP Leg 83, and ODP Leg 111) the quality of the recorded data varied significantly. While the intervals from 275 to 470 mbsf (DSDP Leg 69; Anderson and Zoback, 1983), from 285 to 1285 mbsf (DSDP Leg 83; Newmark et al., 1985; Newmark, Zoback, and Anderson, 1985), and from 1180 to 1535 mbsf (ODP Leg 111; Morin et al., 1989; 1990) were logged, only the intervals from 440 to 1100 mbsf and 1180 to 1530 mbsf proved to consist of reliable data (Moos and Zoback, 1990). These BHTV measurements were recorded with the analog BHTV.

An overlapping of BHTV records with measurements from previous legs would offer one of the few possibilities for a time-dependent study of borehole breakouts, as breakouts were detected on data recorded on the above-mentioned legs (Newmark et al., 1984; Newmark, Zoback, and Anderson, 1985; Morin et al., 1990).

Due to the temperature limit of the BHTV (120°C) the complete hole could not be logged. Without reaching the temperature limit of the tool, an overlapping depth interval was tried as the first stage of open hole logging. After logging the casing, the tool was lowered to 493 mbsf and an upward log of the open hole was started. Because of failure of the tool at 403 mbsf, the log was terminated and no more data could be collected.

Within the logged depth interval (493–403 mbsf), the collected data reveal a wide variation in borehole shape and size. Smooth variations in the cross sections indicate that the borehole wall was deformed by drilling processes. Sharp cut-ins into the borehole wall (Fig. 34) suggest that short intervals are

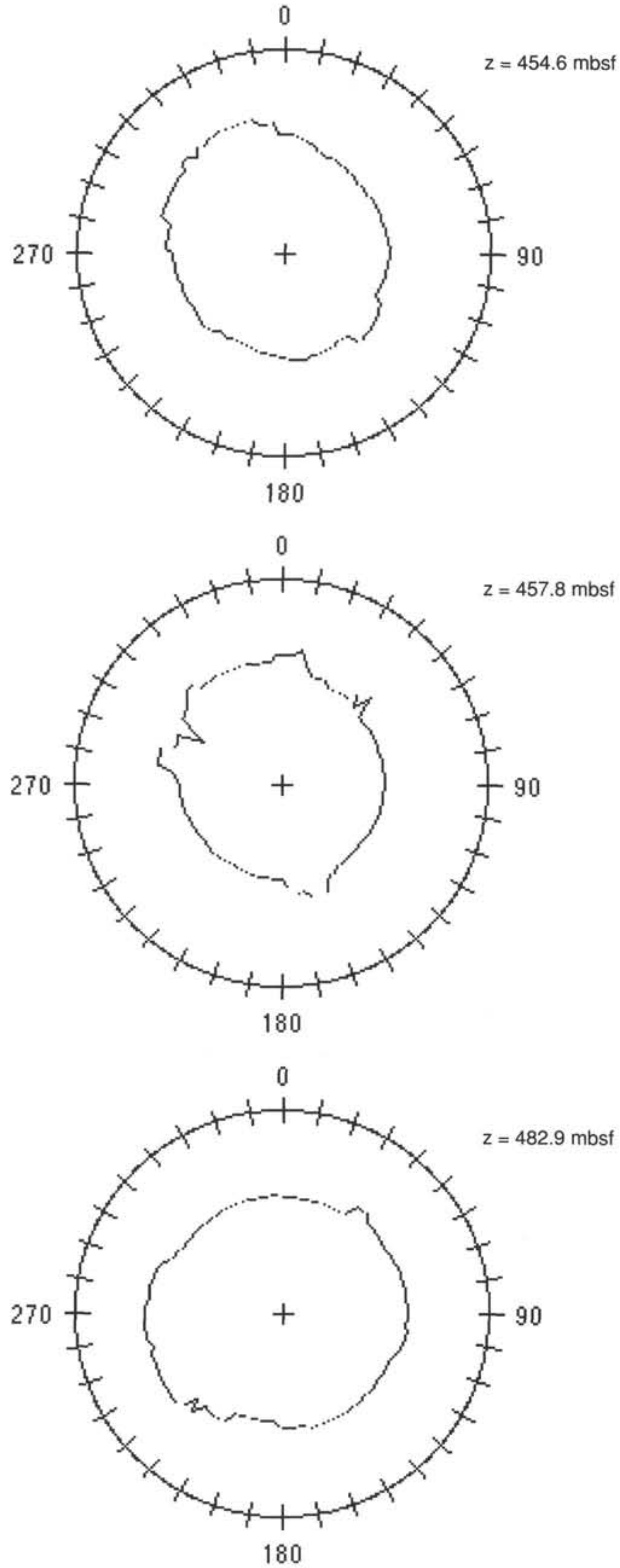

Figure 34. Cross-sections of the borehole at different depths. Cross-sections are oriented with respect to the Earth's magnetic field.

affected by stress-induced borehole deformations. These, however, need more detailed investigation. Various forms of lens-shaped structures intersecting with the borehole show the pillow structure of this depth section (Fig. 35).

FLOWMETER/INJECTION EXPERIMENT

In hydrogeological investigations of the ocean crust, permeability is the key physical property which controls fluid transport and exchange processes. To date, the drill-string packer system (Becker, 1986) is the only shipboard method which has been used by DSDP/ODP to measure permeability *in situ.* The first application of this standard hydrologic field technique to the marine environment occurred at Hole 504B during DSDP Leg 69 (Anderson and Zoback, 1982). Since that initial effort, the method has emerged as a reliable and indispensable part of several other downhole measurements programs which have shared a common hydrogeologic research theme (Hickman et al., 1984; Becker, 1990; Becker, 1991). In the case of Hole 504B, a systematic program of packer testing has been performed which encompasses Legs 69, 83, 92, and 111. These data provide a representation of the vertical distribution of bulk permeability in the oceanic crust at this site to 1500 mbsf (Anderson and Zoback, 1982; Becker et al., 1983b; Anderson, Zoback, et al., 1985; Becker, 1989).

A typical ODP packer test involves the inflation of a single packer which may isolate a fairly long interval between the packer element and the bottom of the hole, with the resulting estimate of permeability being a bulk value often integrated over several hundred meters. In an effort to improve the vertical resolution of these data and to obtain a fine-scale distribution of permeability as a function of depth, a flowmeter/injection experiment was planned for this leg. The flowmeter/injection method was originally proposed by Hufschmied (1984); it combines the concepts of injection to characterize bulk aquifer properties and *in-situ* hydraulic measurements at specific depths to monitor fine-scale variability. This simple and innovative method utilizes constant-rate injection into a sealed well and concurrent logging of flow and pressure to arrive at a detailed vertical profile of permeability. This method has been evaluated and refined at several groundwater wells on land (Morin et al., 1988; Hess, 1989), and a comparison of the permeability values estimated from this technique to those of other standard, established field methods has been excellent (Molz et al., 1989).

The possibility of adapting this flowmeter/injection technique to shipboard operations was first proposed by Morin (1988). There are fundamental differences between the way this experiment is performed on land in a water well and the way it must be conducted onboard a drill ship. In the former case, all fluid injected into the well is assumed to enter the formation (unless there is overflow from surface casing). In the ODP case, fluid injected into the drill pipe from pumps onboard the ship is not ensured of entering the formation unless a packer seals the annulus between drill pipe and surface casing and, thus, prevents injected fluid from short-circuiting up into the open ocean (Fig. 36). It is this part of the field operation which failed during the Leg 137 attempt to complete the first flowmeter/injection test conducted at sea.

The initial stages of this experiment on 28 April 1991 proceeded as designed. A combination flowmeter/pressure/caliper tool was lowered down the drill pipe along with a modified go-devil which was clamped to the logging cable. This new go-devil was specially designed to accommodate the particular requirements imposed by this experiment. This device allows the packer to be inflated, and afterward allows unrestricted movement of the logging cable which passes through it. It also allows fluid injected from the surface to pass

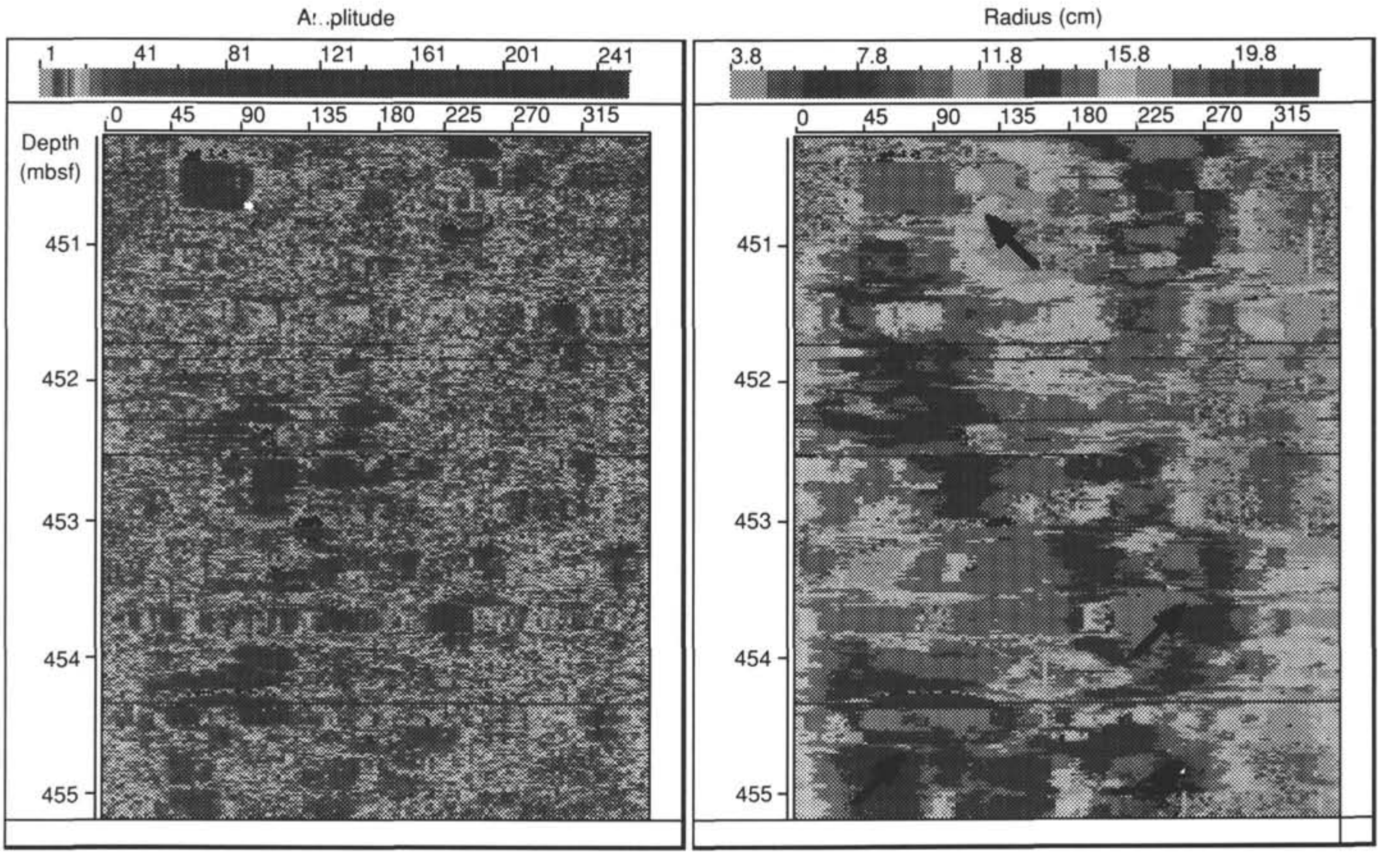

Figure 35. Gray-scale amplitude and traveltime (radius) image of the borehole between 450 and 455 mbsf. Orientation of the images is with respect to Earth's magnetic field. Arrows indicate lens-shaped structures.

through it, enter the well, and be detected by the logging tool. In this first test, the logging tool was lowered until the go-devil landed into the bottom-hole packer assembly. The packer was then successfully inflated against casing at a depth of 100 mbsf. The drill string was subsequently pressurized such that pins in the go-devil were sheared and the logging tool was allowed to continue down into the open hole below the packer. Two hours later, however, as the injection phase of the test was about to proceed, the packer suddenly and inexplicably deflated, essentially negating the experiment. Measurements of flow and pressure during injection from the rig floor would have been meaningless.

The tool and go-devil assembly were quickly retrieved to the rig floor and the go-devil was redressed for another attempt at packer inflation. The experiment was repeated, but the packer started to slide down the hole and again deflated about 10 min after it had been successfully inflated and the logging tool had been lowered into the cased hole below the packer.

It is not clear at this time why the packer deflated. The packer itself was in good condition after recovery and showed no signs of damage. Also, no inherent flaw in the design of the new go-devil could be detected. The most plausible explanation for the packer deflations is that the inflation pressure was too low for the packer to hold adequately against the casing. Insufficient setting pressure would cause the packer to then slide down the casing. With the present packer design, this motion would result in automatic deflation. The logging tool itself worked properly and the concept of applying this experiment at sea appears to be feasible. However, the problem with packer deflation in casing will have to be resolved before this flowmeter/injection experiment can be completed on a future leg.

SUMMARY AND CONCLUSIONS

The principal objective of Leg 137 of the Ocean Drilling Program (ODP) was to revisit Hole 504B in the eastern equatorial Pacific (Fig. 1), to recondition the hole for future ODP operations. Hole 504B is by far the deepest penetration into oceanic crust and perhaps our most important *in-situ* reference section for the structure of the upper oceanic crust. However, its status had been jeopardized when a coring assembly was lost at the bottom of the hole near the end of Leg 111. Therefore, the highest priorities for Leg 137 involved engineering operations, including remedial measures to clean this junk from the hole and tests to prove the feasibility of continued coring on a subsequent expedition. If these objectives were successfully achieved during Leg 137, Leg 140 was committed to returning to the hole for a full scientific leg of coring and downhole measurements.

Leg 137 departed Honolulu on 20 March 1991, and began with a 17½ day transit to Site 504. The leg ended in Balboa, Panama, on 1 May 1991, after 21½ days of operations and a 2 day transit. During its scheduled operations at Hole 504B, Leg 137 focused on removal of the existing junk (Fig. 4), assessment of the condition of the hole and its casing and reentry cone, and development of more efficient coring and drilling techniques for the projected deepening of the hole on Leg 140. Additional objectives involved high-priority downhole measurements that could not be deferred to a later leg, including

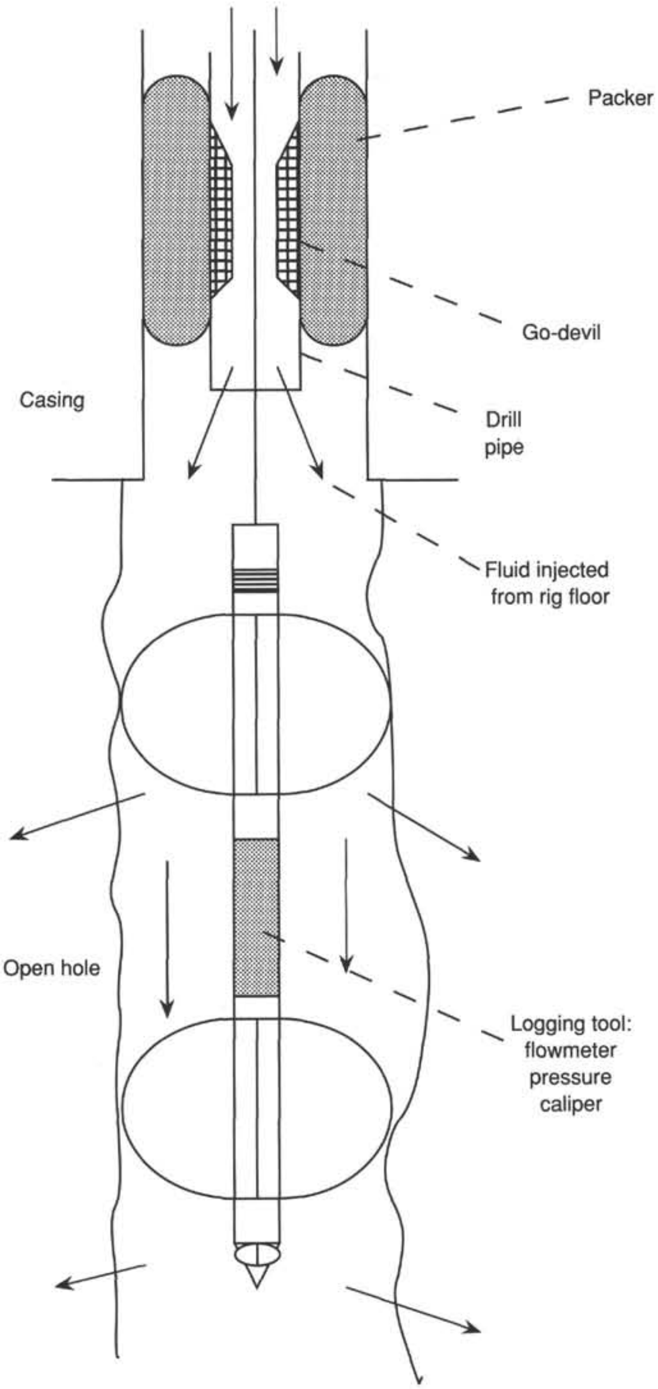

Figure 36. Diagram of flowmeter/injection operation.

temperature logging, borehole fluid sampling, and permeability measurements.

Initial Temperature Log and Fluid Sampling

Before engineering operations were begun, temperatures in the undisturbed hole were logged, and 36 hr was devoted to sampling borehole fluids. Figure 26 shows the Leg 137 temperature log compared to measurements made during past legs to Hole 504B. Temperatures in the deeper kilometer of the hole were consistent with values logged during Leg 111, with a linear gradient of 61°C/km. This gradient extrapolates to a temperature of 165°C at the bottom of the hole at 1562 mbsf. In the upper 350 m of the hole, temperatures were considerably depressed, suggesting an unexpected renewal of the downhole flow of ocean bottom water into the upper levels of basement. Such downhole flow was fairly vigorous when the hole was first drilled during Legs 69 and 70 in 1979, but had decayed to about 1 m/hr, or less than 1% of the original rate, when Leg 111 revisited the hole in 1986. The Leg 137 temperatures are slightly higher than those measured during Leg 83 in 1981, suggesting that the downhole flow has increased since 1986 to a rate on the order of 15 m/hr. This is a surprising result that raises many intriguing questions about the hydrogeology at the site. Some of these questions were planned to be studied with a digital televiewer log and permeability measurements planned at the end the leg, but these measurements were cut short because of developments during coring tests.

Using tools provided by the Lawrence Berkeley and Los Alamos National Laboratories, eight fluid samples were obtained from the hole, at depths ranging from 350 to 1540 mbsf. Initial chemical analyses indicate that seven of these samples contain borehole fluid with characteristics in agreement with past sampling studies of the hole. Some contamination of the samples appears to have occurred, either by entrainment of fluids during the trip down prior to sampling or as a result of leakage during the ascent as the hot sampled fluids cooled and contracted. The fluid chemistry indicates bottom water present down to at least 350 mbsf, corroborating the inference of downhole flow from the temperature log. Interestingly, during subsequent engineering operations at the bottom of the hole, many small pieces of platy anhydrite were recovered, consistent with predictions that anhydrite should reach saturation in the borehole fluids near 150°C and 1500 mbsf.

Hole 504B Clean-out

But the primary purpose of Leg 137 was to salvage Hole 504B—and the clean-out operations succeeded very much according to plan. As noted above, a diamond coring assembly had broken off at the end of Leg 111, which was left with insufficient time to recover all of the lost hardware, and had to abandon the large diamond bit and assorted hardware at the bottom of the hole. There were also suggestions of possible problems with the casing, and it was feared that wall rocks might have caved in on top of the junk since Leg 111.

Despite these uncertainties, Leg 137 was able to run straight to the junk from virtually the beginning of remedial operations. Cleaning the junk from the bottom of the hole required less than 1 week of straightforward operations (Fig. 5), including one fishing attempt with a junk basket and five mill runs with boot baskets to capture pieces of broken-up metal. These returned with parts or whole pieces of all the lost hardware, including recognizable pieces of the diamond bit. This was followed by a run with a tri-cone drill bit to verify that the hole was clean, which deepened the hole without coring by 7.7 m to a total depth of 1570 mbsf.

Coring Tests

Another important priority of Leg 137 was to test coring systems, to assess the feasibility of coring ahead during a full scientific leg. Once the hole was verified to be clean, two coring systems were tested: the standard ODP RCB wireline coring system and a conventional oilfield diamond core barrel. (The latter is a standard oilfield system, completely different from the small-diameter wireline diamond coring system under development at ODP.) These tests yielded mixed results, and unfortunately ended with a frustrating loss of very fishable coring equipment in the hole.

Two runs with the RCB system in a clean hole yielded penetration rates of 1–2 m/hr and average recovery of 14%.

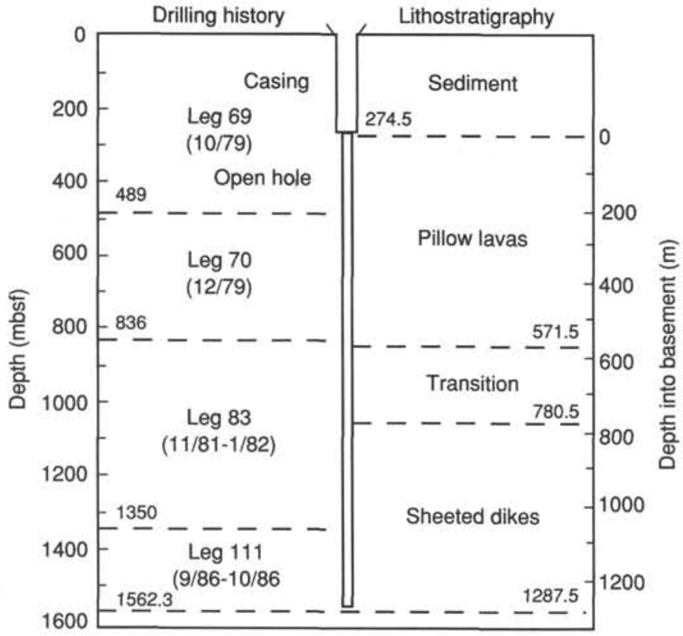

Figure 37. Schematic of drilling history and lithostratigraphy of Hole 504B, as of the end of Leg 137.

This is comparable to results with the same system during Legs 83 and 111. The cutting inserts of the bits failed quickly in a manner that suggested that the formation is extremely hard and abrasive and that a more appropriate grade of bit could make more hole. But, while rotary core and drill bits could be used to advance the hole at a reasonable rate, it is clear that the RCB system cannot be expected to yield core recovery any better than 20% in this lithology.

The diamond core barrel also yielded mixed results, with extremely slow penetration but very good recovery. Two runs resulted in a recorded advance of only 3.1 m (which could be in error because of the effects of tides) and a calculated recovery of 79%. The first diamond bit was extremely worn after less than 2 m of penetration, indicating that the bit matrix material was too soft for the hard, abrasive formation. The second diamond bit behaved in a similar manner downhole, but was not recovered because all 18 m of outer core barrel broke off in the hole, with the bit at the bottom.

Such a long, narrow piece is normally the easiest kind of junk to fish from a hole with the appropriate tools, and in fact the first fishing overshot apparently did engage and lift it some distance up the hole. However, the fishing overshot itself broke off, leaving a compound fish as detailed in Figure 6. This remains eminently fishable with the appropriate fishing tools. Unfortunately, the proper tools were not on board, although a second fishing attempt was made with a modified taper tap. When this failed, the decision was made not to risk damage to the fish by attempting to retrieve it with a "rig-engineered" solution, but instead to leave the fish in its easily retrievable condition, hopefully to be removed with proper equipment during a future leg.

Coring Results

Drilling on Leg 137 deepened Hole 504B by 59.2 m, to a total depth of 1621.5 mbsf or 1347 m into basement (Fig. 37). Of this interval, 48.6 m was cored, with a recovery of 8.77 m. The recovered rocks are all interpreted as a continuation of the sheeted dike complex, although no intrusive dike margins were actually recovered. The physical properties of recovered core support the inference that the formation is very hard and dense massive basalt, and therefore difficult to core. Chlorite and actinolite veins and actinolite-bearing alteration halos are common in the diamond cores with good recovery. It would therefore appear that the trend of increasing proportion of actinolite in the secondary mineral assemblage recognized on Leg 111 continues with depth.

Final Logging

Attempts to fish the lost outer core barrel left time for only an abbreviated program of downhole measurements at the end of the leg. The planned open-hole packer inflation was cancelled because it posed the greatest risk of somehow disturbing or compounding the presentation of the fish. A digital BHTV log of the casing was successfully conducted, but the tool failed shortly after logging only 85–90 m of the open-hole section. The complicated flowmeter/injection experiment was an operational success during two packer inflations in casing, but each time was cut short by premature packer deflations. The packer was recovered in good condition (with outer rubber fully intact), so the most plausible explanation for the packer deflations is that the inflation pressure was insufficient to maintain its grip against the smooth casing.

The casing inspection by borehole televiewer disclosed that the casing flaw suspected after Leg 111 can in fact be attributed to a casing expansion joint, but that some casing damage, apparently due to wear, does exist. The most severe degradation is in the lowermost 30–40 m, where the casing appears to have several small holes connected by some sort of vertical split or separation. To date this has not affected operations at the hole, and it does not appear to require casing repair for the single science leg approved for the 1991-1992 schedule.

Conclusions and Recommendations for Future Operations at Hole 504B

Leg 137 achieved its primary objective, cleaning Hole 504B of the serious junk lost at the end of Leg 111. Operations throughout the leg showed no indication of the supposed problems with the casing, although a borehole televiewer inspection during the last day on site showed flaws in the lower 30–40 m of casing. Leg 137 clearly succeeded in demonstrating that Hole 504B can be advanced to the Layer 2/3 transition, the proposed target for a scientific leg later in 1991.

This important success was tarnished by a frustrating inability to retrieve a much less serious piece of junk lost at the end of coring tests. This disappointment can be attributed to a defective fishing tool and a lack of time to procure and deploy any further appropriate tools, not to any difficult presentation of the junk itself. In fact, such tool losses and fishing jobs are not at all unusual in drilling any deep hole, and in this case it is virtually certain that the lost outer core barrel can readily be fished with the proper tool. Furthermore, Hole 504B has a history of being open to total depth on multiple revisits, so the fish can be expected to remain clean and in easily retrievable condition for a reasonable period of time. With appropriate fishing tools, it should pose little risk to a revisit in the near future.

The more serious dilemma facing future legs to Hole 504B is the inability of both the RCB and diamond coring systems to simultaneously cut core and make hole in this lithology. The RCB system can make hole with recovery on the order of 15%, whereas the diamond core barrel gives excellent recovery with very slow progress. Even with improved bit designs for these coring systems, trade-offs will have to be made between penetration and recovery.

While Leg 137 has shown that the key scientific priorities for deepening and logging Hole 504B to the Layer 2/3 and/or dike/gabbro transition(s) can be achieved on a later leg, these objectives may require compromise strategies for drilling, coring, and logging.

REFERENCES

Adamson, A. C., 1985. Basement lithostratigraphy, DSDP Hole 504B. *In* Anderson, R. N., Honnorez, J., Becker, K., et al., *Init. Repts. DSDP,* 83: Washington (U.S. Govt. Printing Office), 121–127.

Alt, J. C., Anderson, T. F., Bonnell, L., and Muehlenbachs, K., 1989. Mineralogy, chemistry, and stable isotopic compositions of hydrothermally altered sheeted dikes: ODP Hole 504B, Leg 111. *In* Becker, K., Sakai, H., et al., *Proc. ODP, Sci. Results,* 111: College Station, TX (Ocean Drilling Program), 27–40.

Alt, J. C., Honnorez, J., Laverne, C., and Emmermann, R., 1986. Hydrothermal alteration of a 1 km section through the upper oceanic crust, Deep Sea Drilling Project Hole 504B: mineralogy, chemistry, and evolution of seawater-basalt interactions. *J. Geophys. Res.,* 91:10309–10335.

Anderson, R. N., Honnorez, J., Becker, K., Adamson, A. C., Alt, J. C., Emmermann, R., Kempton, P. D., Kinoshita, H., Laverne, C., Mottl, M. J., and Newmark, R. L., 1982. DSDP Hole 504B, the first reference section over 1 km through Layer 2 of the oceanic crust. *Nature,* 300:589–594.

Anderson, R. N., Honnorez, J., et al., 1985. *Init. Repts. DSDP,* 83: Washington (U. S. Govt. Printing Office).

Anderson, R. N., and Zoback, M. D., 1982. Permeability, underpressures, and convection in the oceanic crust near the Costa Rica Rift, eastern equatorial Pacific. *J. Geophys. Res.,* 87:2860–2868.

________, 1983. The implication of fracture and void distribution from bore-hole televiewer imagery for the seismic velocity of the upper oceanic crust at Deep Sea Drilling Project Holes 501 and 504B. *In* Cann, J. R., Langseth, M. G., Honnorez, J., Von Herzen, R. P., White, S. M., et al., *Init. Repts. DSDP,* 69: Washington (U.S. Govt. Printing Office), 255–270.

Anderson, R. N., Zoback, M. D., Hickman, S. H., and Newmark, R. L., 1985. Permeability versus depth in the upper oceanic crust: in situ measurements in DSDP Hole 504B, eastern equatorial Pacific. *J. Geophys. Res.,* 90:3659–3669.

Autio, L. K., and Rhodes, J. M., 1983. Cost Rica Rift Zone basalts: geochemical and experimental data from a possible example of multistage melting. *In* Cann, J. R., Langseth, M., Honnorez, J., and Von Herzen, R. P., and White, S. M., et al., *Init. Repts. DSDP,* 69: Washington (U.S. Govt. Printing Office), 729–746.

Becker, K., 1986. Special report: development and use of packers in ODP. *JOIDES Journal,* 12:51–57.

________, 1989. Measurements of the permeability of the sheeted dikes in Hole 504B, ODP Leg 111. *In* Becker, K., Sakai, H., et al., *Proc. ODP, Sci. Results,* 111: College Station, TX (Ocean Drilling Program), 317–325.

________, 1990. Measurements of the permeability of the upper oceanic crust at Hole 395A, ODP Leg 109. *In* Detrick, R., Honnorez, J., Bryan, W. B., Juteau, T., et al., *Proc. ODP, Sci. Results,* 106/109: College Station, TX (Ocean Drilling Program), 213–222.

________, 1991. In situ bulk permeability of oceanic gabbros in Hole 735B. *In* Robinson, P. T., Von Herzen, R. P., et al., *Proc. ODP, Sci. Results,* 118: College Station, TX (Ocean Drilling Program), 333–348.

Becker, K., Langseth, M. G., and Von Herzen, R. P., 1983a. Deep crustal geothermal measurements, Hole 504B, Deep Sea Drilling Project Legs 69 and 70. *In* Cann, J. R., Langseth, M. G., Honnorez, J., Von Herzen, R. P., White, S. M., et al., *Init. Repts. DSDP,* 69: Washington (U.S. Govt. Printing Office), 223–236.

Becker, K., Langseth, M. G., Von Herzen, R. P., and Anderson, R. N., 1983b. Deep crustal geothermal measurements, Hole 504B, Costa Rica Rift. *J. Geophys. Res.,* 88:3447–3457.

Becker, K., Langseth, M. G., Von Herzen, R. P., Anderson, R. N., and Hobart, M. A., 1985. Deep crustal geothermal measurements, Hole 504B, Deep Sea Drilling Project Legs 69, 70, 83, and 92. *In* Anderson, R. N., Honnorez, J., Becker, K., et al., *Init. Repts. DSDP,* 83: Washington (U.S. Govt. Printing Office), 405–418.

Becker, K., Sakai, H., Adamson, A. C., Alexandrovich, J., Alt, J. C., Anderson, R. N., Bideau, D., Gable, R., Herzig, P. M., Houghton, S., Ishizuka, H., Kawahata, H., Kinoshita, H., Langseth, M. G., Lovell, M. A., Malpas, J., Masuda, H., Merrill, R. B., Morin, R. H., Mottl, M. J., Pariso, J. E., Pezard, P., Phillips, J., Sparks, J., and Uhlig, P., 1989a. Drilling deep into the oceanic crust at Hole 504B, Costa Rica Rift. *Rev. Geophys.,* 27:79–102.

Becker, K., Sakai, H., et al., 1988. *Proc. ODP, Init. Repts.,* 111: College Station, TX (Ocean Drilling Program).

________, 1989. *Proc. ODP, Sci. Results,* 111: College Station, TX (Ocean Drilling Program).

Bell, J. S., and Gough, D. I., 1979. Northeast-southwest compressive stress in Alberta: evidence from oil wells. *Earth Planet. Sci. Lett.,* 45:475–482.

Bryan, W. B., Thompson, G., Frey, F. A., and Dickey, J. S., 1976. Inferred settings and differentiation in basalts from the Deep Sea Drilling Project. *J. Geophys. Res.,* 81:4285–4304.

Cann, J. R., Langseth, M. G., Honnorez, J., Von Herzen, R. P., White, S. M., et al., 1983. *Init. Repts. DSDP,* 69: Washington (U.S. Govt. Printing Office).

Christaras, B., 1989. Weathering of granites and mechanical behavior changing, in northern Greece. *Proc. Int. Symp. Conserv. Monum. Mediter. Basin,* Bari, 335–339.

CRRUST (Costa Rica Rift United Scientific Team), 1982. Geothermal regimes of the Costa Rica Rift, east Pacific, investigated by drilling, DSDP-IPOD legs 68, 69, and 70. *Geol. Soc. Am. Bull.,* 93:862–875.

Dearman, W. R., 1976. Weathering classification in the characterization of rocks: a revision. *Bull. IAEG,* 13:123–127.

Elthon, D., 1981. Metamorphism in oceanic spreading centers. *In* Emiliani, C. (Ed.), *The Sea* (Vol. 7): New York (Wiley), 285–303.

Fisher, A. T., and Becker, K., 1991. The reduction of measured heat flow with depth in Hole 504B: evidence for convection of borehole fluids? *Sci. Drilling,* 2:34–40.

Gable, R., Morin, R. H., and Becker, K., 1989. Geothermal state of Hole 504B: ODP Leg 111 overview. *In* Becker, K., Sakai, H., et al., *Proc. ODP, Sci. Results,* 111: College Station, TX (Ocean Drilling Program), 87–96.

Gieskes, J. M., Kastner, M., Erzinger, J., and Boulegue, J., 1986. Geochemical studies in Hole 504B, Leg 92. *In* Leinen, M., Rea, D. K., et al. *Init Repts. DSDP,* 92: Washington (U.S. Govt. Printing Office), 547–562.

Goff, F., Gardner, J. N., Solbau, R. D., Adams, A., Evans, W. C., Lippert, D. R., Jacobson, R., Bayhhurst, G., Trujillo, P. E., Counce, D., and Dixon, P., 1990. The "art" of *in situ* fluid sampling and remarkable compositional variations in the wellbore fluid of VC-2B, Valles Caldera, New Mexico. *Geothermal Resources Counc. 1990 Internat. Symp.,* Honolulu.

Hess, K. M., 1989. Use of a borehole flowmeter to determine spatial heterogeneity of hydraulic conductivity and macrodispersion in a sand and gravel aquifer, Cape Cod, Massachusetts, *Proc. Conf. on New Field Techniques for Quantifying the Physical and Chemical Properties of Heterogeneous Aquifers.* National Water Well Assoc., Dallas, 497–508.

Hickman, S. H., Langseth, M. G., and Svitek, J. F., 1984. In situ permeability and pore-pressure measurements near the Mid-Atlantic Ridge, Deep Sea Drilling Project Hole 395A. *In* Hyndman, R. D., Salisbury, M. H., et al., *Init. Repts. DSDP,* 78B: Washington (U.S. Govt. Printing Office), 699–708.

Hufschmied, P., 1984. Hydrogeologie emmental, teil IV, modellstudie zur bestimmung des grundwasser-dargebotes im testgeviet emmental, Wasser-u. *Energiewirtschaftsamt des Kantons Bern.*

Jaeger, J. C., and Cook, N.G.W., 1979. *Fundamentals of Rock Mechanics* (3rd ed.): New York (Chapman and Hall).

Kennedy, G. C., and Hosler, W. T., 1966. Pressure-volume-temperature and phase relations of H_2O and CO_2. *In* Clark, S. P. (Ed.), *Handbook of Physical Constants.* Mem. Geol. Soc. Am., 97:374–375.

Kirsch, G., 1898. Die Theorie der Elastizität und die Bedürfnisse der Festigkeitslehre. *VDI Z.,* 42:797–807.

Leinen, M., Rea, D. K., et al., 1986. *Init. Repts. DSDP,* 92: Washington (U.S. Govt. Printing Office).

Lonsdale, P., and Klitgord, K. D., 1978. Structure and tectonic history of the eastern Panama Basin. *Geol. Soc. Am. Bull.,* 89:881–999.

Lysne, P., in press. P, V, T states within the VC-2B Borehole, Valles Caldera, New Mexico. *Appl. Geochem.*

Molz, F. J., Morin, R. H., Hess, A. E., Melville, J. G., and Guven, O., 1989. The impeller meter for measuring aquifer permeability variations: evaluation and comparison with other tests. *Water Resour. Res.,* 25:1677–1683.

Moos, D., and Zoback, M. D., 1990. Utilization of observations of well bore failure to constrain the orientation and magnitude of crustal stresses: application to continental, Deep Sea Drilling Project, and Ocean Drilling Program boreholes. *J. Geophys. Res.,* 95:9305–9325.

Morin, R. H., 1988. Recent developments in measuring permeability at sea. *Colloq. on Hydrothermal Activity in the Oceans,* Brest, France. IFREMER Rept. 88-A553, 34–35.

Morin, R. H., Anderson, R. N., and Barton, C. A., 1989. Analysis and interpretation of the borehole televiewer log: information on the state of stress and the lithostratigraphy at Hole 504B. *In* Becker, K., Sakai, H., et al., *Proc. ODP, Sci. Results,* 111: College Station, TX (Ocean Drilling Program), 109–118.

Morin, R. H., Hess, A. E., and Paillet, F. L., 1988. Determining the distribution of hydraulic conductivity in a fractured limestone aquifer by simultaneous injection and geophysical logging. *J. Ground Water,* 26:587–595.

Morin, R. H., Newmark, R. L., Barton, C. A., and Anderson, R. N., 1990. State of lithospheric stress and borehole stability at Deep Sea Drilling Project Site 504B, eastern equatorial Pacific. *J. Geophys. Res.,* 95:9293–9303.

Mottl, M. J., 1983. Metabasalts, axial hot springs, and structure of hydrothermal systems at mid-ocean ridges. *Geol. Soc. Am. Bull.,* 94:161–180.

Mottl, M. J., Druffel, E.R.M., Hart, S. R., Lawrence, J. R., and Saltzman, E. S., 1985. Chemistry of hot waters sampled from basaltic basement in Hole 504B, Deep Sea Drilling Project Leg 83, Costa Rica Rift. *In* Anderson, R. N., Honnorez, J., et al., *Init. Repts. DSDP,* 83: Washington (U.S. Govt. Printing Office), 315–328.

Mottl, M. J., and Gieskes, J. M., 1990. Chemistry of waters sampled from oceanic basement boreholes, 1979–1988. *J. Geophys. Res.,* 95:9327–9342.

Newmark, R. L., Anderson, R. N., Moos, D., and Zoback, M. D., 1985. Sonic and ultrasonic logging of Hole 504B and its implications for the structure, porosity and stress regime of the upper 1 km of the oceanic crust. *In* Anderson, R. N., Honnorez, J., et al., *Init. Repts. DSDP,* 83: Washington (U.S. Govt. Printing Office), 479–510.

Newmark, R. L., Zoback, M. D., and Anderson, R. N., 1984. Orientation of in situ stresses in the oceanic crust. *Nature,* 311:424–428.

________, 1985. Orientation of in situ stresses near the Costa Rica Rift and Peru-Chile Trench, Deep Sea Drilling Project Hole 504B. *In* Anderson, R. N., Honnorez, J., Becker, K., et al., *Init. Repts. DSDP,* 83: Washington (U.S. Govt. Printing Office), 511–514.

Plumb, R. A., and Hickman, S. H., 1985. Stress-induced borehole elongation. A comparison between the four-arm dipmeter and the borehole televiewer in the Auburn geothermal well. *J. Geophys. Res.,* 90:5513–5521.

Seyfried, W. E., Jr., and Bischoff, J. L., 1979. Low temperature basalt alteration by seawater: an experimental study at 70°C and 150°C. *Geochim. Cosmochim. Acta,* 43:1937–1947.

Shipboard Scientific Party, 1985. Site 504: Costa Rica Rift. *In* Anderson, R. N., Honnorez, J., Becker, K., et al., *Init. Repts. DSDP,* 83: Washington (U.S. Govt. Printing Office).

________, 1988. Site 504: Costa Rica Rift. *In* Becker, K., Sakai., H., et al., *Proc. ODP, Init. Repts,* 111: College Station, TX (Ocean Drilling Program), 35–251.

________, in press. Site 829. *In* Collot, J.-Y., Greene, G., Stokking, L. B., et al., *Proc. ODP, Init. Repts.,* 134: College Station, TX (Ocean Drilling Program).

Williams, C. F., Narasimhan, T. N., Anderson, R. N., Zoback, M. D., and Becker, K., 1986. Convection in the oceanic crust: simulation of observations from Deep Sea Drilling Project Hole 504B, Costa Rica Rift. *J. Geophys. Res.,* 91:4877–4889.

Zemanek, J., Glenn, E. E., Jr., Norton, J. J., and Caldwell, R. L., 1970. Formation evaluation by inspection with the borehole televiewer. *Geophysics,* 35:254–269.

Zoback, M. D., Moos, D., Mastin, L. G., and Anderson, R. N., 1985. Well bore breakouts and in situ stress. *J. Geophys. Res.,* 90:5523–5530.

Ms 137A-102

NOTE: All core description forms ("barrel sheets") and core photographs have been printed on coated paper and bound as Section 3, near the back of the book, beginning on page 59.